Finite-Difference Methods for Second-Order Wave Equations with Reduced Dispersion Errors

Yajun An

A dissertation submitted in partial fulfillment of the
requirements for the degree of

Doctor of Philosophy

University of Washington

2015

Reading Committee:

Kenneth P. Bube, Chair

Hart Smith

Yu Yuan

Program Authorized to Offer Degree:
Mathematics

University of Washington

Abstract

Finite-Difference Methods for Second-Order Wave Equations
with Reduced Dispersion Errors

Yajun An

Chair of the Supervisory Committee:
Professor Kenneth P. Bube
Mathematics

Finite Difference (FD) schemes have been used widely in computing approximations for partial differential equations for wave propagation, as they are simple, flexible and robust. However, even for stable and accurate schemes, waves in the numerical schemes can propagate at different wave speeds than in the true medium. This phenomenon is called numerical dispersion error. Traditionally, FD schemes are designed by forcing accuracy conditions, and in spite of the advantages mentioned above, such schemes suffer from numerical dispersion errors.

Traditionally, two ways have been used for the purpose of reducing dispersion error: increasing the sampling rate and using higher order accuracy. More recently, Finkelstein and Kastner (2007, 2008) propose a unified methodology for deriving new schemes that can accommodate arbitrary requirements for reduced phase or group velocity dispersion errors, defined over any region in the frequency domain. Such schemes are based on enforcing exact phase or group velocity at certain preset wavenumbers. This method has been shown to reduce dispersion errors at large wavenumbers.

In this dissertation, we study the construction and behaviors of FD schemes designed to have reduced numerical dispersion error. We prove that the system of equations to select the coefficients in a centered FD scheme for second order wave equations with specified order of accuracy and exact phase velocity at preset wavenumbers can always be solved.

Furthermore, from the existence of such schemes, we can show that schemes which reduce the dispersion error uniformly in an interval of the frequency domain can be constructed from a Remez algorithm. In these new schemes we propose, we can also specify wavenumbers where the exact phase or group dispersion relation can be satisfied. For an incoming signal consisting of waves of different wavenumbers, our schemes can give more accurate wave propagation speeds. Furthermore, when we apply our schemes in two dimensional media, we can obtain schemes that give small dispersion error at all propagation angles.

TABLE OF CONTENTS

LIST OF FIGURES

ACKNOWLEDGMENTS

I would like to thank my advisor, Ken Bube, for his continued support and guidance.

DEDICATION

To anyone who might benefit from this work.

Chapter 1

INTRODUCTION

In this chapter, we address the main question of focus of this work in section one, review background material in section two, and describe our contributions in section three.

1.1 Numerical dispersion error

Waves are a common phenomenon: there are mechanical waves that propagate through a medium, such as ocean waves and seismic waves; or electromagnetic waves that do not require a medium, such as radio waves and microwaves. All these waves obey their respective wave equations that describe how the disturbance proceeds over time. The speed at which waves travel is often called the wave speed. More precisely, the speed at which a plane wave travels in a homogeneous medium is called the phase velocity, and the speed at which the energy propagates is called the group velocity.

Finite Difference (FD) schemes have been used widely in computing approximations for partial differential equations for wave propagation, as they are simple, flexible and robust (Kelly et al, 1976). The method has thus become very popular, especially in its second-order accurate, central difference variant known as the Leap-frog scheme. However, even for stable and accurate schemes, waves in the numerical schemes can propagate at different wave speeds than in the true medium. This phenomenon is called numerical dispersion error. Traditionally, FD schemes are designed by forcing accuracy conditions, and in spite of the advantages mentioned above, such schemes suffer from numerical dispersion errors. These errors can result in poor approximation to the wave speed for high wavenumbers, and thus cause poor approximations to the wave propagation as time spans get larger.

In many real life applications, it is useful to be able to model wave speeds accurately. For example, in weather forecasting, we wish to know precisely when a weather front will arrive so we know when to stay home to avoid storms. Predicting well when a weather front

will arrive requires accurate numerical wave speeds. It is our goal in this work to design Finite Difference schemes that approximate wave speeds well, so that we can simulate wave propagation and generate synthetic waves that travel at speeds close to the true wave speeds.

Traditionally, two ways have been used for the purpose of reducing dispersion error: increasing the sampling rate and using higher order accuracy (Levander, 1988). Staggered grids have also been introduced (Virieux, 1984, 1986).

More recently, Finkelstein and Kastner (2007, 2008) propose a unified methodology for deriving new schemes that can accommodate arbitrary requirements for reduced phase or group velocity dispersion errors, defined over any region in the frequency domain. Such schemes are based on enforcing exact phase or group velocity at certain preset wavenumbers. This method has been shown to reduce dispersion errors at large wavenumbers. Liu and Sen (2009) give explicit expression of such schemes in their work. We build on the work of Finkelstein and Kastner, Liu and Sen and others.

In this dissertation, we study the construction and behaviors of FD schemes designed to have reduced numerical dispersion error. We prove that the system of equations to select the coefficients in a centered FD scheme for second order wave equation with specified order of accuracy and exact phase velocity at preset wavenumbers can always be solved. Furthermore, from the existence of such schemes, we can show that schemes which reduce the dispersion error uniformly in an interval of the frequency domain can be constructed from a Remez-like algorithm. In these new schemes we propose, we can also specify wavenumbers where exact phase or group dispersion relation can be satisfied. For an incoming signal consisting of waves of different wavenumbers, our scheme can give better synthetic wave propagation. Furthermore, when we apply our schemes in two dimensional media, we can obtain schemes that give small dispersion error at all propagation angles. We show in numerical experiments that choosing schemes to have accuracy conditions at angle $\pi/4$ is the best option in designing schemes, as it guarantees the existence of schemes, and the error is not much bigger should we choose $\pi/8$ as used by Liu and Sen.

1.2 Background material: Wave equations, Finite difference schemes and Mathematical seismology

In this section, we introduce related background material to our work. We describe wave equations, talk about plane wave solutions to the acoustic wave equations, the speed at which the waves propagate, and how to approximate them with finite difference schemes. We will also introduce present definition of order of accuracy called spectral accuracy that has been commonly used in the geophysics community. Since our results can be used for solving elastic equations, we will also describe the equations used in continuum mechanics.

Wave propagation in real media is governed by complicated systems of wave equations which allow anisotropy, heterogeneity, and a variety of other physical phenomena. For elastic media with waves of small amplitude, wave propagation is governed by the linearized elastic system, which is commonly written either as a first-order system of differential equations with nine state variables (three particle velocities and six stresses), or as a second-order system with just the three particle velocities. Computations with the second-order system, because of the second time derivatives, must be at least two-step schemes, meaning that we must save two previous time levels at each step. The first-order system allows the use of staggered-grid schemes, but computationally, it is more efficient to use the second-order system because we have to store only six wavefields at a time instead of nine for the first-order system.

For very large earth models, storage is a concern, even with large distributed-memory parallel computations. It is thus common practice to use two-step schemes for second-order equations or systems, which appears to limit accuracy in time to second order. However, using the differential equation to write higher order time derivatives in terms of space derivatives, a methodology commonly attributed to Lax and Wendroff who introduced it as a way to get higher-order one-step schemes for first-order systems, accuracy is not limited to second-order, even with two-step schemes.

With these considerations in mind, we will study second-order wave equations in this work, and will consider only the efficient two-step schemes.

While the ideas of this work can be applied to more general second-order wave equations

or systems, we will focus mainly on the second order wave equation

$$\partial_t^2 u - c^2 \Delta u = 0. \tag{1.1}$$

where $u(x,t)$ describes the motion, a function of the spatial variable x and the time variable t. Solutions of this equation describe propagation of disturbances at a fixed speed in one or in all spatial directions, as do physical waves from plane or localized sources; the constant c has the dimension of velocity, and is identified with the propagation speed of the wave. This equation is linear, therefore the superposition principle applies, and we can study the plane wave solutions of it.

1.2.1 Plane wave solutions and the dispersion relation for the acoustic media

Plane waves approximate solutions to wave equations locally nicely in a homogeneous medium. We study plane wave solutions to the wave equations in this work. In a heterogeneous medium, locally wavefronts behave like plane waves as well. Moreover, the familiar Radon transform solution to the homogeneous wave equation can be expressed as a superposition of plane waves (Lax). Arbitrary initial conditions can be satisfied by choosing appropriate linear combinations of plane waves.

In an acoustic medium, the wave propagation is described by the following scalar equation:

$$\partial_t^2 u - c^2 \Delta u = 0. \tag{1.2}$$

The plane wave solution we will use (in three dimension for example) is

$$u = e^{i\mathbf{x}\cdot\mathbf{k} - i\omega t} = e^{i\omega(\mathbf{x}\cdot\mathbf{k}/\omega - t)}, \tag{1.3}$$

where $\mathbf{k} = (k_1, k_2, k_3)$ and ω denote the wavenumber and the frequency, respectively. Substituting the plane wave solution into the acoustic wave equation, we get the following *dispersion relation* in three dimensions:

$$c^2(k_1^2 + k_2^2 + k_3^2) - \omega^2 = 0. \tag{1.4}$$

Hence for plane wave solutions to exist, the wavenumber and the frequency need to satisfy the above relation. This relation indicates how fast a true wave should propagate in a homogeneous acoustic medium, and $c_p = \dfrac{\omega}{|\mathbf{k}|} = c$ computes the phase velocity.

Since locally the wavefront looks like a plane wave, a plane wave solution is a common choice for a trial solution. Our work focuses on the acoustic equation, its plane wave solutions and FD approximations to its dispersion relation.

1.2.2 Numerical analysis and Finite difference schemes

This subsection reviews definitions and theorems used in numerical analysis. Much of it follows Kreiss and Oliger (1973), modified for equations with second order time derivatives. We discuss two step methods, or their equivalent one step methods for 2×2 systems.

First we introduce difference operators, and denote the translation operator for f by

$$(E_j^m f)(\mathbf{x}) = f(x_1, \ldots, x_{j-1}, x_j + m\Delta x, x_{j+1}, \ldots, x_n) = f(\mathbf{x} + m\Delta x \mathbf{e_j}) \tag{1.5}$$

where Δx denotes grid size in space, and $\mathbf{e_j}$ the standard basis in $\mathbb{R}^n$. Then in one dimension, for example, we can approximate the second order derivative of f by

$$f''(x) \approx \frac{E^1 - 2I + E^{-1}}{\Delta x^2} f = \frac{f(x + \Delta x) - 2f(x) + f(x - \Delta x)}{\Delta x^2} = \frac{f_{j+1} - 2f_j + f_{j-1}}{\Delta x^2}. \tag{1.6}$$

Using similar notations, we write the 2-step methods of interest in the following general form in one dimension:

$$U_j^{n+1} + U_j^{n-1} + \sum_{m=0}^{M} c_m (U_{j+m}^n + U_{j-m}^n) = 0, \tag{1.7}$$

and

$$U_{l,j}^{n+1} + U_{l,j}^{n-1} + \sum_{m=0}^{M} c_m (U_{l+m,j}^n + U_{l-m,j}^n) + \sum_{m=0}^{M} d_m (U_{l,j+m}^n + U_{l,j-m}^n) = 0 \tag{1.8}$$

in two dimensions. Here U_j^n denotes the approximation to $u(x,t)$ at $x = j\Delta x$ and $t = n\Delta t$, and $U_{l,j}^n$ denotes the approximation to $u(x,z,t)$ at $x = l\Delta x$, $z = j\Delta z$ and $t = n\Delta t$.

Using notations from Kreiss and Oliger, the schemes we study assume the following form

$$Q_1 U(\mathbf{x}, t + \Delta t) = \sum_{n=0}^{1} Q_{-n} U(\mathbf{x}, t - n\Delta t) \tag{1.9}$$

where $Q_1 = I$, $Q_{-1} = -I$, and $Q_0 = \sum_m A_{m,n}(E_1^m + E_1^{-m}) + (E_2^m + E_2^{-m})$, $A_{m,n}$ are constants, $m = 0, \ldots, M$, $n = 0, 1$.

Remarks:

- In this work, we always take $Q_1 = I$; all the schemes are *explicit*.

- Design of new schemes comes down to design of different Q_0's. With wider stencils in space, it is possible to get higher order accuracy in space-time by Lax-Wendroff analysis for one dimension despite using two-step schemes based on the second order difference in time.

- We define the solution operator $S_h = S_h(t, t_0, \Delta x, \Delta t)$ by

$$U(x,t) = S_h(t, t_0, \Delta x, \Delta t)U(x, t_0), \tag{1.10}$$

  where $t - t_0$ is a non-negative multiple of Δt. We will use the solution operator for stability analysis. In one step methods, the solution operator is always $S_h(t, t_0, \Delta x, \Delta t) = Q_0^{(t-t_0)/\Delta t}$ due to the normalization of $Q_1 = I$ and the time-independence of the coefficients. For multi-step schemes, to study stability we convert the schemes into one-step schemes for a system. This is how Kreiss and Oliger handle multi-step methods. We will show in Example 1.2.5, that stability can be studied with roots of a quadratic polynomial.

We illustrate the motivation of above general schemes in the following example, and see that equal weights in symmetric grid points in space is natural for the wave equation.

Example 1.2.1 (Leap-frog scheme for the 1D wave equation)**.** Consider the wave equation in one dimension:

$$u_{tt} = c^2 u_{xx}. \tag{1.11}$$

Using $\partial_t^2 u \approx \dfrac{u^{n+1} - 2u^n + u^{n-1}}{\Delta t^2}$, and $\partial_x^2 u \approx \dfrac{u_{j+1} - 2u_j + u_{j-1}}{\Delta t^2}$, we get the Leap-frog scheme for the wave equation:

$$\frac{U(x,t+\Delta t) - 2U(x,t) + U(x,t-\Delta t)}{\Delta t^2} = c^2 \frac{U(x+\Delta x,t) - 2U(x,t) + U(x-\Delta x,t)}{\Delta x^2}. \tag{1.12}$$

Normalizing to get $Q_1 = I$, we obtain $Q_0 = \left(\frac{c\Delta t}{\Delta x}\right)^2 (E^1 - 2I + E^{-1}) + 2I$ and $Q_{-1} = -I$, write

$$\widetilde{U}(x,t) = \begin{pmatrix} U(x,t) \\ U(x,t-\Delta t) \end{pmatrix}, \tag{1.13}$$

and then the scheme can be written as

$$\begin{pmatrix} Q_1 & 0 \\ 0 & I \end{pmatrix} \widetilde{U}(x, t+\Delta t) = \begin{pmatrix} Q_0 & Q_{-1} \\ I & 0 \end{pmatrix} \widetilde{U}(x,t). \tag{1.14}$$

The one-step solution operator is

$$S_h = \begin{pmatrix} Q_0 & Q_{-1} \\ I & 0 \end{pmatrix}. \tag{1.15}$$

Remark: We define the ratio $\gamma = \frac{c\Delta t}{\Delta x}$ to be the CFL number. It is related to the stability of FD schemes, as we will see later.

Now that we have set up the general schemes, we will discuss their properties with the following concepts in the theory of numerical analysis.

Definition 1.2.2 (Stability for one-step methods)**.** A one-step difference scheme is stable for a sequence $(\Delta x_j, \Delta t_j) \to 0$ if there exist constants α_s, K_s such that $\forall t_0$, $\forall t \geq t_0$ (with $t - t_0$ a multiple of Δt), $||S_h(t, t_0, \Delta x, \Delta t)|| \leq K_s e^{\alpha_s (t-t_0)}$.

In this work, we will use the von Neumann condition for stability analysis:

Theorem 1.2.3 (von Neumann condition)**.** *A necessary condition for stability is that* $\exists\ \alpha_s$*, such that* $|\lambda_j(\widehat{S}_h(k))| \leq e^{\alpha_s \Delta t}$*, i.e.*

$$|\lambda_j(\widehat{S}_h(k))| \leq 1 + O(\Delta t) \tag{1.16}$$

where $\lambda_j(\widehat{S}_h(k))$ *are the eigenvalues of the symbol* $\widehat{S}_h(k)$ *of* S_h*. Here* k *denotes the wavenumber.*

Remark: If $\widehat{S}_h(k)$ is normal, the von Neumann condition is also sufficient.

One way to decide how well a FD scheme works is the order of accuracy:

Definition 1.2.4 (Order of accuracy)**.** A two-step difference scheme with $Q_1 = I$ is accurate of order (q_1, q_2) for the particular solution $U(x,t)$ if there is a function $C(t)$, bounded on every finite interval $[0, T]$, such that for $(\Delta x, \Delta t)$ sufficient small, $||Q_1 u(\cdot, t+\Delta t) - \sum_{n=0}^{1} Q_{-n} u(\cdot, t - n\Delta t)|| \leq \Delta t^2 C(t)(\Delta t^{q_1} + \Delta x^{q_2})$.

If an approximation is accurate of order (q_1, q_2) for all sufficiently smooth solutions, we say it is accurate of order (q_1, q_2). The approximation is called consistent if it is accurate of order at least (1,1).

Remarks:

- The above definition is equivalent to the common definition of order of accuracy.
- Accuracy can be easily determined by Taylor series. Here we give an example:

Example 1.2.5 (Difference scheme for the wave equation, order of accuracy and stability)**.** For the wave equation $u_{tt} = c^2 u_{xx}$ with approximation defined in Example 1.2.1

$$\frac{U(x,t+\Delta t) - 2U(x,t) + U(x,t-\Delta t)}{\Delta t^2} = c^2 \frac{U(x+\Delta x,t) - 2U(x,t) + U(x-\Delta x,t)}{\Delta x^2} \tag{1.17}$$

Let $u(x,t)$ be a true solution to the wave equation; then

$$u(x,t+\Delta t) - Q_0 u - Q_{-1} u = (\Delta t)^2 \left((\Delta t)^2 \frac{2}{4!} \partial_t^4 u - (\Delta x)^2 \frac{2c^2}{4!} \partial_x^4 u \right) + O(\Delta t^4, \Delta x^4); \tag{1.18}$$

therefore the Leap-frog scheme is accurate of order $(2,2)$.

Since S_h is given by (1.15), we have

$$\widehat{S}_h = \begin{pmatrix} 2\left(\left(\frac{c\Delta t}{\Delta x}\right)^2 (\cos(k\Delta x) - 1) + 1\right) & -1 \\ 1 & 0 \end{pmatrix}. \tag{1.19}$$

The eigenvalues of the matrix are solutions to the quadratic equation

$$g^2 - 2\left(\left(\frac{c\Delta t}{\Delta x}\right)^2 (\cos(k\Delta x) - 1) + 1\right) g + 1 = 0. \tag{1.20}$$

To get stability, we enforce $|g| \leq 1$ and we need $\left|\left(\frac{c\Delta t}{\Delta x}\right)^2 (\cos(k\Delta x) - 1) + 1\right| \leq 1$ for all $k\Delta x$ with $\gamma = \frac{c\Delta t}{\Delta x}$ fixed.

When we design a FD scheme, we consider both the order of accuracy and stability, as convergence of schemes is guaranteed by:

Theorem 1.2.6 (Lax Equivalence Theorem)**.** *Given a well-posed initial value problem and a consistent finite-difference approximation, the scheme is convergent if and only if it is stable.*

In the next subsection, we discuss the definition of spectral order of accuracy. This concept was discussed in Finkelstein and Kastner (2009).

1.2.3 Dispersion relation and spectral order of accuracy

The concept of spectral order of accuracy (for the wave equation) was proposed by Finkelstein and Kastner in 2009 as a combination of the order of accuracy and the numerical dispersion relation. Here we generalize the concept of spectral accuracy to constant linear difference operators. Since we will often see the product of k and Δx, we will define a *normalized wavenumber* $K = k\Delta x$. Similarly, we define the *normalized frequency* $\Omega = \omega\Delta t$.

Definition 1.2.7 (Spectral order of accuracy)**.** A two-step finite difference scheme is spectrally accurate of order (q_1, q_2) for the particular solution $u(x,t)$ if there is a function $C(\widehat{u})$, bounded for $K, \Omega \in [0, 2\pi]$ such that for Ω, K sufficiently small,

$$||\widehat{Q}_1\widehat{u} - \sum_{n=0}^{1} \widehat{Q}_{-n}\widehat{u}|| \leq C(\widehat{u})(\Omega^{q_1+2} + K^{q_2+2}) \tag{1.21}$$

where $\widehat{Q}$ denotes the symbol of Q and $\widehat{u}$ denotes the Fourier transform of u. The approximation is called *spectrally consistent* if it is spectrally accurate of order at least $(1, 1)$.

Remark: Since all the difference operators have constant coefficients, $\widehat{Q}\widehat{u} = \widehat{Qu}$.

The spectral order of accuracy can also be determined by Taylor expansion. We compute the spectral order of accuracy for the Leap-frog scheme for the one dimension wave equation:

Example 1.2.8 (Spectral order of accuracy for the wave equation)**.** Fourier Transform of the wave equation $u_{tt} = c^2 u_{xx}$ gives the true dispersion relation

$$\omega = \pm ck. \tag{1.22}$$

If we take the particular mesh widths into consideration, the true dispersion would be (without the loss of generality, we consider the right moving wave)

$$\Omega = \gamma K \tag{1.23}$$

Here $\gamma = \frac{c\Delta t}{\Delta x}$ is the CFL number previously defined. With the same finite difference scheme shown in Example 1.2.5, we get

$$\widehat{Q}_1\widehat{u} - \widehat{Q}_0\widehat{u} - \widehat{Q}_{-1}\widehat{u} = 2\left(\cos(\Omega) - \gamma^2\cos(K) + \gamma^2 - 1\right)\widehat{u}(K,\Omega). \tag{1.24}$$

Here $\widehat{u}(K,\Omega)$ is a smooth function of K and Ω. Taylor expansion of $\cos(\Omega)-\gamma^2\cos(K)+\gamma^2-1$ at $(K,\Omega) = (0,0)$ gives

$$\begin{aligned}\widehat{Q}_1\widehat{u} - \widehat{Q}_0\widehat{u} &= 2\left(\sum_{n=0}^{\infty}\frac{(-1)^n\Omega^{2n}}{(2n)!} - \gamma^2\sum_{n=0}^{\infty}\frac{(-1)^nK^{2n}}{(2n)!} + \gamma^2 - 1\right)\widehat{u} \\ &= \frac{2}{4!}(\Omega^4 - \gamma^2K^4)\widehat{u} + O(\Omega^6 + K^6),\end{aligned} \tag{1.25}$$

where the cancellation of the lower order terms are due to plugging in the true dispersion relation (1.23). By definition, this scheme is of spectral order $(2,2)$.

We see order of accuracy and spectral order of accuracy are equivalent:

Theorem 1.2.9 (Equivalence of order of accuracy and spectral order of accuracy)**.** *A finite difference scheme is accurate of order (q_1,q_2) if and only if it is spectrally accurate of order (q_1,q_2). Thus order of accuracy and spectral order of accuracy are equivalent.*

Proof. We take the L^2 norm and use the relation $\Omega = \omega\Delta t$ and $K = k\Delta x$, then we apply the Plancherel theorem to $||Q_1u - \sum_{n=0}^{1}Q_{-n}u||$ and the equivalence follows. □

The main objective of this work is to investigate the error between true dispersion and the numerical dispersion. Here we write the frequency as a function of wavenumber:

$$\Omega = \Omega(K), \tag{1.26}$$

with the assumption that $\gamma = \frac{c\Delta t}{\Delta x}$ is a fixed constant. This reduces the dependence of dispersion to only the normalized wavenumber. We are interested in reducing $||\Omega_{true} - \Omega_{numerical}||$. However, Finkelstein and Kastner, Liu and Sen both designed schemes aiming to reduce $||\cos(\Omega_{true}) - \cos(\Omega_{numerical})||$. From the continuity of $\cos(\cdot)$ and $\arccos(\cdot)$, small dispersion error implies small spectral error and vice verse. Computational results also show reduction of spectral error guarantees the reduction of dispersion error.

1.2.3.1 Higher dimensional case

Similarly, we can talk about the general n dimensional case for both types of accuracy. Both the definitions in one dimensional case carries through.

Definition 1.2.10 (Spectral order of accuracy: n dimensions)**.** A two-step finite difference scheme is spectrally accurate of order $(q_1, q_2, \ldots, q_{n+1})$ if there is a function $C(\widehat{u})$, bounded for $K_1, \ldots, K_n, \Omega \in [0, 2\pi]$ such that for Ω, K sufficiently small,

$$||\widehat{Q}_1\widehat{u} - \sum_{n=0}^{1} \widehat{Q}_{-n}\widehat{u}|| \leq C(\widehat{u})(\Omega^{q_1+2} + K_1^{q_2+2} + \cdots + K_n^{q_n+2}) \tag{1.27}$$

The approximation is called *spectrally consistent* if it is spectrally accurate of order at least $(1, \ldots, 1)$.

Example 1.2.11 (Leap-frog scheme for 2D wave equation, order of accuracy)**.** For the wave equation $u_{tt} = c^2(u_{xx} + u_{zz})$ with approximation

$$\frac{U(x,t+\Delta t) - 2U(x,t) + U(x,t-\Delta t)}{\Delta t^2} = \\ c^2\frac{U(x+\Delta x,t) - 2U(x,t) + U(x-\Delta x,t)}{\Delta x^2} + c^2\frac{U(z+\Delta z,t) - 2U(z,t) + U(z-\Delta z,t)}{\Delta z^2}, \tag{1.28}$$

we will compute the order of accuracy and spectral accuracy, dispersion accuracy. Similar to the previous example, let $u(x,t)$ be a true solution to the wave equation; we obtain

$$u(x,t+\Delta t) - Q_0 u - Q_{-1}u = (\Delta t)^2\left((\Delta t)^2\frac{2}{4!}\partial_t^4 u - (\Delta x)^2\frac{2c^2}{4!}\partial_x^4 u - (\Delta z)^2\frac{2c^2}{4!}\partial_z^4 u\right) \\ + O(\Delta t^4, \Delta x^4, \Delta z^4); \tag{1.29}$$

therefore the Leap frog scheme is of order $(2, 2, 2)$.

1.2.3.2 Example: Elliptical anisotropic case

A direct generalization an acoustic medium is an elliptically anisotropic VTI medium. In such a medium, we study wave equations of the form

$$u_{tt} - \left(c_x^2 u_{xx} + c_z^2 u_{zz}\right) = 0. \tag{1.30}$$

In practice, we normally take $c_x^2 = (1+2\epsilon)c_z^2$ where ϵ is the Thomsen anisotropy parameter ϵ. Since horizontal reflectors act as a decelerator for energy propagation, waves propagate slower vertically than horizontally, so usually $\epsilon > 0$.

Similar to the Leap-frog scheme for isotropic media, we can discretize the differential equation to get

Example 1.2.12.

$$U_{l,j}^{n+1} - 2U_{l,j}^n + U_{l,j}^{n-1} = \frac{c_x^2\Delta t^2}{\Delta x^2}\left(U_{l+1,j}^n - 2U_{l,j}^n + U_{l-1,j}^n\right) + \frac{c_z^2\Delta t^2}{\Delta z^2}\left(U_{l,j+1}^n - 2U_{l,j}^n + U_{l,j-1}^n\right). \tag{1.31}$$

Similar to FD schemes for isotropic media, consider:

$$U_{l,j}^{n+1} + U_{l,j}^{n-1} + \sum_{m=0}^{M}(1+2\epsilon)c_m(U_{l+m,j}^n + U_{l-m,j}^n) + \sum_{m=0}^{M} c_m(U_{l,j+m}^n + U_{l,j-m}^n) = 0, \tag{1.32}$$

here the grid size in x and z directions are equal, $\Delta x = \Delta z$.

The true dispersion relation for the elliptical anisotropic media is $\Omega^2 = \gamma_x^2 K_x^2 + \gamma_z^2 K_z^2$.

1.2.4 Review of continuum mechanics and elastic waves

In this subsection, we review general elastic wave equations and provide the background for the wave equations we discuss. The main part is based on Chapter two of Burridge's notes on mathematical topics in seismology.

The wave equation for general anisotropic elastic media can be obtained from the following two equations:

$$\text{the linear momentum equation: } \frac{d}{dt}\int_V \rho\dot{\mathbf{u}}dV = \int_{\partial V}\mathbf{T}(\mathbf{x},\mathbf{n})dS + \int_V \rho\mathbf{f}dV, \tag{1.33}$$

and

$$\text{the conservation of mass: } \int_V \rho dV = \int_{V_0}\rho_0 dV_0, \tag{1.34}$$

where ρ and ρ_0 are the density in the reference and the current state, $\mathbf{u}$ is the displacement, $\mathbf{T}$ is the contact force in a volume V, and $\mathbf{f}$ denotes the body force (say for example, gravity). Let F denote the deformation gradient from the reference state to the current state; then

the conservation of mass gives $\int_V \rho dV = \int_{V_0} \rho |F| dV_0 = \int_{V_0} \rho_0 dV_0$, and since V is arbitrary, we conclude $\rho_0 = \rho|F|$. This fact together with the linear momentum equation give

$$\frac{d}{dt}\int_V \rho \dot{\mathbf{u}} dV = \frac{d}{dt}\int_{V_0} \rho_0 \frac{1}{|F|}\dot{\mathbf{u}}|F| dV_0 = \int_{V_0} \rho_0 \ddot{\mathbf{u}} dV_0 = \int_V \rho \ddot{\mathbf{u}} dV. \tag{1.35}$$

Hence we can write the linear momentum equation as

$$\int_{\partial V} \mathbf{T}(\mathbf{x}, \mathbf{n}) dS = \int_V \rho(\ddot{\mathbf{u}} - \mathbf{f}) dV. \tag{1.36}$$

To study traction as a function of the unit normal, consider traction on four faces of a tetrahedron. We can write

$$\mathbf{T}(\mathbf{x}, \mathbf{n}) = \boldsymbol{\sigma}(\mathbf{x})\mathbf{n}, \tag{1.37}$$

where $\boldsymbol{\sigma}$ is a second-order tensor, called the *stress tensor*:

$$\boldsymbol{\sigma} = \begin{pmatrix} \sigma_{11} & \sigma_{12} & \sigma_{13} \\ \sigma_{21} & \sigma_{22} & \sigma_{23} \\ \sigma_{31} & \sigma_{32} & \sigma_{33} \end{pmatrix}. \tag{1.38}$$

In an equilibrium medium, there should be no torque. This requires that the stress tensor is symmetric, i.e. $\boldsymbol{\sigma} = \boldsymbol{\sigma}^T$. With this notation, we can apply the divergence theorem to the linear momentum equation component-wise:

$$\int_{\partial V} \sigma_{ij} n_j dS = -\int_V \frac{\partial \sigma_{ij}}{\partial x_j} dV. \tag{1.39}$$

This implies

$$\int_V \rho \ddot{u}_i - \frac{\partial \sigma_{ij}}{\partial x_j} - \rho f_i dV = 0. \tag{1.40}$$

Since V is arbitrary, we get the wave equation for general anisotropic heterogeneous media

$$\rho \frac{\partial^2 u_i}{\partial t^2} - \frac{\partial \sigma_{ij}}{\partial x_j} = f_i. \tag{1.41}$$

The unknowns in the above wave equation are the displacement vector $\mathbf{u}$ and the stress tensor $\boldsymbol{\sigma}$. To complete the system for elastic media, we will introduce the constitutive relation between stress and displacement:

$$\sigma_{ij} = c_{ijkl} e_{kl}, \tag{1.42}$$

where $e_{kl} = \frac{1}{2}(\frac{\partial u_k}{\partial x_l} + \frac{\partial u_l}{\partial x_k})$ denotes the *strain tensor* and c_{ijkl} constants related to the properties of the media. The strain tensor is symmetric, i.e. $\mathbf{e} = \mathbf{e}^T$.

In this work, we will focus on **homogeneous media**, hence $\frac{\partial c_{ijkl}}{\partial x_j} = 0$. Plugging in the constitutive relation, the wave equation becomes

$$\rho \frac{\partial^2 u_i}{\partial t^2} - c_{ijkl} \frac{\partial^2 u_k}{\partial x_j \partial x_l} = f_i. \tag{1.43}$$

The symmetry of the stress tensor implies that $c_{ijkl} = c_{jikl}$; the symmetry of the strain tensor implies that $c_{ijkl} = c_{ijlk}$. A thermodynamic argument[1] implies that $c_{ijkl} = c_{klij}$. These symmetry conditions help reduce the number of independent elastic coefficients for the most general homogeneous anisotropic media down to 21. We will write these stiffness parameters c_{ijkl} with the *Voigt notation* of the indices:

$$\{ij\} \to m \text{ where } \{11\} \to 1, \{22\} \to 2, \{33\} \to 3, \{23\} \to 4, \{31\} \to 5, \{12\} \to 6$$

We then define the new parameters $C_{mn} = c_{ijkl}$ with $\{ij\} \to m$ and $\{kl\} \to n$. The constitutive relation can be rewritten as

$$\begin{pmatrix} \sigma_{11} \\ \sigma_{22} \\ \sigma_{33} \\ \sigma_{23} \\ \sigma_{31} \\ \sigma_{12} \end{pmatrix} = \begin{pmatrix} C_{11} & C_{12} & C_{13} & C_{14} & C_{15} & C_{16} \\ & C_{22} & C_{23} & C_{24} & C_{25} & C_{26} \\ & & C_{33} & C_{34} & C_{35} & C_{36} \\ & & & C_{44} & C_{45} & C_{46} \\ & & & & C_{55} & C_{56} \\ & & & & & C_{66} \end{pmatrix} \begin{pmatrix} e_{11} \\ e_{22} \\ e_{33} \\ 2e_{23} \\ 2e_{31} \\ 2e_{12} \end{pmatrix} \tag{1.44}$$

We only write the 21 independent parameters for the *stiffness matrix*. We will discuss some special types of media and their wave equations, where the stiffness matrix is even simpler.

1.2.4.1 Acoustic media

Acoustic waves propagate in a fluid. A perfect fluid is defined as a medium in which shear stresses are always zero. It is necessary that the stress tensor be isotropic, i.e. $\sigma_{11} = \sigma_{22} =$

[1] The existence of a unique, internal strain energy function from work done by stress tensor. See Chapman, section 4.4.

$\sigma_{33} = -P$ thus the stress tensor is

$$\boldsymbol{\sigma} = \frac{1}{3} tr(\boldsymbol{\sigma})\mathbf{I} = -P\mathbf{I}, \tag{1.45}$$

where $\mathbf{I}$ is the identity tensor [2]. We assume the fluid is isotropic, so the linear constitutive relation can be written as

$$\nabla \cdot \mathbf{u} = -\frac{1}{\kappa} P, \tag{1.46}$$

or

$$\frac{\partial P}{\partial t} = -\kappa \nabla \cdot \dot{\mathbf{u}}. \tag{1.47}$$

Substituting the stress tensor (1.45) in the (1.41), we get

$$\ddot{\mathbf{u}} = -\frac{1}{\rho} \nabla P + \frac{1}{\rho} \mathbf{f}. \tag{1.48}$$

Together we get the acoustic wave equation:

$$\rho \ddot{\mathbf{u}} = -\nabla P + \mathbf{f}, \tag{1.49}$$

$$P = -\kappa \nabla \cdot \mathbf{u}, \tag{1.50}$$

which simplifies to:

$$\ddot{\mathbf{u}} = \frac{\kappa}{\rho} \nabla(\nabla \cdot \mathbf{u}) + \mathbf{f}. \tag{1.51}$$

Taking $\mathbf{f} = \mathbf{0}$ and writing $c^2 = \frac{\kappa}{\rho}$, then we obtain the standard acoustic wave equation

$$\ddot{\mathbf{u}} - c^2 \Delta \mathbf{u} = 0. \tag{1.52}$$

---

[2] Define $P = -\frac{1}{3} tr(\boldsymbol{\sigma})$, the hydrostatic pressure. The negative sign is from the fact that pressure and stress are measured in opposite directions.

1.2.4.2 Isotropic media

When all directions of wave propagation are equivalent, the medium is isotropic, and we obtain the following stiffness matrix:

$$\mathbf{C} = \begin{pmatrix} \lambda+2\mu & \lambda & \lambda & 0 & 0 & 0 \\ \lambda & \lambda+2\mu & \lambda & 0 & 0 & 0 \\ \lambda & \lambda & \lambda+2\mu & 0 & 0 & 0 \\ 0 & 0 & 0 & \mu & 0 & 0 \\ 0 & 0 & 0 & 0 & \mu & 0 \\ 0 & 0 & 0 & 0 & 0 & \mu \end{pmatrix}, \tag{1.53}$$

or

$$c_{ijkl} = \lambda\delta_{ij}\delta_{kl} + \mu(\delta_{ik}\delta_{jl} + \delta_{il}\delta_{jk}).$$

The coefficients λ and μ are the Lamé parameters; they describe the elastic properties of the isotropic medium. μ in particular is the shear modulus, defined as the ratio of the shear stress to the shear strain. The wave equation in this case is then

$$\rho\frac{\partial^2 u_i}{\partial t^2} - (\lambda+\mu)\frac{\partial^2 u_j}{\partial x_i \partial x_j} - \mu\frac{\partial^2 u_i}{\partial x_j \partial x_j} = f_i. \tag{1.54}$$

1.2.4.3 Transversely isotropic elastic media

In transversely isotropic (TI) media, there is a single axis of rotational symmetry and a symmetry plane which is perpendicular to the symmetry axis. In particular, we discuss TI media with a vertical symmetry axis (VTI). The stiffness matrix of VTI media is given by

$$\mathbf{C} = \begin{pmatrix} C_{11} & C_{11}-2C_{66} & C_{13} & 0 & 0 & 0 \\ C_{11}-2C_{66} & C_{11} & C_{13} & 0 & 0 & 0 \\ C_{13} & C_{13} & C_{33} & 0 & 0 & 0 \\ 0 & 0 & 0 & C_{55} & 0 & 0 \\ 0 & 0 & 0 & 0 & C_{55} & 0 \\ 0 & 0 & 0 & 0 & 0 & C_{66} \end{pmatrix} \tag{1.55}$$

with five independent parameters.

1.2.4.4 Pseudo-acoustic approximation to the elastic wave equations in VTI media

In this section, we will present the pseudo-acoustic VTI approximation proposed by Duveneck et al. in 2008, which increases computational efficiency. It consists of describing the medium in terms of the *Thomsen parameters* ϵ and δ, and vertical P- and S- wave velocities V_{P0} and V_{S0}. Then the vertical S- wave velocity V_{S0} is set to be zero (Alkhalifah, 1998). We will derive the wave equations for acoustic VTI media from the linear stress-strain relationship for VTI media together with the equations of motion.

The stiffnesses are expressed in terms of Thomsen parameters (where ρ denotes the density):

$$\begin{aligned} V_{P0} &= \sqrt{\frac{C_{33}}{\rho}} \\ V_{S0} &= \sqrt{\frac{C_{55}}{\rho}} \\ \epsilon &= \frac{C_{11} - C_{33}}{2C_{33}} \\ \delta &= \frac{(C_{13} + C_{55})^2 - (C_{33} - C_{55})^2}{2C_{33}(C_{33} - C_{55})} \\ \gamma &= \frac{C_{66} - C_{55}}{2C_{55}}. \end{aligned} \tag{1.56}$$

Then the stiffnesses are:

$$\begin{aligned} C_{11} &= (1 + 2\epsilon)\rho V_{P0}^2 \\ C_{13} &= \sqrt{(\rho V_{P0}^2 - \rho V_{S0}^2)((1 + 2\delta)\rho V_{P0}^2 - \rho V_{S0}^2)} - \rho V_{S0}^2 \\ C_{33} &= \rho V_{P0}^2 \\ C_{55} &= \rho V_{S0}^2 \\ C_{66} &= (1 + 2\gamma)\rho V_{S0}^2. \end{aligned} \tag{1.57}$$

We assume $V_{S0} = 0$. Hooke's law becomes (in Voigt notation):

$$\begin{pmatrix} \sigma_{11} \\ \sigma_{22} \\ \sigma_{33} \\ \sigma_{23} \\ \sigma_{31} \\ \sigma_{12} \end{pmatrix} = \rho \begin{pmatrix} V_{P0}^2(1+2\epsilon) & V_{P0}^2(1+2\epsilon) & V_{P0}^2\sqrt{1+2\delta} & 0 & 0 & 0 \\ V_{P0}^2(1+2\epsilon) & V_{P0}^2(1+2\epsilon) & V_{P0}^2\sqrt{1+2\delta} & 0 & 0 & 0 \\ V_{P0}^2\sqrt{1+2\delta} & V_{P0}^2\sqrt{1+2\delta} & V_{P0}^2 & 0 & 0 & 0 \\ 0 & 0 & 0 & 0 & 0 & 0 \\ 0 & 0 & 0 & 0 & 0 & 0 \\ 0 & 0 & 0 & 0 & 0 & 0 \end{pmatrix} \begin{pmatrix} e_{11} \\ e_{22} \\ e_{33} \\ 2e_{23} \\ 2e_{31} \\ 2e_{12} \end{pmatrix} \tag{1.58}$$

We use the indices $i, j = 1, 2, 3$ corresponding to the x, y, z axes. Using horizontal isotropy, we write $\sigma_H = \sigma_{11} = \sigma_{22}$ and $\sigma_V = \sigma_{33}$ and reduce the system into two linearly independent equations:

$$\begin{aligned} \sigma_H &= \rho V_{P0}^2(1+2\epsilon)e_{11} + \rho V_{P0}^2(1+2\epsilon)e_{22} + \rho V_{P0}^2\sqrt{1+2\delta}e_{33} \\ \sigma_V &= \rho V_{P0}^2\sqrt{1+2\delta}e_{11} + \rho V_{P0}^2\sqrt{1+2\delta}e_{22} + \rho V_{P0}^2 e_{33}. \end{aligned} \tag{1.59}$$

Combining the two equations with the equations of motion (1.41), and assuming the external force is zero, we obtain the following 5×5 first order system:

$$\begin{aligned} \frac{\partial^2 u_x}{\partial t^2} &= \frac{1}{\rho}\frac{\partial \sigma_H}{\partial x} \\ \frac{\partial^2 u_y}{\partial t^2} &= \frac{1}{\rho}\frac{\partial \sigma_H}{\partial y} \\ \frac{\partial^2 u_z}{\partial t^2} &= \frac{1}{\rho}\frac{\partial \sigma_V}{\partial z} \\ \frac{\partial \sigma_H}{\partial t} &= \rho V_{P0}^2\left[(1+2\epsilon)\left(\frac{\partial^2 u_x}{\partial x \partial t} + \frac{\partial^2 u_y}{\partial y \partial t}\right) + \sqrt{1+2\delta}\frac{\partial^2 u_z}{\partial z \partial t}\right] \\ \frac{\partial \sigma_V}{\partial t} &= \rho V_{P0}^2\left[\sqrt{1+2\delta}\left(\frac{\partial^2 u_x}{\partial x \partial t} + \frac{\partial^2 u_y}{\partial y \partial t}\right) + \frac{\partial^2 u_z}{\partial z \partial t}\right]. \end{aligned} \tag{1.60}$$

Differentiating the resulting equations with respect to t, with the constant density assumption, and eliminating the velocity (u_x, u_y, u_z) in the above system, we get the following 2×2 second-order system:

$$\frac{\partial^2 \sigma_H}{\partial t^2} = V_{P0}^2\left[(1+2\epsilon)\left(\frac{\partial^2 \sigma_H}{\partial x^2} + \frac{\partial^2 \sigma_H}{\partial y^2}\right) + \sqrt{1+2\delta}\frac{\partial^2 \sigma_V}{\partial z^2}\right] \tag{1.61}$$

$$\frac{\partial^2 \sigma_V}{\partial t^2} = V_{P0}^2\left[\sqrt{1+2\delta}\left(\frac{\partial^2 \sigma_H}{\partial x^2} + \frac{\partial^2 \sigma_H}{\partial y^2}\right) + \frac{\partial^2 \sigma_V}{\partial z^2}\right]. \tag{1.62}$$

We can write the above system in matrix form:

$$\partial_t^2 \begin{pmatrix} \sigma_H \\ \sigma_V \end{pmatrix} = V_{P0}^2 \begin{pmatrix} (1+2\epsilon) & \sqrt{1+2\delta} \\ \sqrt{1+2\delta} & 1 \end{pmatrix} \begin{pmatrix} \partial_x^2 \sigma_H + \partial_y^2 \sigma_H \\ \partial_z^2 \sigma_V \end{pmatrix}. \tag{1.63}$$

Since the medium is isotropic in the xy- plane,we can get some insight by studying wave propagation in a single vertical plane. Here we take the vertical plane to be the xz- plane, and then the system can be simplified to

$$\partial_t^2 \begin{pmatrix} \sigma_H \\ \sigma_V \end{pmatrix} = V_{P0}^2 \begin{pmatrix} (1+2\epsilon) & \sqrt{1+2\delta} \\ \sqrt{1+2\delta} & 1 \end{pmatrix} \begin{pmatrix} \partial_x^2 \sigma_H \\ \partial_z^2 \sigma_V \end{pmatrix} \tag{1.64}$$

1.2.4.5 Elliptically anisotropic VTI media

Elliptically anisotropic media are a special case of VTI media, where the Thomsen parameters satisfy $\epsilon = \delta$. In this case, the two linearly independent equations (1.59) satisfy $\sigma_H = \sqrt{1+2\epsilon}\sigma_V$, and then the 2×2 system further reduces to one single equation. We obtain the acoustic wave equation for the elliptically anisotropic media:

$$\frac{\partial^2 \sigma_H}{\partial t^2} = V_{P0}^2 \left[(1+2\epsilon) \left(\frac{\partial^2 \sigma_H}{\partial x^2} + \frac{\partial^2 \sigma_H}{\partial y^2} \right) + \frac{\partial^2 \sigma_H}{\partial z^2} \right]. \tag{1.65}$$

Similar to the VTI equations, in 2D we will not consider the y dependence. Denoting $u = \sigma_H$ and $c = V_{P0}$, then the equation is

$$\partial_t^2 u = c^2(1+2\epsilon)\partial_x^2 u + c^2 \partial_z^2 u. \tag{1.66}$$

1.3 Comparison of previous and new results

Traditionally, FD schemes are designed by enforcing accuracy conditions only at the point $u(x,t)$ (or equivalently, at the zero wavenumber). As we see in the following chapters, the numerical phase velocity is a good approximation to the real phase velocity if the wavenumber is small. For large wavenumbers, the numerical velocity is in general smaller than the true value from the differential equation. In this work, we design schemes that target good approximations to the wave speed at all wavenumbers up to the Nyquist wavenumber. The schemes are modified from the well-known Remez algorithm, and are guaranteed to exist, from a theorem presented in Chapter two.

In two dimensional media, we fix a propagation angle, and look for schemes that give small dispersion error for all wavenumbers, or we fix a wavenumber, and look for schemes that give good dispersion approximation in all propagation directions. We show in numerical experiments that choosing schemes to have accuracy conditions at $\pi/4$ is the best option in design of schemes, as it guarantees the existence of schemes, and does not increase numerical anisotropy in the wavefront compared to $\pi/8$ proposed by Liu and Sen.

Chapter 2

ONE DIMENSIONAL ACOUSTIC WAVE EQUATION

In this chapter, we develop Finite difference schemes for the one dimensional acoustic wave equation. Let the u in (1.2) depend on the one-dimensional space variable x and time t; the equation we will study is

$$\frac{\partial^2 u}{\partial t^2} - c^2 \frac{\partial^2 u}{\partial x^2} = f. \tag{2.1}$$

Without loss of generality, we take the phase velocity $c = 1$. f on the right hand side is a source term. In the following, we will either work with a source-less medium with an initial pulse, or a medium with a source term and zero initial conditions. For the purpose of simplicity, we do all analysis for the former situation.

We are interested in schemes of general form

$$U_j^{n+1} + U_j^{n-1} + \sum_{m=0}^{M} c_m (U_{j+m}^n + U_{j-m}^n) = 0 \tag{2.2}$$

with wide stencil of size $(2, 2M)$ (stencil as seen in Figure 2.6). A Remez-like algorithm will be applied to determine the coefficients c_m for the above scheme, with the goal of decreasing numerical dispersion errors over a range of wavenumbers.

2.1 Motivation of choices of schemes

To motivate these two choices (wider spatial stencil and the Remez-like algorithm), we first show some computational results comparing dispersion computed with narrow versus wide spatial stencils, and accuracy-oriented schemes versus dispersion-oriented schemes. These comparisons make our choice for the general scheme natural.

2.1.1 Comparison of narrow and wide spatial stencils

In this section, we take different M in (2.2), and show that numerical dispersion error decreases as M gets larger. All the schemes we use in this section are derived via Taylor

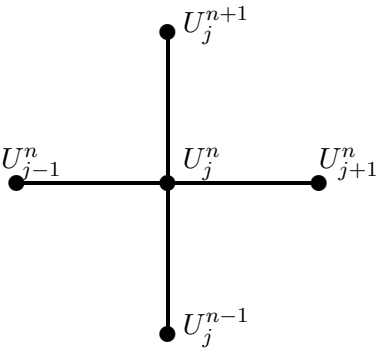

Figure 2.1: Stencil for Leap-Frog scheme

expansion, based on getting highest order of accuracy at (x, t).

Example 2.1.1 (Leap-frog scheme)**.** The Leap-frog scheme is derived from (2.2) with $M = 2$ (stencil in Figure 2.1), by enforcing second order accuracy at (x, t).

$$U_j^{n+1} - 2U_j^n + U_j^{n-1} - \gamma^2 \left(U_{j+1}^n - 2U_j^n + U_{j-1}^n\right) \approx 0. \tag{2.3}$$

Here $\gamma = c\dfrac{\Delta t}{\Delta x}$ denotes the CFL number (the CFL number is related to the stability condition for the scheme, as seen in Chapter One), and U_{j+m}^{n+l} denotes the grid function approximating $u(x + m\Delta x, t + l\Delta t)$.

The numerical dispersion relation is

$$1 - \cos(\Omega) - \gamma^2 + \gamma^2 \cos(K) \approx 0. \tag{2.4}$$

Solving for Ω gives

$$\Omega(K) = \arccos(1 - \gamma^2 + \gamma^2 \cos(K)), \tag{2.5}$$

and the numerical phase velocity is

$$c(K) = \frac{c}{\gamma K} \arccos(1 - \gamma^2 + \gamma^2 \cos(K)) \tag{2.6}$$

In Figure 2.2, we show the numerical phase velocity plotted for different stencil widths with schemes enforcing accuracy conditions at (x, t) (given by (2.11) in next section). We

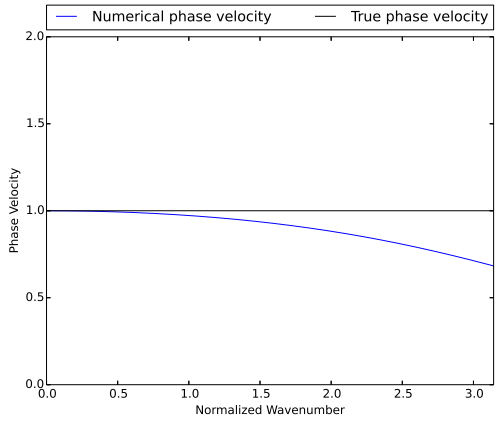

(a) Numerical phase velocity, max error=0.31722411766955516

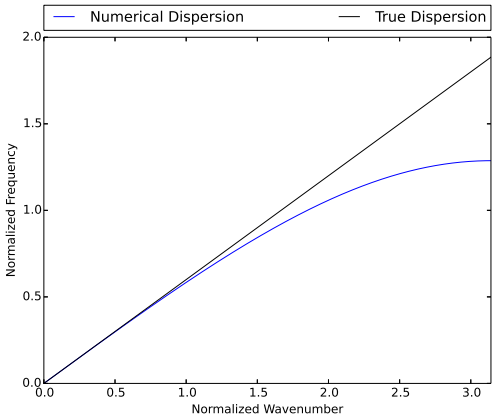

(b) Numerical Dispersion, max error=0.59795337456730713

Figure 2.2: Numerical dispersion/phase velocity for the Leap-frog scheme, with $\gamma = 0.6$

see that regardless of the stencil width, the computed velocity is in general smaller than the true velocity, and it gets further away from the true velocity as the wavenumber gets bigger. Hence we expect the wave propagation simulated by the scheme to be slower than the true propagation, especially for waves with big wavenumber. Wave propagation Figures 2.3a and 2.3b justify our expectation.

In Figure 2.4, we see that as we increase M, the lag of wave speed near $K = \pi$ decreases.

2.1.2 Comparison of accuracy focused schemes and dispersion focused schemes

In this section, we will motivate the choice of our methodology to derive schemes focused on the dispersion relation. In their work of 2008 and 2009, Finkelstein and Kastner proposed that, instead of putting all the restraints on order of accuracy at the zero wavenumber, using some of the conditions to force exact dispersion relation at some non-zero wavenumbers. As we have seen that dispersion error increases as wavenumber gets closer to π, it is natural to force the exact dispersion at large wavenumbers. Note the schemes we get will still have some

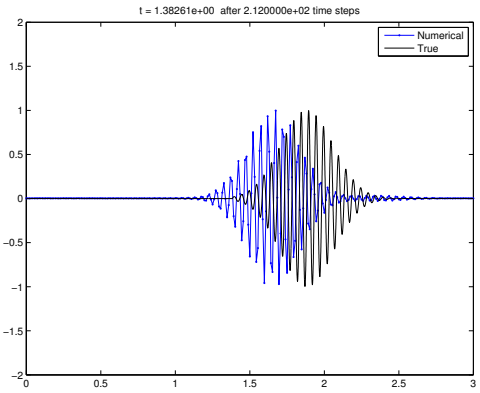

(a) Wave packet $\phi(t) = e^{-16(x-0.5)^2} \sin(125.7x)$

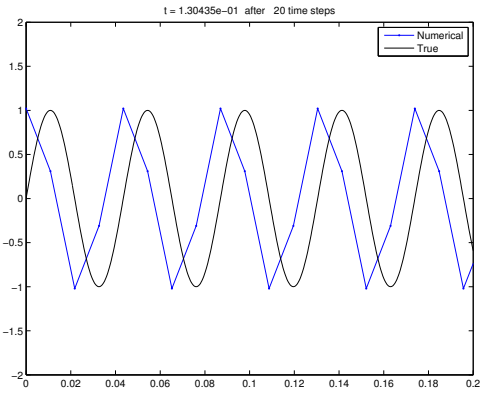

(b) Single wave $\phi(t) = \sin(72.2566x)$

Figure 2.3: True and numerical wave propagation computed by Leap-frog scheme, with $\gamma = 0.6$

accuracy conditions at the zero wavenumber, only lower order. Figure 2.5 shows several comparisons of schemes obtained by enforcing the exact dispersion relation at different wavenumbers (given by (2.12) in the next section). As seen from Figure 2.5, replacing order of accuracy with exact dispersion at non-zero wavenumbers decreases the numerical dispersion error uniformly.

2.2 General schemes for the wave equation- accuracy and stability analysis

From the previous section, we have concluded the following:

- Wider stencil in space decreases numerical dispersion error. (Figure 2.4)

- To increase dispersion accuracy on the whole interval $[0, \pi]$, we need dispersion reduction targeted schemes. (Figure 2.5)

Hence the design of our general scheme will follow these rules. We study a general (3,2M+1) stencil, with two steps in time and $2M + 1$ grid points in space (see Figure2.6). The $\{c_m\}$'s

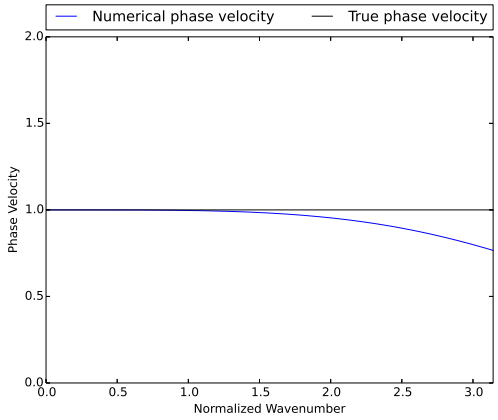

(a) $M = 2$, max error=0.23390380741442984

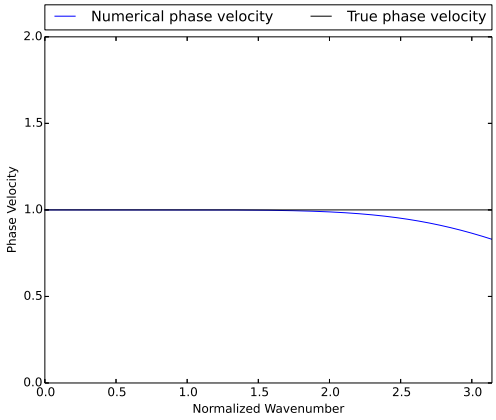

(b) $M = 4$, max error=0.16976836377423321

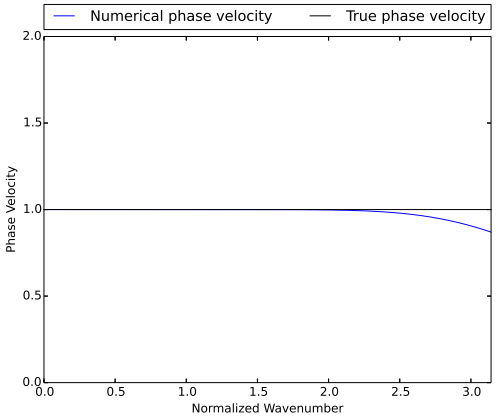

(c) $M = 7$, max error=0.13018373811829442

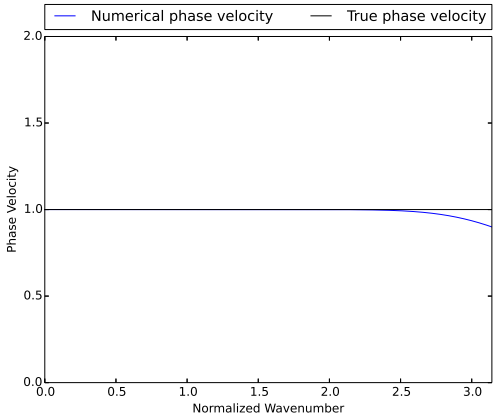

(d) $M = 12$, max error=0.10042897825001129

Figure 2.4: Comparison of numerical phase velocity for different stencil widths M, $\gamma = 0.6$. As M gets bigger, the overall dispersion error decreases. Schemes obtained from (2.11).

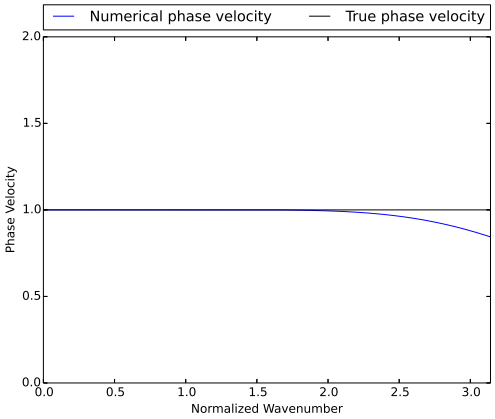

(a) $M = 4$, $\pi/2$, max error=0.15600852977771806

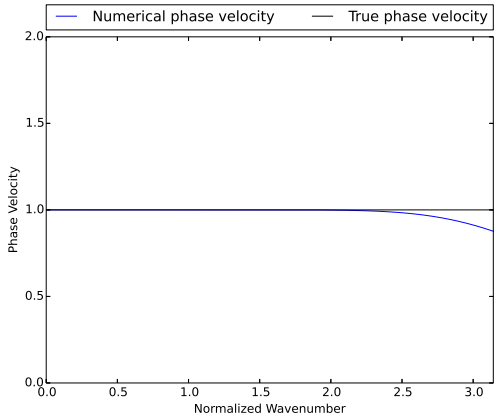

(b) $M = 7$, $\pi/2$, max error=0.12321155804448247

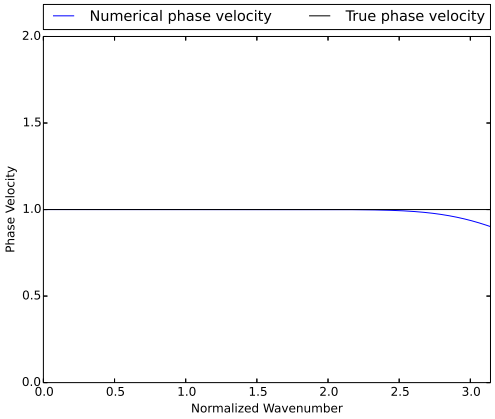

(c) $M = 12$, $\pi/2$, max error=0.098543775268695177

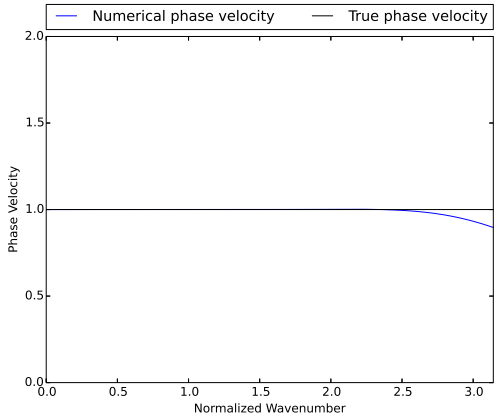

(d) $M = 12$, $.75\pi$, max error=0.10366091159125002

Figure 2.5: Comparison of numerical phase velocity for different stencil width M and exact dispersion relation at different wavenumbers, $\gamma = 0.6$.

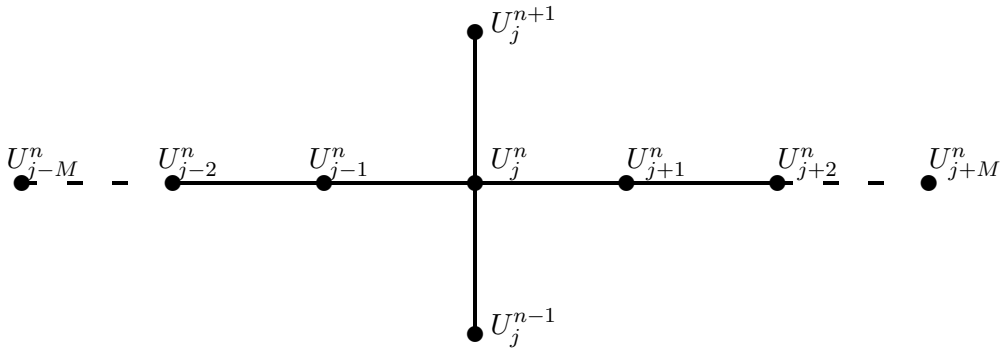

Figure 2.6: Stencil for general scheme

denote coefficients to be determined in the schemes, and the general difference equation is:

$$U_j^{n+1} + U_j^{n-1} + \sum_{m=0}^{M} c_m (U_{j+m}^n + U_{j-m}^n) \approx 0. \tag{2.7}$$

As mentioned in Example 1.2.1, it is natural to assign equal weight for symmetric grid points.

For the rest of this section, we will discuss accuracy and stability analysis for the stencil shown in Figure 2.6. This analysis will get us ready for scheme design in the next section.

2.2.1 Accuracy analysis of the general scheme

We compute explicitly the accuracy conditions at the zero wavenumber. We will use the fact that the true solution satisfies the wave equation and is infinitely differentiable (that is, given smooth initial conditions). U_{j+m}^{n+l} still approximates the true solution u at the point $(x + m\Delta x, t + l\Delta t)$. Due to the symmetry of the stencil, odd order terms can be canceled out and we can get second order accuracy in time (and $2M$-th order accuracy in space). From the differential equation $(\frac{\partial^2}{\partial x^2} - \frac{1}{c^2}\frac{\partial^2}{\partial t^2})u = 0$, by differentiating with respect to time and space we get that for even orders $(2n)$ of derivatives, $\frac{\partial^{2n}}{\partial x^{2n}}u = \frac{1}{c^{2n}}\frac{\partial^{2n}}{\partial t^{2n}}u$. This allows us to compute the $2n$-th time derivative with the $2n$-th space derivative. With the wider spatial stencil (thus higher spatial order of accuracy) and Lax-Wendroff analysis, we can obtain higher temporal accuracy despite only having three grid points in time. Write the

Taylor expansion at (x,t) to get the local truncation error:

$$LTE = u(x,t+\Delta t) + u(x,t-\Delta t) + \sum_{m=0}^{M} c_m \left(u(x+m\Delta x,t) + u(x-m\Delta x,t)\right) \tag{2.8}$$

$$= \left(u(x,t) + \Delta t\frac{\partial}{\partial t}u + (\Delta t)^2\frac{\partial^2}{2!\partial t^2}u + \dots\right) + \left(u(x,t) - \Delta t\frac{\partial}{\partial t}u + (\Delta t)^2\frac{\partial^2}{2!\partial t^2}u - \dots\right)$$

$$+ 2c_0u(x,t) + \sum_{m=1}^{M} c_m\left(2u(x,t) + 2(m\Delta x)^2\frac{\partial^2}{2!\partial x^2}u + 2(m\Delta x)^4\frac{\partial^4}{4!\partial x^4}u + \dots\right)$$

$$= 2u(x,t) + 2(\Delta t)^2\frac{\partial^2}{2!\partial t^2}u + 2(\Delta t)^4\frac{\partial^4}{4!\partial t^4}u + \dots$$

$$+ 2c_0u(x,t) + \sum_{m=1}^{M} c_m\left(2u(x,t) + 2(m\Delta x)^2\frac{\partial^2}{2!\partial x^2}u + 2(m\Delta x)^4\frac{\partial^4}{4!\partial x^4}u + \dots\right)$$

(replace the time derivative with space derivative)

$$= 2u(x,t) + 2(c\Delta t)^2\frac{\partial^2}{2!\partial x^2}u + 2(c\Delta t)^4\frac{\partial^4}{4!\partial x^4}u + \dots$$

$$+ 2c_0u(x,t) + \sum_{m=1}^{M} c_m\left(2u(x,t) + 2(m\Delta x)^2\frac{\partial^2}{2!\partial x^2}u + 2(m\Delta x)^4\frac{\partial^4}{4!\partial x^4}u + \dots\right)$$

$$= \left(2 + 2c_0 + \sum_{m=1}^{M} 2c_m\right)u(x,t) + \left(2(c\Delta t)^2 + \sum_{m=1}^{M} 2c_m(m\Delta x)^2\right)\frac{\partial^2}{2!\partial x^2}u$$

$$+ \left(2(c\Delta t)^4 + \sum_{m=1}^{M} 2c_m(m\Delta x)^4\right)\frac{\partial^4}{4!\partial x^4}u + \dots \tag{2.9}$$

Make the lowest $l+1$ terms vanish to get:

$$1 + \sum_{m=0}^{M} c_m = 0, \tag{2.10}$$

$$(\gamma^2)^j + \sum_{m=1}^{M} c_m(m^2)^j = 0, \qquad j = 1,\dots,l, \tag{2.11}$$

where we replace $\gamma = \dfrac{c\Delta t}{\Delta x}$.

These conditions are the building blocks of our schemes, and guarantee $2l$-order accuracy in both time and space (with consistency given by the first equation), which is the highest possible order of accuracy with $l+1$ restrictions.

We derive the numerical dispersion relation for (2.7) by the Fourier transform:

$$\cos(\Omega) + \sum_{m=0}^{M} c_m \cos(mK) \approx 0 \tag{2.12}$$

We compute the Taylor expansion at $\Omega = 0$ and $K = 0$:

$$\begin{aligned}
\epsilon &= \cos(\Omega) + \sum_{m=0}^{M} c_m \cos(mK) \\
&= \sum_{j=0}^{\infty} \frac{(-1)^j}{(2j)!}\Omega^{2j} + \sum_{m=0}^{M} c_m \left(\sum_{j=0}^{\infty} \frac{(-1)^j}{(2j)!}(mK)^{2j} \right) \\
&= \sum_{j=0}^{\infty} \frac{(-1)^j}{(2j)!} \left[\Omega^{2j} + \sum_{m=0}^{M} c_m (mK)^{2j} \right].
\end{aligned} \tag{2.13}$$

Making the first $l+1$ terms in the infinite series vanish gives error of size $O(\Omega^{2l+2}, K^{2l+2})$, equivalent to the previous accuracy conditions obtained for the general scheme.

Take $l = M$ to get $M + 1$ equations for the $M + 1$ unknown coefficients:

$$\begin{pmatrix} 1 & 1 & \dots & 1 \\ 0 & 1^2 & \dots & M^2 \\ \vdots & \vdots & \vdots & \vdots \\ 0 & 1^{2M} & \dots & M^{2M} \end{pmatrix} \begin{pmatrix} c_0 \\ c_1 \\ \vdots \\ c_M \end{pmatrix} = \begin{pmatrix} -1 \\ -\gamma^2 \\ \vdots \\ -\gamma^{2M} \end{pmatrix}. \tag{2.14}$$

In this case, the coefficient matrix is a Vandermonde matrix, and there is a unique solution to the system. Liu and Sen gave the explicit solution in their work in 2009:

$$c_m = \frac{-\gamma^2 \prod_{1 \le n < m} (\gamma^2 - n^2) \prod_{m < n \le M} (n^2 - \gamma^2)}{m^2 \prod_{1 \le n \le m} (m^2 - n^2) \prod_{m < n \le M} (n^2 - m^2)}. \tag{2.15}$$

2.2.2 Stability analysis for the stencil

Since we are studying the constant coefficient, linear case with periodic boundary conditions, we can apply the von Neumann analysis to discuss stability of the FD schemes. Set $U_j^n = g^n(\xi) e^{ij\xi\Delta x}$ plug into (2.7) to obtain the amplification polynomial

$$g^2 + 2g \sum_{m=0}^{M} c_m \cos(m\xi\Delta x) + 1 = 0. \tag{2.16}$$

Denote $z = \sum_{m=0}^{M} c_m \cos(m\xi\Delta x)$. Then the boundary of stability region can be found by plotting $z = -\dfrac{g^2+1}{2g}$, where we plug in $g = e^{i\theta}$ and we let θ vary between $[0, 2\pi]$. Any

value of z in the region guarantees that $|g| \leq 1$. As we can see on Figure 2.7, the stability condition is $|z| \leq 1$. Note the same region works for higher dimension schemes with similar amplification polynomial $g^2 + 2zg + 1 = 0$.

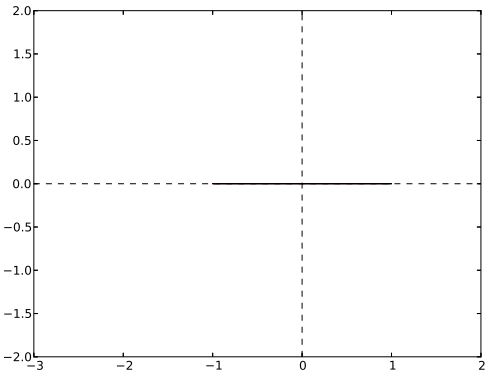

Figure 2.7: Stability region for amplification polynomial $g^2 + 2zg + 1 = 0$: $|z| \leq 1$

2.3 Schemes to reduce numerical dispersion error: interpolation

So far we have presented schemes obtained by enforcing traditional order of accuracy conditions at (x, t) (corresponding to the grid point at j-th grid point and n-th time step). Since these conditions are equivalent to the accuracy of the dispersion relation at the zero wavenumber, schemes obtained this way guarantee small dispersion error for small wavenumbers. As seen in Figure 2.4, such schemes do not guarantee small dispersion error at high wavenumbers. It is of our interest to sacrifice some accuracy at zero wavenumber to obtain schemes with reduced dispersion error at wavenumbers closer to the Nyquist wavenumber $K_{Nyquist} = \pi$.

Such schemes can be obtained using several methods. As shown in Figure 2.5, enforcing exact phase velocity at some preset wavenumber K_0 away from zero reduces dispersion error near K_0 (Finkelstein and Kastner (2007, 2008)). We obtain the *zero-th order derivative accuracy* of dispersion relation at wavenumber K_0. Similarly, we can force further exact first order derivative, second order derivative, etc. Enforcing exact first-order derivative

accuracy naturally gives exact group velocity, so we will also discuss this case. Another approach takes the uniform norm as measurement of error, and we apply a Remez algorithm to generate new schemes that minimize numerical dispersion error for all wavenumbers up to some maximum wavenumber $K_{max} <$ Nyquist wavenumber. We will discuss the these methods in detail in the next three subsections.

2.3.1 Interpolation of phase velocity

Proposed by Finkelstein and Kastner (2007,2008), the first method we will discuss decreases numerical dispersion error for large wavenumbers by forcing exact dispersion at preset nonzero wavenumbers. In equation (2.11), take l strictly less than M, so the system has $M - l$ degrees of freedom. We choose $M - l$ distinct nonzero wave numbers $\{K_j\}_{j=l+1}^{M}$, and plug the true dispersion relation $\Omega_j = \gamma K_j$ for wavenumbers $K_{l+1}, \ldots, K_M$ into equation(2.12). This guarantees exact numerical dispersion at those wavenumbers. The system we obtain is:

$$\begin{aligned} 1 + \sum_{m=0}^{M} c_m &= 0, \\ (\gamma^2)^j + \sum_{m=1}^{M} c_m (m^2)^j &= 0, \qquad j = 1, \ldots, l, \\ \cos(\gamma K_j) + \sum_{m=0}^{M} c_m \cos(m K_j) &= 0, \qquad j = l+1, \ldots, M. \end{aligned} \tag{2.17}$$

The number l can be changed to adjust the number of accuracy conditions at the zero wavenumber. We can rewrite the equations into the system:

$$\begin{pmatrix} 1 & 1 & \ldots & 1 \\ 0 & 1^2 & \ldots & M^2 \\ \vdots & \vdots & \vdots & \vdots \\ 0 & 1^{2l} & \ldots & M^{2l} \\ 1 & \cos(K_{l+1}) & \ldots & \cos(MK_{l+1}) \\ \vdots & \vdots & \vdots & \vdots \\ 1 & \cos(K_M) & \ldots & \cos(MK_M) \end{pmatrix} \begin{pmatrix} c_0 \\ c_1 \\ \vdots \\ c_l \\ c_{l+1} \\ \vdots \\ c_M \end{pmatrix} = \begin{pmatrix} -1 \\ -\gamma^2 \\ \vdots \\ -\gamma^{2l} \\ -\cos(\gamma K_{l+1}) \\ \vdots \\ -\cos(\gamma K_M) \end{pmatrix}. \tag{2.18}$$

To obtain schemes with order of accuracy $2l$ and exact dispersion relation at wavenumbers $\{K_j\}_{j=l+1}^{M}$, we solve the above system for $\{c_m\}_{m=0}^{M}$. Denote the coefficient matrix of the above system by $C(M, l+1)$. Then the following theorem guarantees the existence and uniqueness of such schemes:

Theorem 2.3.1. *The above system* (2.18) *has a unique solution for any choice of distinct* $\{K_j\}_{j=l+1}^{M} \subset (0, \pi]$. *Moreover, the determinant of the coefficient matrix is*

$$|C(M, l+1)| = 2^1 \cdots 2^M \left(\prod_{n=l+1}^{M} (\cos(K_n) - 1) \right)^{l+1} \prod_{l+1 \le m < n \le M} (\cos(K_n) - \cos(K_m)) .$$

Note: The theorem also implies that any r rows ($r \le M+1$) in the coefficient matrix are mutually linearly independent. We will use this fact later to justify the possibility of uniform approximation.

Remark: This way of reducing dispersion error can guarantee exact dispersion for a preset wavenumber, and dispersion errors will be reduced near those preset wavenumbers. However, the wavenumbers we choose influence the accuracy, as seen in Figure 2.5d and Figure 2.5c. This method works well for signals composed of a single wavenumber.

As shown in Figures 2.5 and 2.4, by enforcing exact dispersion at non-zero wavenumbers, dispersion errors decrease for stencils of the same width. Moreover, as seen in Figure 2.8, narrower stencils can give similar error as wider stencils with no exact dispersion conditions.

2.3.1.1 Proof of Theorem 2.3.1

Here we compute the determinant of the coefficient matrix in system 2.17. We show that as long as the wavenumbers K_j are distinct, the determinant is non zero. Moreover, we give an explicit expression of the determinant. The proof is done by induction on l.

We would like to compute the determinant of the following matrix, as noted in Theorem

2.3.1:

$$C(M,l+1)=\begin{pmatrix}1 & 1 & 1 & \cdots & 1 & 1\\ 0 & 1 & 2^2 & \cdots & (M-1)^2 & M^2\\ \vdots & \vdots & \vdots & \vdots & \vdots & \vdots\\ 0 & 1^{2l} & 2^{2l} & \cdots & (M-1)^{2l} & M^{2l}\\ 1 & \cos(K_{l+1}) & \cos(2K_{l+1}) & \cdots & \cos((M-1)K_{l+1}) & \cos(MK_{l+1})\\ 1 & \cos(K_{l+2}) & \cos(2K_{l+2}) & \cdots & \cos((M-1)K_{l+2}) & \cos(MK_{l+2})\\ \vdots & \vdots & \vdots & \vdots & \vdots & \vdots\\ 1 & \cos(K_M) & \cos(2K_M) & \cdots & \cos((M-1)K_M) & \cos(MK_M)\end{pmatrix} \tag{2.19}$$

Case for $l+1=0$

If $l+1=0$, we have a full trigonometric matrix:

$$C(M,0)=\begin{pmatrix}1 & \cos(K_0) & \cos(2K_0) & \cdots & \cos((M-1)K_0) & \cos(MK_0)\\ \vdots & \vdots & \vdots & \vdots & \vdots & \vdots\\ 1 & \cos(K_M) & \cos(2K_M) & \cdots & \cos((M-1)K_M) & \cos(MK_M)\end{pmatrix}. \tag{2.20}$$

All $\{K_j\}_{j=0}^{M}$ are distinct variables in $[0,\pi]$.

With the identity

$$\cos((m+1)K)=2\cos(K)\cos(mK)-\cos((m-1)K) \tag{2.21}$$

$|C(M,0)|$ in (2.20) can be transformed into

$$|C(M,0)|=\begin{vmatrix}1 & \cos(K_0) & 2\cos^2(K_0) & \cdots & 2^{M-2}\cos^{M-1}(K_0) & 2^{M-1}\cos^{M}(K_0)\\ \vdots & \vdots & \vdots & \vdots & \vdots & \vdots\\ 1 & \cos(K_M) & 2\cos^2(K_M) & \cdots & 2^{M-2}\cos^{M-1}(K_M) & 2^{M-1}\cos^{M}(K_M)\end{vmatrix}.$$

This is the determinant of a Vandermonde matrix:

$$\begin{aligned}|C(M,0)| &= 2^0\cdot 2^1\cdot\ldots\cdot 2^{M-1}\begin{vmatrix}1 & \cos(K_0) & \cdots & \cos^{M-1}(K_0) & \cos^{M}(K_0)\\ \vdots & \vdots & \vdots & \vdots & \vdots\\ 1 & \cos(K_M) & \cdots & \cos^{M-1}(K_M) & \cos^{M}(K_M)\end{vmatrix}\\ &= 2^0\cdot 2^1\cdot\ldots\cdot 2^{M-1}\prod_{0\le m<n\le M}(\cos(K_n)-\cos(K_m)).\end{aligned} \tag{2.22}$$

This concludes the case for $l+1=0$.

Case for $l+1=1$

For $l+1=1$, we compute $|C(M,1)|$ by computing the zero-th derivative of $|C(M,0)|$ in (2.22) with respect to K_0, and evaluate the result at $K_0=0$:

$$|C(M,1)| = \begin{vmatrix} 1 & 1 & 1 & \cdots & 1 & 1 \\ 1 & \cos(K_1) & \cos(2K_1) & \cdots & \cos((M-1)K_1) & \cos(MK_1) \\ \vdots & \vdots & \vdots & \vdots & \vdots & \vdots \\ 1 & \cos(K_M) & \cos(2K_M) & \cdots & \cos((M-1)K_M) & \cos(MK_M) \end{vmatrix}$$
$$= 2^0 \cdot 2^1 \cdot \cdots \cdot 2^{M-1} \prod_{1\le m<n\le M} (\cos(K_n)-\cos(K_m)) \cdot \prod_{1\le n\le M} (\cos(K_n)-1). \quad (2.23)$$

Case for $l+1=2$

For $l+1=2$, we show that $|C(M,2)|$ is computed by taking $K_0, K_1 \to 0$ in $\dfrac{\partial^2 |C(M,1)|}{\partial K_1^2}$. Recall

Lemma 2.3.2 (Cramer's rule)**.** *Let A be an $n\times n$ matrix. Denote its (i,j)-th entry as a_{ij}, with cofactor A_{ij}. The determinant of A can be computed by cofactor expansion along any i-th row or j-th column:*

$$|A| = a_{i1}A_{i1} + a_{i2}A_{i2} + \cdots + a_{in}A_{in} \quad (2.24)$$
$$= a_{1j}A_{1j} + a_{2j}A_{2j} + \cdots + a_{nj}A_{nj} \quad (2.25)$$

where $A_{ij} = (-1)^{i+j}M_{ij}$, M_{ij} the determinant of the (i,j)-th minor of A.

In equation (2.23) do cofactor expansion for $|C(M,1)|$ along the second row. Denote the (i,j)-th cofactor as C_{ij}.

$$|C(M,1)| = 1\cdot C_{21} + \cos(K_1)\cdot C_{22} + \cdots + \cos(MK_1)C_{2,M+1}, \quad (2.26)$$

where

$C_{2j} = (-1)^{2+j}$.

$$\begin{vmatrix} 1 & 1 & \cdots & 1 & 1 & 1 & 1 \\ 1 & \cos(K_2) & \cdots & \cos((j-1)K_2) & \cos((j+1)K_2) & \cos(M-1)K_2) & \cos(MK_2) \\ \vdots & \vdots & \vdots & \vdots & \vdots & & \\ 1 & \cos(K_M) & \cdots & \cos((j-1)K_M) & \cos((j+1)K_M) & \cos(M-1)K_M) & \cos(MK_M) \end{vmatrix}$$

is a function independent of K_1. Differentiate twice with respect to K_1 in equation (2.26) to get

$$\frac{\partial^2 |C(M,1)|}{\partial K_1^2} = 0 \cdot C_{21} + (-1)\cos(K_1) \cdot C_{22} + \cdots + (-1)M^2 \cos(MK_1) C_{2,M+1} \tag{2.27}$$

which is $-|C(M,2)|$ in (2.19).

To compute the explicit expression of $|C(M,2)|$, we differentiate (2.23) twice with respect to K_1. We first take out all the terms with $\cos(K_1)$.

$$\begin{aligned} |C(M,1)| &= 2^0 \cdot 2^1 \cdot \cdots \cdot 2^{M-1} \prod_{1 \le m < n \le M} (\cos(K_n) - \cos(K_m)) \prod_{1 \le n \le M} (\cos(K_n) - 1)) \\ &= 2^0 \cdot 2^1 \cdot \cdots \cdot 2^{M-1} \prod_{1 \le n \le M} (\cos(K_n) - 1) \prod_{2 \le n \le M} (\cos(K_n) - \cos(K_1)) \cdot \\ &\quad \prod_{2 \le m < n \le M} (\cos(K_n) - \cos(K_m)) \\ &= \left[-2^0 \cdot 2^1 \cdot \cdots \cdot 2^{M-1} \prod_{2 \le n \le M} (\cos(K_n) - 1) \prod_{2 \le m < n \le M} (\cos(K_n) - \cos(K_m)) \right] \cdot \\ &\quad \prod_{0 \le n \le M, n \ne 1} (\cos(K_n) - \cos(K_1)). \end{aligned} \tag{2.28}$$

Now when we differentiate above equation with respect to K_1, we only need to differentiate the last term. By the product rule,

$$\frac{\partial}{\partial K_1} \left(\prod_{0 \le n \le M, n \ne 1} (\cos(K_n) - \cos(K_1)) \right) \tag{2.29}$$

$$= \sin(K_1) \left(\prod_{\substack{0 \le n \le M \\ n \ne 1,0}} (\cos(K_n) - \cos(K_1)) + \cdots + \prod_{0 \le n \le M, n \ne 1, M} (\cos(K_n) - \cos(K_1)) \right).$$

Now we take the second derivative. Notice that we will evaluate both K_0 and K_1 at zero, so all the terms multiplied with $\sin(K_1)$ or $\cos(K_0) - \cos(K_1)$ will vanish.

$$\begin{aligned}
&\frac{\partial}{\partial K_1}\left[\sin(K_1)\left(\prod_{0\le n\le M, n\neq 1,0}(\cos(K_n)-\cos(K_1)) + \cdots + \prod_{0\le n\le M, n\neq 1, M}(\cos(K_n)-\cos(K_1))\right)\right] \\
&= \cos(K_1)\left(\prod_{0\le n\le M, n\neq 1,0}(\cos(K_n)-\cos(K_1)) + \cdots + \prod_{0\le n\le M, n\neq 1, M}(\cos(K_n)-\cos(K_1))\right) \\
&+ \sin(K_1)\frac{\partial}{\partial K_1}\left(\prod_{0\le n\le M, n\neq 1,0}(\cos(K_n)-\cos(K_1)) + \cdots + \prod_{0\le n\le M, n\neq 1, M}(\cos(K_n)-\cos(K_1))\right).
\end{aligned} \tag{2.30}$$

Evaluating $\dfrac{\partial^2 |C(M,1)|}{\partial K_1^2}$ with the above computation at $K_0 = K_1 = 0$, we get

$$|C(M,2)| = 2^0 \cdot 2^1 \cdot \cdots \cdot 2^{M-1}\left(\prod_{2\le n\le M}(\cos(K_n)-1)\right)^2 \prod_{2\le m<n\le M}(\cos(K_n)-\cos(K_m)). \tag{2.31}$$

This concludes the case for $l+1 = 2$.

Case for general $l+1$

Now we will prove Theorem 2.3.1 by induction.

Proof. We have proved the case for $l+1 = 0, 1, 2$. We will do induction on l. Suppose result holds for $l+1 = p$, i.e.

$$|C(M,p)| = 2^0 \cdot 2^1 \cdots 2^{M-1}\left(\prod_{n=p}^{M}(\cos(K_n)-1)\right)^p \prod_{p\le m<n\le M}(\cos(K_n)-\cos(K_m)). \tag{2.32}$$

To compute $|C(M,p+1)|$, we take the $2p$-th derivative of $|C(M,p)|$ with respect to K_p and

evaluate the result at $K_p = \cdots = K_0 = 0$.

$$\frac{\partial^{2p}|C(M,p)|}{\partial K_p^{2p}} = 2^0 \cdot 2^1 \cdots 2^{M-1} \frac{\partial^{2p}}{\partial K_p^{2p}} \left[\left(\prod_{n=p}^{M} (\cos(K_n) - 1) \right)^p \prod_{p \le m < n \le M} (\cos(K_n) - \cos(K_m)) \right] \tag{2.33}$$

$$= 2^0 \cdot 2^1 \cdots 2^{M-1} \left(\prod_{n=p+1}^{M} (\cos(K_n) - 1) \right)^p \prod_{p+1 \le m < n \le M} (\cos(K_n) - \cos(K_m)) \tag{2.34}$$

$$\cdot \frac{\partial^{2p}}{\partial K_p^{2p}} \left[(\cos(K_p) - 1))^p \prod_{p+1 \le n \le M} (\cos(K_n) - \cos(K_p)) \right]. \tag{2.35}$$

With $K_p = \cdots = K_0 = 0$, the left hand side is $(-1)^p |C(M, p+1)|$ from Cramer's rule. We compute the right hand side. Write

$$f_m(K_p) = \cos(K_p) - 1$$

for $m = 1, \ldots, p$ and

$$f_{p+1}(K_p) = \prod_{p+1 \le n \le M} (\cos(K_n) - \cos(K_p)).$$

By the product rule,

$$\frac{\partial^{2p}}{\partial K_p^{2p}} \left[(\cos(K_p) - 1))^p \prod_{p+1 \le n \le M} (\cos(K_n) - \cos(K_p)) \right] \tag{2.36}$$

$$= \sum_{q_1 + q_2 + \cdots + q_{p+1} = 2p} \binom{2p}{q_1, q_2, \ldots, q_{p+1}} \prod_{1 \le m \le p+1} f_m^{(q_m)}. \tag{2.37}$$

1. As long as one of the $q_1, \ldots, q_p$ is odd, evaluation of $f_m^{(q_m)}$ at $K_p = 0$ will vanish.

2. If all $q_1, \ldots, q_p$ are even, but $q_1 + q_2 + \cdots + q_p < 2p$, then at least one of the $\cos(K_p) - 1$ factors remains, evaluation of $\cos(K_p) - 1$ at $K_p = 0$ will vanish.

Therefore, the only remaining term is

$$(-1)^p \prod_{p+1 \le n \le M} (\cos(K_n) - \cos(K_p)), \tag{2.38}$$

and

$$\frac{\partial^{2p}|C(M,p)|}{\partial K_p^{2p}} \tag{2.39}$$

$$= 2^0 \cdot 2^1 \cdots 2^{M-1} \left(\prod_{n=p+1}^{M} (\cos(K_n) - 1) \right)^p \prod_{p+1 \le m < n \le M} (\cos(K_n) - \cos(K_m)) \tag{2.40}$$

$$\cdot (-1)^p \prod_{p+1 \le n \le M} (\cos(K_n) - \cos(K_p)) \tag{2.41}$$

$$= 2^0 \cdot 2^1 \cdots 2^{M-1} \left(\prod_{n=p+1}^{M} (\cos(K_n) - 1) \right)^{p+1} \prod_{p+1 \le m < n \le M} (\cos(K_n) - \cos(K_m)). \tag{2.42}$$

This concludes the general case.

□

Figure 2.8a shows the dispersion relation with exact phase velocity requirement at three wavenumbers. The maximum dispersion error for stencil width 5 is less than that of stencil width 7 as shown in Figure 2.4c. As shown in Figure 2.5d and Figure 2.8a, the stencil with width 5 here gives smaller dispersion error than stencil with 12 there, due to the enforcing of exact dispersion at higher wavenumber.

2.3.2 Interpolation of group velocity

In this subsection, we investigate higher order approximation to the dispersion curve. As stated in Chapter One, the energy of a wave packet propagates at the group velocity. In the acoustic case, the true group velocity is computed by differentiating the frequency:

$$c_g = \frac{d}{dk}\omega = \frac{d}{dk}(ck) = c \tag{2.43}$$

We see that in gas or fluid, energy propagates at the phase velocity. To find the numerical group velocity dispersion relation, we differentiate the numerical phase velocity dispersion relation (2.12) with respect to the normalized wavenumber:

$$\sin(\Omega)\frac{d\Omega}{dK} + \sum_{m=0}^{M} c_m \sin(mK)m \approx 0. \tag{2.44}$$

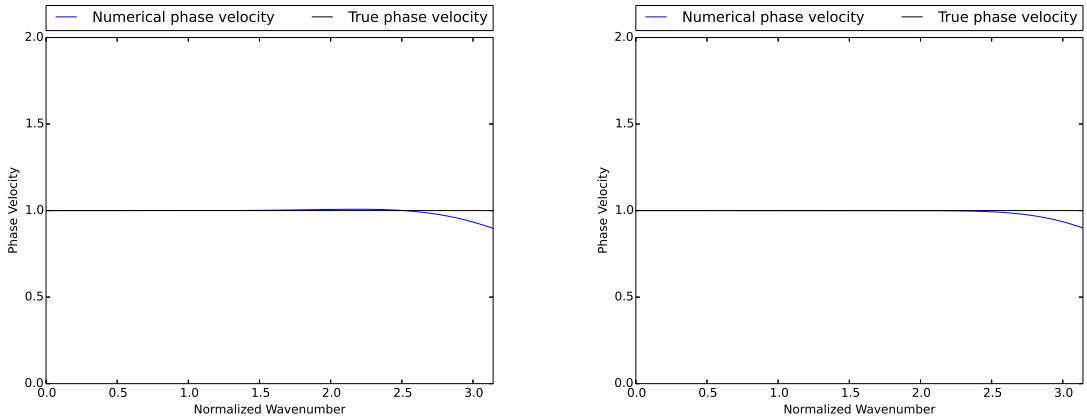

(a) Numerical phase velocity with $M = 5$, exact phase velocity at $K = [0.2\pi, 0.3\pi, 0.8\pi]$, $\gamma = 0.6$, max error=0.10269580347306029

(b) Numerical phase velocity with $M = 12$, only accuracy at zero wavenumber, $\gamma = 0.6$, max error=0.10038631249141738

Figure 2.8: Numerical phase velocities drawn with exact phase velocity for $M = 5$ and only accuracy condition with $M = 12$.

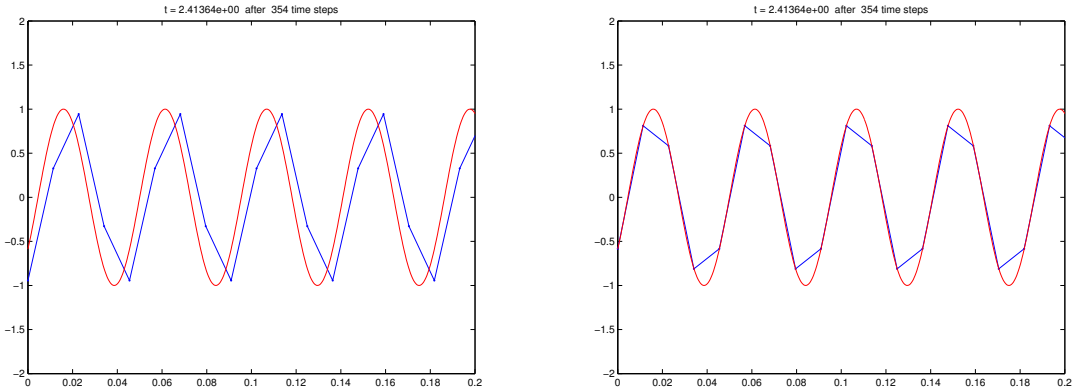

(a) Wave propagation computed with Figure 2.8a

(b) Wave propagation computed with Figure 2.8b

Figure 2.9: Wave propagation computed by schemes corresponding to Figure 2.8. Notice that enforcing exact dispersion reduces the max error, but the numerical waves might propagate faster than the true wave.

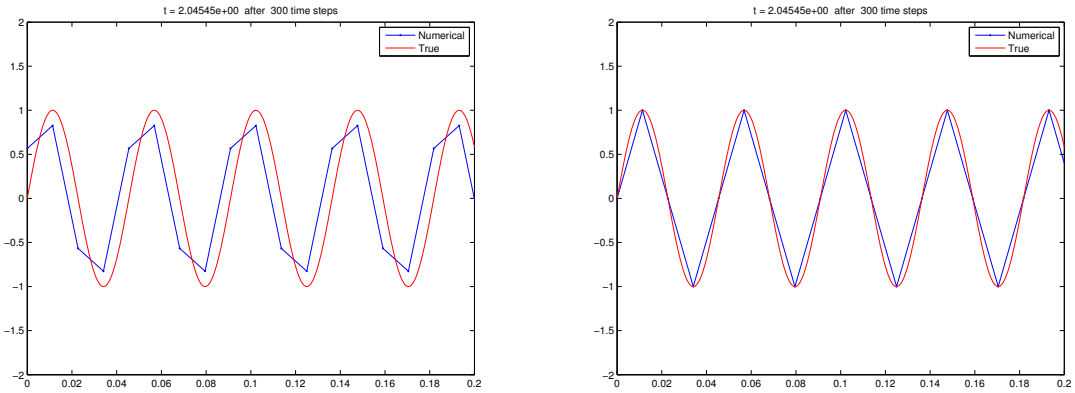

(a) Wave propagation computed with Figure 2.4b (b) Wave propagation computed with Figure 2.5a

Figure 2.10: Wave propagation computed by schemes corresponding to Figures 2.4b and 2.5a. Numerical wave lags 1/4 cycle after 300 time steps.

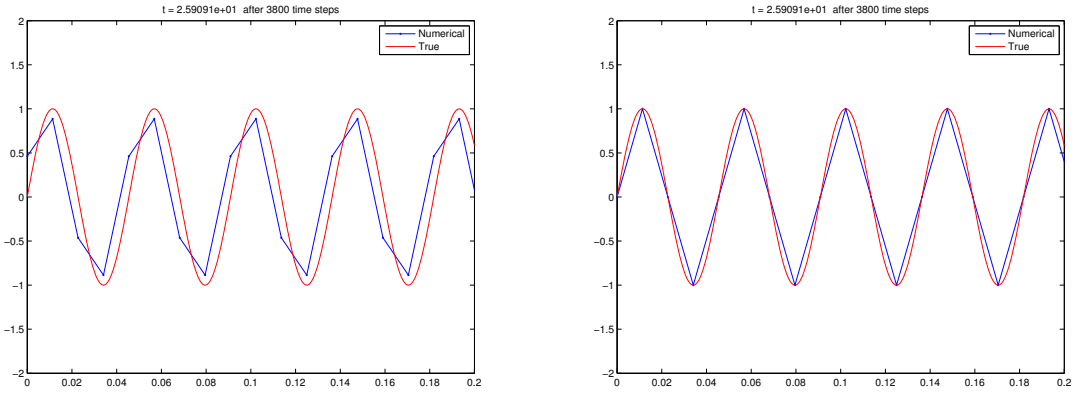

(a) Wave propagation computed with Figure 2.4c (b) Wave propagation computed with Figure 2.5b

Figure 2.11: Wave propagation computed by schemes corresponding to Figures 2.4c and 2.5b. Numerical wave lags 1/4 cycle after 3800 time steps.

To enforce exact group dispersion in the FD scheme, we plug in the true group dispersion corresponding to the scheme obtained from $\Omega = \gamma K$:

$$\frac{d}{dK}\Omega = \frac{d}{dK}(\gamma K) = \gamma. \tag{2.45}$$

Then we obtain exact numerical group velocity:

$$\sin(\Omega)\gamma + \sum_{m=0}^{M} c_m \sin(mK)m \approx 0. \tag{2.46}$$

Note that in above equation, only enforcing true group velocity does not eliminate the dependence on Ω, therefore we still use the true dispersion relation corresponding to the scheme, $\Omega = \gamma K$. This implies that when we enforce exact group velocity for the scheme, we automatically enforce exact phase velocity. In (2.17), replace exact phase velocity at K_M by exact group velocity at K_{M-1} to obtain the following system:

$$\begin{aligned}
1 + \sum_{m=0}^{M} c_m &= 0, \\
(\gamma^2)^j + \sum_{m=1}^{M} c_m (m^2)^j &= 0, \qquad j = 1, \ldots, l. \\
\cos(\gamma K_j) + \sum_{m=0}^{M} c_m \cos(mK_j) &= 0, \qquad j = l+1, \ldots, M-1 \\
\sin(\gamma K_{M-1})\gamma + \sum_{m=0}^{M} c_m \sin(mK_{M-1})m &= 0,
\end{aligned} \tag{2.47}$$

which can be rewritten as the system:

$$\begin{pmatrix}
1 & 1 & \ldots & 1 \\
0 & 1^2 & \ldots & M^2 \\
\vdots & \vdots & \vdots & \vdots \\
0 & 1^{2l} & \ldots & M^{2l} \\
1 & \cos(K_{l+1}) & \ldots & \cos(MK_{l+1}) \\
\vdots & \vdots & \vdots & \vdots \\
1 & \cos(K_{M-1}) & \ldots & \cos(MK_{M-1}) \\
0 & \sin(K_{M-1}) & \ldots & \sin(MK_{M-1})
\end{pmatrix}
\begin{pmatrix}
c_0 \\ c_1 \\ \vdots \\ c_l \\ c_{l+1} \\ \vdots \\ c_{M-1} \\ c_M
\end{pmatrix}
=
\begin{pmatrix}
-1 \\ -\gamma^2 \\ \vdots \\ -\gamma^{2l} \\ -\cos(\gamma K_{l+1}) \\ \vdots \\ -\cos(\gamma K_{M-1}) \\ -\sin(\gamma K_{M-1})
\end{pmatrix}. \tag{2.48}$$

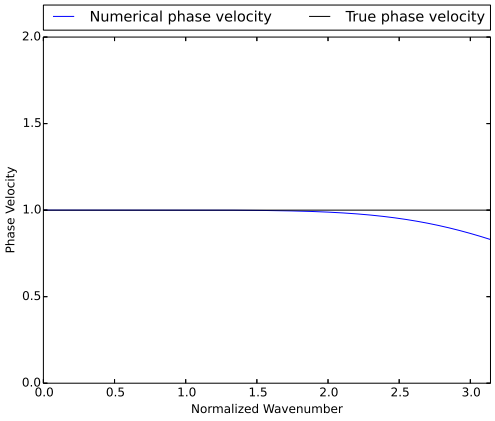

(a) M=4,only accuracy at zero wavenumber, max error=0.16976836377423321

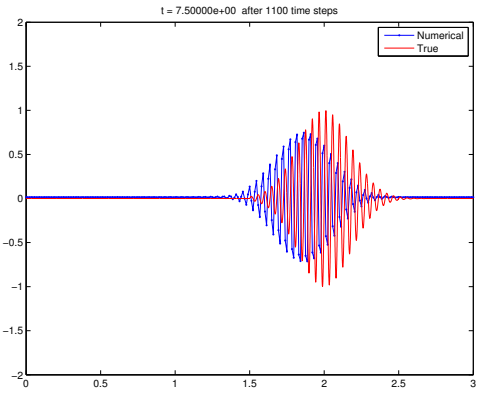

(b) Wave packet propagation: only accuracy at zero wavenumber, $M = 4$

Figure 2.12: Group dispersion curve and wave propagation drawn with schemes that gives accuracy at the zero wavenumber.

Such schemes exist, since the determinant of the coefficient matrix (denote as $C_g(M, l+1, 1)$) can be shown to be nonzero, by a proof similar to the proof of Theorem 2.3.1.

Theorem 2.3.3. *The above system* (2.48) *has a unique solution for any choice of* $\{K_j\}_{j=l+1}^{M-1}$ *distinct and nonzero. Moreover, the determinant of the coefficient matrix is*

$$|C_g(M, l+1, 1)| = 2^1 \cdots 2^M \sin(K_M) \left(\prod_{n=l+1}^{M} (\cos(K_n) - 1) \right)^{l+1} \cdot \left(\prod_{l+1 \le m < n \le M-1} (\cos(K_n) - \cos(K_m)) \right) \left(\prod_{l+1 \le m \le M-2} (\cos(K_M) - \cos(K_m)) \right).$$

where we take $K_M = K_{M-1}$.

Exact group velocities can be enforced at several distinct wavenumbers. Moreover, second order approximation can be achieved by differentiating. We differentiate $|C(M, l+1)|$ with respect to K_M and K_{M-1}, then let the two wavenumbers approach to K_{M-2}.

In general, we can prescribe any phase or group velocities at distinct wavenumbers.

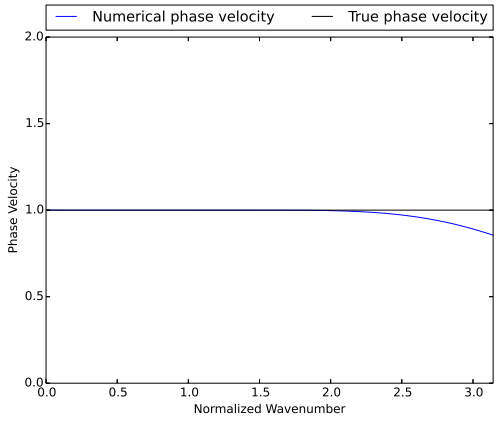

(a) M=4,exact phase and group velocity at 0.5π, max error=0.14467278814415996

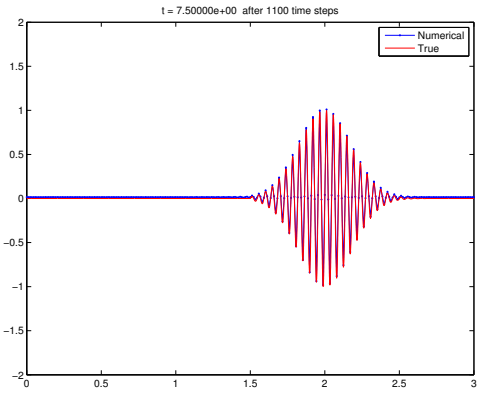

(b) Wave packet propagation: exact phase and group velocity at 0.5π

Figure 2.13: Group dispersion curve and wave propagation drawn with schemes that gives accuracy at the zero wavenumber and exact phase and group velocity at 0.5π.

2.4 Dispersion reduction scheme by minimax approximation

Since we are interested in reducing dispersion error for general wavenumbers, we consider reducing the L^∞ norm :

$$|| \cos(\Omega_{true}) - \cos(\Omega_{numerical})|| = \left|\left|\cos(\gamma K) + \sum_{m=0}^{M} c_m \cos(mK)\right|\right| \tag{2.49}$$

Write the following error function:

$$\epsilon(K) = \cos(\gamma K) + \sum_{m=0}^{M} \cos(mK). \tag{2.50}$$

Then we consider the following approximation problem:

Given the continuous function $f(K) = \cos(\gamma K)$, take a trigonometric polynomial of the form $p(K) = -\sum_{m=0}^{M} c_m \cos(mK)$, and we look for $\{c_m\}_{m=0}^{M}$ such that the following value is minimized:

$$\max_{K\in[0,\pi]} |f(K) - p(K)|. \tag{2.51}$$

Notice that the functions $\{\cos(mK)\}_{m=0}^{M}$ span a linear subspace of the continuous functions on $K \in [0, \pi]$. Hence we are looking for coefficients $\{c_m\}$'s such that the distance between f and the subspace spanned by $\{\cos(mK)\}_{m=0}^{M}$ is minimized.

Comparing with system (2.17), then we want the polynomial $p(K) = -\sum_{m=0}^{M} c_m \cos(mK)$ to satisfy the conditions

$$\begin{aligned} &p(0) = 1, \qquad j = 0 \\ &p^{(2j)}(0) = (-1)^j \gamma^{2j}, \qquad j = 1, \ldots, l \\ &p(K_j) = \cos(\gamma K_j), \qquad j = l+1, \ldots, M. \end{aligned} \tag{2.52}$$

Remark: For exact group dispersion at K_j, the condition is $p^{(1)}(K_j) = \sin(\gamma K)\gamma$.

The question transforms into an optimization problem with above restrictions on c_m. Take the number of restrictions strictly less than $M + 1$, and we solve the optimization problem with restraints.

Consider the space corresponding to the above restraints:

$$\begin{aligned} &P = \{p | p \in span\{\cos(mK)\}_{m=0}^{M}, K \in [0, \pi], \\ &p^{(2j)}(0) = (-1)^j \gamma^{2j},\ j = 0 \ldots, l, p(K_m) = \cos(\gamma K_m), m = 1, \ldots n\} \end{aligned} \tag{2.53}$$

with associated null space

$$\begin{aligned} &P_0 = \{p | p \in span\{\cos(mK)\}_{m=0}^{M}, K \in [0, \pi], \\ &p^{(2j)}(0) = 0,\ j = 0 \ldots, l, p(K_m) = 0, m = 1, \ldots n\}. \end{aligned} \tag{2.54}$$

The following theorem about P extends the famous Kolmogorov Theorem (Lorenz, 1966):

Theorem 2.4.1. *Let $f \in \mathcal{C}[0, \pi]$ and $p \in P$ given. Then p is a best approximation to f from P if and only if for each $p_0 \in P_0$*

$$\max_{K \in A} [f(K) - p(K)] p_0(K) \geq 0$$

where $A = A(f, p) = \{K \big| |f(K) - p(K)| = ||f - p||_\infty\}$

The proof of Theorem 2.4.1 is essentially identical to the proof of the Kolmogorov Theorem.

Proof. Take $p \in P$ to be a best approximation to f, let $E = ||f - p||$. Assume there exists a $p_0 \in P_0$ such that $\max_{K \in A}[f(K) - p(K)]p_0(K) = -2\epsilon$ for some ϵ positive. By the continuity of the functions, there is an open subset G of $[0, \pi]$, such that $A \subset G$ and for all $K \in G$,

$$[f(K) - p(K)]p_0(K) < -\epsilon$$

Take $p_1 = p - cp_0 \in P$, where $c > 0$ is small. Let M denote the maximum of $|p_0|$ on $[0, \pi]$.

If $K \in G$:

$$\begin{aligned}
&(f(K) - p_1(K))^2 \\
=&(f(K) - p(K) + cp_0(K))^2 \\
=&(f(K) - p(K))^2 + 2c(f(K) - p(K))p_0(K) + c^2 p_0^2(K) \\
<&E^2 - 2c\epsilon + c^2 M^2.
\end{aligned}$$

Taking $c < M^{-2}\epsilon$, then $c^2 M^2 < c\epsilon$ and we get

$$(f(K) - p_1(K))^2 < E^2 - c\epsilon,$$

contradicting with p being the best approximation.

If $K \notin G$, then by the definition of G, $|f(K) - p(K)| < E$. Since $F = G^c$ is a closed set in $[0, \pi]$, there is some $\delta > 0$, such that $|f(K) - p(K)| \leq E - \delta$, for all $K \in F$. If we take c small enough that $c < (2M)^{-1}\delta$, we would have

$$|f(K) - p_1(K)| \leq |f(K) - p(K)| + c|p_0(K)| \leq E - \delta + \frac{1}{2}\delta = E - \frac{1}{2}\delta.$$

Hence p_1 approximates f better than p_0, which is a contradiction. This shows the necessity.

Now we show sufficiency. If for the given $p \in P$, the inequality holds for all $p_0 \in P_0$, in particular, it holds for $p_0 = p - p_1$, where $p_1 \in P$ is arbitrary. Then there is a point $K_0 \in A$

such that:

$$\begin{aligned}
&(f(K_0) - p_1(K_0))^2 \\
=&(f(K_0) - p(K_0) + cp_0(K_0))^2 \\
=&(f(K_0) - p(K_0))^2 + 2c(f(K_0) - p(K_0))p_0(K_0) + c^2 p_0^2(K_0) \\
\geq&(f(K_0) - p(K_0))^2 = \epsilon^2
\end{aligned}$$

since $K_0 \in A$ (with ϵ as before). Hence p is the best approximation. □

We will use Theorem 2.4.1 to find a generalized alternating property, and obtain a Remez algorithm for computing the $\{c_m\}$'s. First we need to discuss *Haar spaces*.

Definition 2.4.2. Let A be an $(n+1)$ dimensional linear subspace of the continuous functions on $(0, \pi)$. If any non trivial function in A has at most n zeros, we call A a *Haar space* of dimension $n+1$.

In the next few subsections, we will study the null spaces as in (2.54) and use it to develop algorithms that guarantee the best minimax approximation.

2.4.1 Only keep accuracy conditions at the zero wavenumber

To begin with, we will keep the $l+1$ restraints of the derivative conditions at the zero wavenumber and leave the other $M-l$ conditions free for the L^∞ approximation. Here we are looking for a minimax approximation to f from the space

$$P = \{p | p \in span\{\cos(mK)\}_{m=0}^{M}, K \in [0, \pi],\, p^{(2j)}(0) = (-1)^j \gamma^{2j},\, j = 0 \ldots, l\} \tag{2.55}$$

with the associated null space denoted as P_0:

$$P_0 = \{p | p \in span\{\cos(mK)\}_{m=0}^{M}, K \in [0, \pi],\, p^{(2j)}(0) = 0,\, j = 0 \ldots, l\}. \tag{2.56}$$

Lemma 2.4.3. *The space P_0 is a Haar space over $(0, \pi)$ of dimension $M - l$.*

Proof. Pick any non trivial $p_0 \in P_0$; then we show

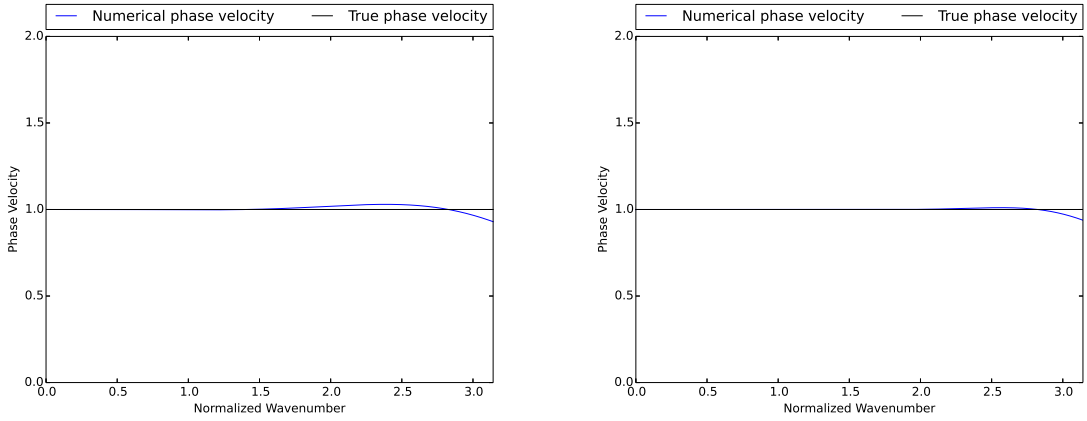

(a) M=4, max error=0.070441171046992324 (b) M=7, max error=0.061921947514832709

Figure 2.14: Dispersion relation with Remez algorithm schemes. With order of accuracy 2, $M = 4, 7$, optimization interval $(0, 0.9\pi)$ and $\gamma = 0.6$. Error is reduced compared to Figures 2.4b and 2.4c. Note that numerical speed is higher than true speed at big wavenumber for both schemes. This should result in a faster numerical wave, as shown below.

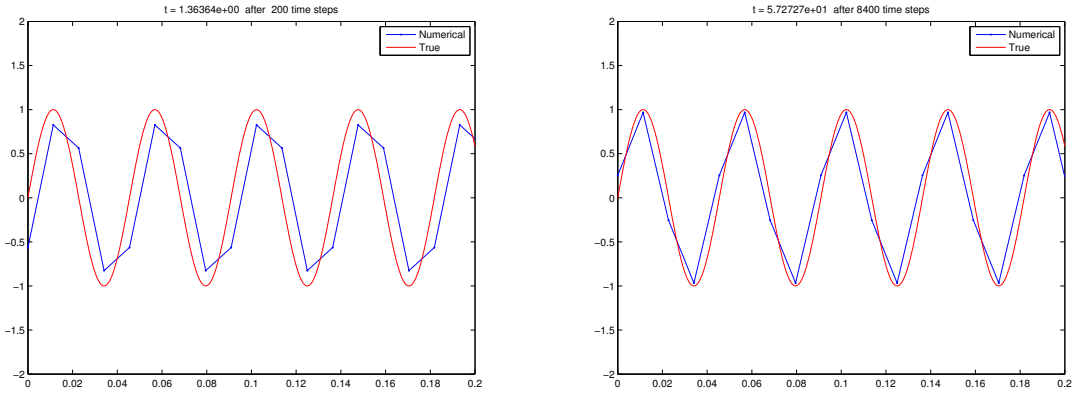

(a) $M = 4$, $l = 2$, $kmax = 0.9\pi$, Remez algorithm (b) $M = 7$, $l = 2$, $kmax = 0.9\pi$, Remez algorithm

Figure 2.15: Propagation of a single wave with schemes computed from Figure 2.14.

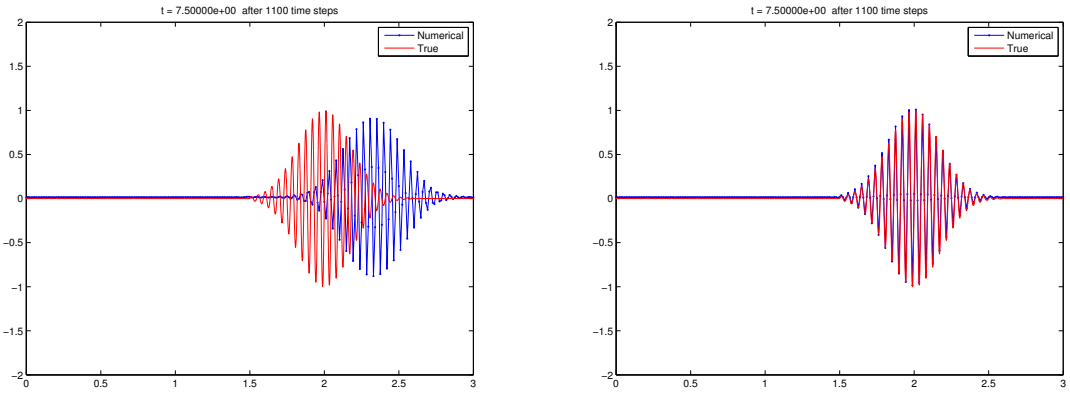

(a) $M = 4$, $l = 2$, $kmax = 0.9\pi$, Remez algorithm (b) $M = 7$, $l = 2$, $kmax = 0.9\pi$, Remez algorithm

Figure 2.16: Propagation of a wave packet with schemes computed from Figure 2.14

Claim 2.4.4. p_0 has at most $M - l - 1$ zeros in $(0, \pi)$.

Proof. If $p_0(K)$ has at least $M - l$ zeros in $(0, \pi)$, we show that $p_0(K)$ is identically zero. We write the zeros of p_0 to be K_j where $j = 1, \ldots, M - l$, then p_0 satisfies

$$\begin{aligned} p_0^{(2j)}(0) &= 0, \qquad j = 0, \ldots l, \\ p_0(K_j) &= 0, \qquad j = 1, M - l. \end{aligned} \tag{2.57}$$

By Theorem 2.3.1, such system has only trivial solution. □

Claim 2.4.5. P_0 is of dimension $M - l$ on $(0, \pi)$.

Proof. By Theorem 2.3.1, we know the first $l + 1$ rows are linearly independent. Since there are $M + 1$ undetermined coefficients, the dimension of solution space is $M - l$. □

With these two claims, P_0 is a Haar space over $(0, \pi)$. □

From this lemma, we will prove the following generalized alternating property:

Theorem 2.4.6. *Let $p \in P$ be a best minimax approximation to f . Then there exists $M+1-l$ consecutive points $K_i \in (0,\pi]$ such that*

$$|f(K_i) - p(K_i)| = ||f-p||_\infty$$

$i = 1, 2, \ldots, M+1-l$ and

$$sign[f(K_i) - p(K_i)] = (-1)^{i-1} sign[f(K_1) - p(K_1)].$$

Proof. The proof is similar to the one given in Kimchi and Richter-Dyn. Divide the interval $[0,\pi]$ into consecutive closed intervals in which the maximal change of the error function $\epsilon(K) = f(K) - p(K)$ is less than $\frac{\epsilon_0}{2}$, where $\epsilon_0 = ||f-p||_\infty$. The interval containing zeros of ϵ does not have an extreme point since ϵ(zero of ϵ) $= 0$ but all intervals containing extreme points satisfy $\epsilon(K) = \epsilon_0 > \frac{\epsilon_0}{2}$. We group these intervals into consecutive groups, starting a new group only when there is a change of sign of $\epsilon(K)$. Pick the groups where there is a point $\{K_i\}_{i=1}^{\rho}$ such that $\epsilon(K_i) = \epsilon_0$. We claim $\rho \geq M+1-l$, i.e., there are at least $M+1-l$ consecutive points where they attain the maximum and such that their signs are opposite. Suppose $1 \leq \rho \leq M-l$; then by above construction there is an open interval between any two consecutive groups. From each interval we choose one point y_i, where $i = 1, \ldots, \rho-1$ such that $\epsilon(y_i) \neq 0$. By Lemma 2.4.1, P_0 is a Haar space over $(0,\pi)$, so we can construct a polynomial $p_0 \in P_0$ with $\rho-1$ simple zeros at $y_1, \ldots, y_{\rho-1}$ and non-zero elsewhere in $(0,\pi)$. By the choice of $\{y_i\}_1^{\rho-1}$, $\epsilon(k)p_0(K)$ is of constant sign on K_i, i.e., $(f(K_i) - p(K_i))p_0(K_i)$ is of constant sign, for all i. By specifying the value of p_0 at one of K_j, taking either p_0 or $-p_0$, we get a contradiction to Theorem 2.4.1. □

The converse to above theorem is also true:

Theorem 2.4.7. *Suppose $p \in P$, and $A(f,p)$ has at least $M+1-l$ points $\{K_i\}_{i=1}^{M+1-l}$ satisfying the above alternating property. Then p is a best minimax approximation from P to f.*

Proof. Suppose p_1 is a better approximation to f, i.e. $||\epsilon_1|| = ||f-p_1|| < ||f-p|| = ||\epsilon||$. Notice $p_0 = p - p_1$ is in P_0, and that $|\epsilon_1(K_i)| \leq ||\epsilon_1|| < ||\epsilon|| = |\epsilon(K_i)|$, $p_0(K_i) = -f(K_i) -$

$p_1(K_i) + p(K_i) + f(K_i) = -\epsilon(K_i) + \epsilon_1(K_i)$. Notice $sign(p_0(K_i)) = -sign(\epsilon(K_i))$ for all $i = 1, \ldots, M + 1 - l$, and p_0 has at least $M - l$ zeros. Since $p_0 \in P_0$, by Lemma 2.4.1, $p_0 \equiv 0$. □

With the alternating property, we can design the following exchange algorithm similar to Remez algorithm for computing the coefficients of the scheme.

2.4.1.1 Remez Algorithm I

1. Pick a set of reference points $\{K_i\}_{i=1}^{M+1-l}$, denote $h = f(K_1) - p(K_1)$.

2. Find the first polynomial $p(K) = \sum_{m=0}^{M} c_m \cos(mK)$ with

$$\begin{aligned} p(0) &= 1, \qquad j = 0 \\ p^{(2j)}(0) &= (-1)^j \gamma^{2j}, \qquad j = 1, \ldots, l \\ p(K_i) &= (-1)^{i+1} h, \qquad i = 2, \ldots, M+1-l. \end{aligned}$$

3. Compute the error function $e(K) = f(K) - p(K)$. Find η, a point where $|f(\eta) - p(\eta)| = ||f - p||$, and denote $\delta = |f(\eta) - p(\eta)| - |h|$. If the difference δ is within the preset accuracy, stop and take p to be the best approximation.

4. If not, replace a point from $\{K_i\}_{i=1}^{M+1-l}$ with η, denote the new set of reference points by $\{K_i^+\}_{i=1}^{M+1-l}$. Let $h = f(K_1^+) - p(K_1^+)$.

5. Repeat above until the difference is below the preset error bound.

Remez algorithm with specified order of accuracy at the zero wavenumber.

We claim $|h| \leq ||f - p^*|| \leq ||f - p||$, where p^* denotes the best approximation in theory. By this inequality, $\delta \geq ||f - p|| - ||f - p^*||$. This is the critical reason that the algorithm converges. Now we prove the claim.

Lemma 2.4.8. *Take $p^* \in P$, and $\{K_i\}_{i=1}^{M+1-l}$ a reference set satisfying*

$$sign[f(K_{i+1}) - p^*(K_{i+1})] = -sign[f(K_i) - p^*(K_i)]$$

then for all $p \in P$ we have

$$\begin{aligned}
&\min_{i=1,\ldots,M+1-l} |f(K_i) - p^*(K_i)| \\
&\leq \min_{p \in P} \max_{i=1,\ldots,M+1-l} |f(K_i) - p(K_i)| \\
&\leq \min_{p \in P} ||f - p|| \leq ||f - p^*||.
\end{aligned}$$

Proof. The second and third inequalities are clear. For the first one, assume not, then there exists a $q^* \in P$, such that $\min_{i=1,\ldots,M+1-l} |f(K_i) - p^*(K_i)| \geq \max_{i=1,\ldots,M+1-l} |f(K_i) - q^*(K_i)|$. Write $r^* = q^* - p^*$. If $q^* = p^*$, then for all i, $|f(K_i) - p^*(K_i)|$ are equal and the inequality holds. If not, write $r^* = q^* - p^* = -(f - q^*) + (f - p^*)$, then $r^*(K_i)$ are all of the same sign as $f(K_i) - p^*(K_i)$, and continuity implies r^* has at least $M - l$ zeros. But $r^* \in P_0$, and this means $r^* = 0$. □

2.4.2 Keep accuracy conditions at the zero wavenumber and exact phase dispersion

Now we add in more restraints on the polynomial p: we enforce exact phase dispersion at the wavenumbers $\{K_m\}_{m=1}^n$ (with $l + n < M$) while we keep the accuracy condition at the zero wavenumber. The space we consider is:

$$\begin{aligned}
&P = \{p | p \in span\{\cos(mK)\}_{m=0}^M, K \in [0, \pi], \\
&p^{(2j)}(0) = (-1)^j \gamma^{2j},\ j = 0 \ldots, l, p(K_m) = \cos(\gamma K_m), m = 1, \ldots n\},
\end{aligned} \tag{2.58}$$

with associated null space

$$P_0 = \{p | p \in span\{\cos(mK)\}_{m=0}^{M}, K \in [0, \pi],$$
$$p^{(2j)}(0) = 0,\ j = 0 \ldots, l, p(K_m) = 0, m = 1, \ldots n\}. \tag{2.59}$$

Same as in the previous section, it is crucial that the null space is a Haar space for the alternating property to hold. Due to the exact phase velocity requirements, P_0 is a Haar space only if we avoid the preset wavenumbers.

Lemma 2.4.9. *P_0 is a Haar space of dimension $M - l - n$ on (K_j, K_{j+1}), for all $j = 1, \ldots, n-1$.*

Proof. P_0 is of dimension $M-l-n$. If p_0 has $M-l-n$ zeros, say$\{y_j\}_{j=1}^{M-l-n}$, in (K_j, K_{j+1}) (for any $j = 1, \ldots, n-1$), then p_0 has to satisfy:

$$\begin{aligned} p_0^{(2j)}(0) &= 0, \qquad j = 0, \ldots l \\ p_0(K_j) &= 0, \qquad j = 1, \ldots, n \\ p_0(y_j) &= 0, \qquad j = 1, \ldots, M-l-n. \end{aligned} \tag{2.60}$$

Theorem 2.3.1 guarantees that such p_0 has to be trivial. □

Remark on choices of optimization intervals:

- Since we have the freedom to choose the interval to do minimization, it is natural to choose an interval closer to the Nyquist wavenumber, π. Therefore we might want to take (K_n, π).

- As shown in the work by Kimchi and Richter-Dyn (1975), if we want to do the optimization on the whole interval $(0, K_{max})$, we need to divide out the zeros.

We also have a corresponding alternating property, wihch guarantees a Remez-type algorithm.

Theorem 2.4.10. *$p^* \in P$ is a best minimax approximation to f if and only if there exists $M - n - l + 1$ consecutive points $K_i \in (0, \pi]$ such that*

$$|f(K_i) - p(K_i)| = ||f - p||_\infty$$

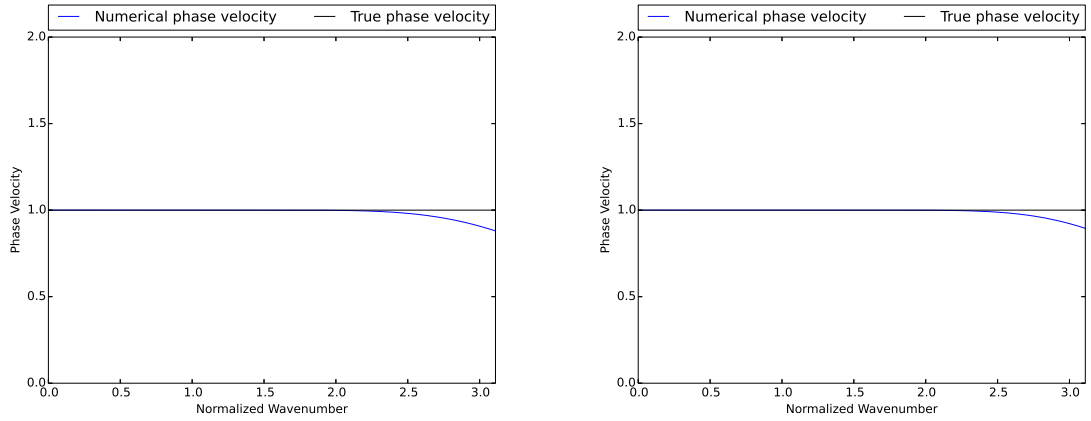

(a) M=5, order of accuracy 0, max error= 0.12005077705647949

(b) M=7, order of accuracy 2, max error=0.10518835061686271

Figure 2.17: Dispersion relation with Remez algorithm schemes. With stencil width $M = 5, 7$, and exact phase velocity at $\pi/2$. Error is reduced compared to Figures 2.4b and 2.4c. The Remez interval is (kmin,kmax)= $(0, 0.49\pi)$

$i = 1, 2, \ldots, M - n - l + 1$ *and*

$$sign\{[f(K_i) - p(K_i)]\} = (-1)^{i-1} sign\{[f(K_1) - p(K_1)]\}.$$

Since we need at least three points for Remez algorithm, it is important to pick M big enough. This is why we have decreased the order of accuracy at zero and increased the stencil width to 5 in Figure 2.17a.

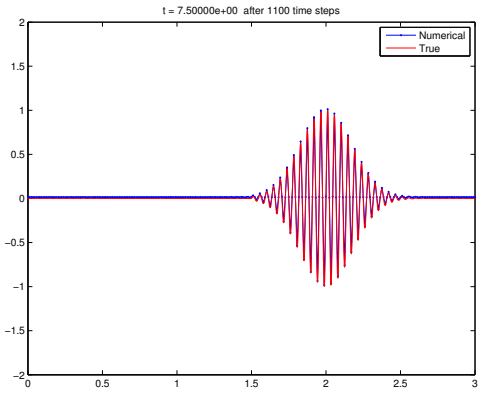

(a) $M = 5$, $l = 0$, wave packet

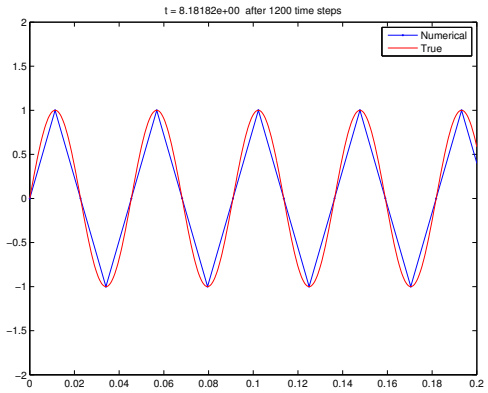

(b) $M = 5$, $l = 0$, single wave

Figure 2.18: Propagation of a wave packet and single wave with schemes computed from Figure 2.17a.

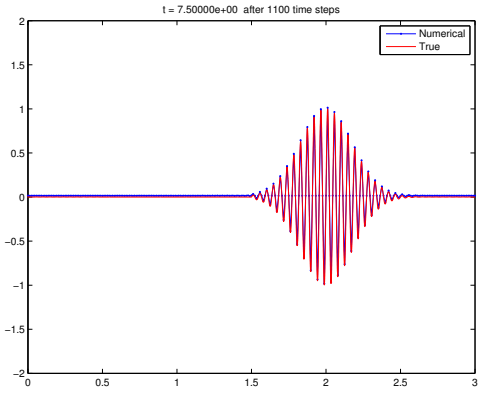

(a) $M = 7$, $l = 2$, wave packet

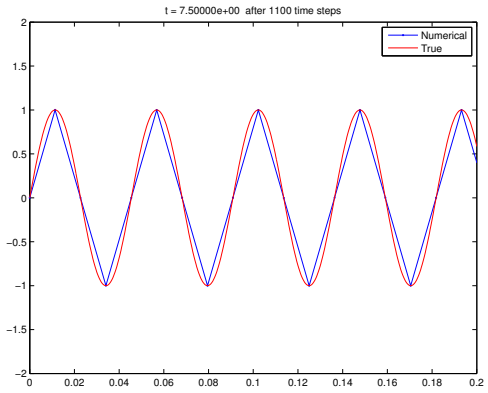

(b) $M = 7$, $l = 2$, single wave

Figure 2.19: Propagation of a wave packet and single wave with schemes computed from Figure 2.17b.

2.4.2.1 Remez Algorithm II

1. Pick a set of reference points $\{y_i\}_{i=1}^{M-n-l+1}$ in (K_j, K_{j+1}), denote $h = f(y_1) - p(y_1)$.

2. Find the first polynomial $p(K) = \sum_{m=0}^{M} c_m \cos(mK)$ with

$$\begin{aligned} p(0) &= 1, \qquad j = 0 \\ p^{(2j)}(0) &= (-1)^j \gamma^{2j}, \qquad j = 1, \ldots, l \\ p(K_j) &= \cos(K_j), \qquad j = 1, \ldots, n \\ p(y_i) &= (-1)^{i+1} h, \qquad i = 1, \ldots, M - l - n + 1. \end{aligned}$$

3. Compute the error function $e(K) = f(K) - p(K)$. Find η, a point where $|f(\eta) - p(\eta)| = ||f - p||$, and denote $\delta = |f(\eta) - p(\eta)| - |h|$. If the difference δ is within the preset accuracy, stop and take p to be the best approximation.

4. If not, replace a point from $\{y_i\}_{i=1}^{M-l-n+1}$ with η, denote the new set of reference points by $\{y_i^+\}_{i=1}^{M-l-n+1}$. Let $h = f(y_1^+) - p(y_1^+)$.

5. Repeat above until the difference is below the preset error bound.

Remez algorithm with specified order of accuracy at the zero wavenumber and exact phase velocity at wavenumbers K_j, $j = 1, \ldots n$.

2.4.3 Keep accuracy conditions at the zero wavenumber, exact phase and group velocity

Now we look for a new scheme to obtain a best minimax approximation to the velocity function over all the wave numbers satisfying the accuracy conditions, and with exact phase and group velocity at a preset nonzero wave number. The continuous function we are looking to approximate is still

$$f(K) = \cos(\gamma K) \tag{2.61}$$

The approximation function we are looking for is $p(K) = -\sum_{m=0}^{M} c_m \cos(mK)$ as before. The function space now is

$$P = \{p | p \in span\{\cos(mK)\}_{m=0}^{M}, K \in [0,\pi], p^{(2j)}(0) = (-1)^j \gamma^{2j},$$
$$j = 0 \ldots, l, p(K_1) = \cos(\gamma K_1), p'(K_1) = \gamma \sin(\gamma K_1)\}.$$

Again consider the null space of P:

$$P_0 = \{p_0 | p_0 \in span\{\cos(mK)\}_{m=0}^{M}, K \in [0,\pi], p_0^{(2j)}(0) = 0,$$
$$j = 0 \ldots, l, p_0(K_1) = 0, p_0'(K_1) = 0\}.$$

Similar as before, we use the fact that the null space P_0 is a Haar space to obtain an alternating property.

Lemma 2.4.11. *P_0 is a Haar space of dimension $M - l - 2$ on $(0, K_1)$ and (K_1, π)*

Proof. By Theorem 2.3.3. □

As before, we have the alternating property

Theorem 2.4.12. *$p^* \in P$ is a best minimax approximation to f if and only if there exist $M - 1 - l$ consecutive points $K_i \in (0, \pi]$ such that*

$$|f(K_i) - p(K_i)| = ||f - p||_\infty$$

$i = 1, 2, \ldots, M - 1 - l$ and

$$sign\{[f(K_i) - p(K_i)]\} = (-1)^{i-1} sign\{[f(K_1) - p(K_1)]\}.$$

Now we have an algorithm:

2.4.3.1 Remez Algorithm III

1. Pick a set of reference points $\{y_i\}_{i=1}^{M-1-l}$, denote $h = f(y_1) - p(y_1)$.

2. Find the first polynomial $p(K) = \sum_{m=0}^{M} c_m \cos(mK)$ with

$$\begin{aligned} p(0) &= 1, \qquad j = 0 \\ p^{(2j)}(0) &= (-1)^j \gamma^{2j}, \qquad j = 1, \ldots, l \\ p(K_1) &= \cos(K_1) \\ p'(K_1) &= \gamma \sin(K_1) \\ p(y_i) &= (-1)^{i+1} h, \qquad i = 1, \ldots, M - l - 1. \end{aligned}$$

3. Compute the error function $e(K) = f(K) - p(K)$. Find η, a point where $|f(\eta) - p(\eta)| = ||f - p||$, and denote $\delta = |f(\eta) - p(\eta)| - |h|$. If the difference δ is within the preset accuracy, stop and take p to be the best approximation.

4. If not, replace a point from $\{y_i\}_{i=1}^{M-l-1}$ with η, denote the new set of reference points by $\{y_i^+\}_{i=1}^{M-l-1}$. Let $h = f(y_1^+) - p(y_1^+)$.

5. Repeat above until the difference is below the preset error bound.

Remez algorithm with specified order of accuracy at the zero wavenumber and exact phase and group velocity at wavenumber K_1.

2.4.4 Interval for optimization

Note that, as $K \to \pi$, the theoretical distance from P to f gets bigger. So one question to consider is, without sacrificing too much information, what might be a good upper bound $K_{max} \leq \pi$ to choose, so that we look for the minimax approximation on the subinterval $[0, K_{max}]$. This issue is mentioned in Kosloff's work (2008). In our experiments, we have used $K_{max} = 0.9\pi$, as seen in Figure 2.14. When we specify exact phase velocity at 0.5π, we take the optimization interval to be $[0, 0.49\pi]$, as seen in Figure 2.17.

Chapter 3

TWO DIMENSIONAL ACOUSTIC WAVE EQUATION

In this chapter, we construct finite difference operators to approximate the differential operator in

$$\left(c_x^2\partial_x^2 + c_z^2\partial_z^2 - \partial_t^2\right) u = 0 \tag{3.1}$$

where c_x and c_z denote the propagation speed along the x and z directions. The finite difference operator assumes the form:

$$U_{l,j}^{n+1} + U_{l,j}^{n-1} + \sum_{m=0}^{M} c_m(U_{l+m,j}^n + U_{l-m,j}^n) + \sum_{m=0}^{M} d_m(U_{l,j+m}^n + U_{l,j-m}^n) = 0. \tag{3.2}$$

If the medium is isotropic, then in the differential equation $c_x = c_z$, and it is reasonable to take $d_m = c_m$ for all $m = 0, \ldots, M$ in the FD scheme. These schemes will be our main focus in the two dimensional case. In the wave propagation experiments, we apply periodic boundary conditions and use a Ricker wavelet as the source term.

As in one dimension case, our goal is to find FD operators that give good approximation to the wave speed. As wave propagation depends on both wavenumber magnitude and direction in two dimension, the schemes we design will also depend on wavenumbers and propagation directions.

3.1 Isotropic media

The following equation describes the acoustic wave in an isotropic media:

$$(\frac{\partial^2}{\partial x^2} + \frac{\partial^2}{\partial z^2} - \frac{1}{c^2}\frac{\partial^2}{\partial t^2})u = 0 \tag{3.3}$$

As before, parameter c denotes the phase velocity. We still take $c = 1$ without loss of generality. Unlike the one dimension case where the propagation direction of a wave is either left or right, in the two dimension case, diving waves exist where waves might propagate at any angle between 0 and π for example. Therefore it is reasonable that we look for schemes

that give good dispersion approximation for all propagation angles in $[0, \pi]$. The differential equation for the isotropic media is symmetric in the x and z direction, and we will take advantage of the symmetry in the design of schemes by taking $d_m = c_m$. We first study the classical Leap-frog scheme and obtain a generalized scheme of the same stencil width.

3.1.1 Example: Leap-frog and generalized Leap-frog scheme

We obtain the Leap-frog scheme in two dimension by using three points in time, the x-direction and the z-direction to approximate the second derivatives. Similar to Example 1.2.5 (we denote the stencil by (3,3,3)):

$$U_{l,j}^{n+1} - 2U_{l,j}^{n} + U_{l,j}^{n-1} - \gamma_x^2 \left[U_{l+1,j}^{n} - 2U_{l,j}^{n} + U_{l-1,j}^{n}\right] - \gamma_z^2 \left[U_{l,j+1}^{n} - 2U_{l,j}^{n} + U_{l,j-1}^{n}\right] = 0, \quad (3.4)$$

where $\gamma_x = \dfrac{c\Delta t}{\Delta x}$ and $\gamma_z = \dfrac{c\Delta t}{\Delta z}$ and $U_{l+I,j+J}^{n+N} \approx u(x + I\Delta x, z + J\Delta z, t + N\Delta t)$ denotes the approximation to u at the grid points $(x + I\Delta x, z + J\Delta z, t + N\Delta t)$. Group the terms by symmetry

$$U_{l,j}^{n+1} + U_{l,j}^{n-1} + 2(-1 + \gamma_x^2 + \gamma_z^2)U_{l,j}^{n} - \gamma_x^2(U_{l+1,j}^{n} + U_{l-1,j}^{n}) - \gamma_z^2(U_{l,j+1}^{n} + U_{l,j-1}^{n}) = 0, \quad (3.5)$$

and replace the coefficients by undetermined coefficients to obtain a general scheme for the (3,3,3) stencil

$$U_{l,j}^{n+1} + U_{l,j}^{n-1} + 2c_1 U_{l,j}^{n} + c_2(U_{l+1,j}^{n} + U_{l-1,j}^{n}) + c_3(U_{l,j+1}^{n} + U_{l,j-1}^{n}) = 0. \quad (3.6)$$

Now we have a generalized Leap-frog scheme (Finkelstein and Kastner, 2007). As in the one dimension case, we plug the true solution into the FD scheme and use Taylor expansion to study accuracy:

$$\begin{aligned} LTE = {} & (2 + 2c_1 + 2c_2 + 2c_3)u + 2\partial_t^2 u \frac{(\Delta t)^2}{2!} + 2\partial_t^4 u \frac{(\Delta t)^4}{4!} + \dots \\ & + c_2 \left(2u_{xx} \frac{(\Delta x)^2}{2!} + 2\partial_x^4 u \frac{(\Delta x)^4}{4!} + \dots \right) \\ & + c_3 \left(2u_{zz} \frac{(\Delta z)^2}{2!} + 2\partial_z^4 u \frac{(\Delta z)^4}{4!} + \dots \right). \end{aligned}$$

Schemes based on accuracy conditions at (x, z, t) are obtained by eliminating lower order terms in the series:

$$1 + c_1 + c_2 + c_3 = 0$$
$$-c^2(\Delta t)^2 = c_2(\Delta x)^2$$
$$-c^2(\Delta t)^2 = c_3(\Delta z)^2,$$

where the second and third equations are obtained from Lax-Wendroff analysis, and eliminating u_{xx} and u_{zz} terms respectively. This coincides with the Leap-frog scheme.

Remark:

If we use a wider stencil for higher order of accuracy, the next lowest order terms made to vanish will be the forth order derivatives:

$$2\partial_t^4 u\frac{(\Delta t)^4}{4!} + 2c_2\partial_x^4 u\frac{(\Delta x)^4}{4!} + 2c_3\partial_z^4 u\frac{(\Delta z)^4}{4!}.$$

But this can not be done with the cross shaped stencil set up, as there are no terms like $\partial_x^2\partial_z^2 u$ from the stencil. Hence increasing space-time accuracy with this stencil is problematic.

In Chapter One, we have shown that using spectral order of accuracy in place of order of accuracy in the scheme design is adequate. In two dimensions, we will also focus mainly on the spectral order of accuracy, which is naturally linked to the dispersion relation.

Fourier transforming equation (3.6) gives the trigonometric dispersion relation

$$\cos(\Omega) + c_1 + c_2\cos(K_x) + c_3\cos(K_z) = 0. \tag{3.7}$$

Here $K_x = k_x\Delta x$ and $K_z = k_z\Delta z$ denote the x and z direction normalized wave numbers, and $\Omega = \omega\Delta t$ the normalized frequency. The true dispersion is

$$\Omega^2 = \gamma_x^2 K_x^2 + \gamma_z^2 K_z^2. \tag{3.8}$$

We compute the Taylor expansion at $(\Omega, K_x, K_z) = (0, 0)$ for the numerical dispersion

relation:

$$\begin{aligned} LTE &= 1 - \frac{1}{2!}\Omega^2 + \frac{1}{4!}\Omega^4 \cdots + c_1 + c_2\left(1 - \frac{1}{2!}K_x^2 + \frac{1}{4!}K_x^4 + \dots\right) \\ &+ c_3\left(1 - \frac{1}{2!}K_z^2 + \frac{1}{4!}K_z^4 + \dots\right) \\ &= (1 + c_1 + c_2 + c_3) - \frac{1}{2!}(\Omega^2 + c_2K_x^2 + c_3K_z^2) \\ &+ \frac{1}{4!}(\Omega^4 + c_2K_x^4 + c_3K_z^4) + \dots . \end{aligned}$$

Similar to the time domain case, we eliminate the lowest order terms to obtain accuracy conditions on the dispersion relation:

$$1 + c_1 + c_2 + c_3 = 0$$

$$\Omega^2 + c_2K_x^2 + c_3K_z^2 = 0 \tag{3.9}$$

$$\Omega^4 + c_2K_x^4 + c_3K_z^4 = 0. \tag{3.10}$$

To eliminate the second order term, we plug in the true Ω as a function of K_x and K_z in (3.8); equation (3.9) becomes

$$(\gamma_x^2 + c_2)K_x^2 + (\gamma_z^2 + c_3)K_z^2 = 0. \tag{3.11}$$

Making both of the coefficients vanish, we get $c_2 = -\gamma_x^2$ and $c_3 = -\gamma_z^2$. This is equivalent to the traditional order of accuracy.

Take $\Delta x = \Delta z$, then we write $\gamma = \frac{c\Delta t}{\Delta x}$ and write the true dispersion as $\Omega = \gamma K = \gamma\sqrt{K_x^2 + K_z^2}$. As we see, the true dispersion is independent of angle (see Figure 3.1). We replace the Cartesian K_x and K_z with the polar coordinates $K\cos(\phi)$ and $K\sin(\phi)$, where ϕ is the propagation angle. The previously mentioned dispersion relation is now

$$\cos(\Omega) + c_1 + c_2\cos(K\cos(\phi)) + c_3\cos(K\sin(\phi)) = 0. \tag{3.12}$$

This dispersion relation makes the angle dependence explicit and fits our purpose, so we will write dispersion relation in polar form in the future. Taylor expansion in the angle

dependent dispersion gives:

$$\begin{aligned} LTE &= 1 - \frac{1}{2!}\Omega^2 + \frac{1}{4!}\Omega^4 \cdots + c_1 + c_2 \left(1 - \frac{1}{2!}K^2\cos^2(\phi) + \frac{1}{4!}K^4\cos^4(\phi) + \dots\right) \\ &+ c_3 \left(1 - \frac{1}{2!}K^2\sin^2(\phi) + \frac{1}{4!}K^4\sin^4(\phi) + \dots\right) \\ &= (1 + c_1 + c_2 + c_3) - \frac{1}{2!}(\Omega^2 + c_2K^2\cos^2(\phi) + c_3K^2\sin^2(\phi) \\ &+ \frac{1}{4!}(\Omega^4 + c_2K^4\cos^4(\phi) + c_3K^4\sin^4(\phi)) + \dots . \end{aligned}$$

Eliminating the coefficient for K^2 by plugging in $\Omega = \gamma K$ in (3.9) gives

$$\gamma^2 + c_2\cos^2(\phi) + c_3\sin^2(\phi) = 0. \tag{3.13}$$

The second formulation makes the angle dependence explicit (controlled by different grid sizes in the first formulation). In equation (3.10), if we use the true dispersion relation $\Omega^4 = \gamma^4 K^4$, we get the following restriction

$$\gamma^4 + c_2\cos^4(\phi) + c_3\sin^4(\phi) = 0, \tag{3.14}$$

which is angle dependent.

Remarks:

- From (3.11), we see that the coefficients are proportional to each other with respect to the grid sizes, i.e., $\frac{c_2}{c_3} = \frac{(\Delta z)^2}{(\Delta x)^2}$. For isotropic media, we will always assign equal grid sizes in the x and z directions, $h = \Delta x = \Delta z$, and denote $\gamma = \frac{c\Delta t}{h}$.

- If we wish to take advantage of Lax-Wendorff analysis for higher order space-time accuracy, we will need to introduce cross derivative terms by introducing diagonal grids in the stencil. As one of the main results we have concerns the Remez algorithm, and the algorithm doesn't apply for denser stencils with diagonal grid points. We will not discuss on such stencils further here.

- With the sparse cross shaped stencil, we will use the dispersion relation $\Omega = \gamma K$ and get angle dependent restrictions on the undetermined coefficients.

- Traditional order of accuracy in x and z is equivalent to order of accuracy of dispersion in Cartesian coordinates. This is a special case for the general angle dependent dispersion.

3.1.2 General schemes with wider stencil

In this section, we set up a general scheme for the two dimensional acoustic wave equation and produce schemes that satisfy certain criteria for order of accuracy. From the analysis of the Leap-frog scheme, we see that angle dependent accuracy for dispersion relation is more general than the traditional accuracy in the time domain for the cross shaped stencil. Therefore, we will focus on schemes based on the cross shaped stencils with accuracy obtained by spectral order of accuracy for the dispersion relation.

Similar to the one dimension case, we exploit wider stencils in space in two dimensions. Due to the equivalence of x and z as spatial variables in isotropic media, we apply the same stencil and weight in both directions:

$$U_{l,j}^{n+1} + U_{l,j}^{n-1} + \sum_{m=0}^{M} c_m (U_{l+m,j}^{n} + U_{l-m,j}^{n}) + \sum_{m=0}^{M} c_m (U_{l,j+m}^{n} + U_{l,j-m}^{n}) = 0. \tag{3.15}$$

As analyzed in the example, for the sparse cross shaped stencil, we will use spectral order of accuracy. First recall the true dispersion relation corresponding to the grid size and time step is $\Omega = \gamma K$. Discrete Fourier transform gives numerical dispersion relation

$$\cos(\Omega) + \sum_{m=0}^{M} c_m [\cos(mK\cos(\phi)) + \cos(mK\sin(\phi))] = 0. \tag{3.16}$$

As analyzed in Chapter one, reducing dispersion error can be simplified to reducing:

$$|| \cos(\Omega_{true}) - \cos(\Omega_{numerical})|| = \left|\left| \cos(\gamma K) + \sum_{m=0}^{M} c_m [\cos(mK\cos(\phi)) + \cos(mK\sin(\phi))] \right|\right|. \tag{3.17}$$

3.1.3 Stability analysis for the generalized scheme

From equation (3.15) with $U_{l,j}^{n} = g^n e^{i(lK_x + jK_z)}$, we get the following amplification polynomial

$$g^2 + 2g \sum_{m=0}^{M} c_m [\cos(mK_x) + \cos(mK_z)] + 1 = 0. \tag{3.18}$$

Similar to the one dimensional situation, the schemes are stable if

$$|z| = \left| \sum_{m=0}^{M} c_m[\cos(mK_x) + \cos(mK_z)] \right| \leq 1 \tag{3.19}$$

for all K_x and K_z. The stability check is integrated in the our algorithms, so that we perform the stability check whenever we obtain a new scheme.

3.1.4 Accuracy analysis for the general scheme

In this section, we present accuracy analysis for the general scheme with Taylor expansion. We will do the analysis in both time and frequency domain, and in the frequency domain, we use polar coordinates. This analysis validates our choice of using spectral accuracy in our scheme designs.

3.1.4.1 Accuracy analysis in time domain

For the general scheme in the time domain (3.15), we plug in the true solution $u(x, z, t)$ that satisfies the wave equation; Taylor expansion at the point (x, z, t) gives

$$\begin{aligned}
LTE &= u(x,z,t+\Delta t) + u(x,z,t-\Delta t) + \sum_{m=0}^{M} c_m(u(x+m\Delta x,z,t) + u(x-m\Delta x,z,t)) \\
&+ \sum_{m=0}^{M} c_m(u(x,z+m\Delta z,t) + u(x,z-m\Delta z,t)) \\
&= \left(2u(x,z,t) + 2(\Delta t)^2 \frac{\partial^2}{2!\partial t^2}u + 2(\Delta t)^4 \frac{\partial^4}{4!\partial t^4}u \dots\right) \\
&+ \sum_{m=0}^{M} c_m \left(2u(x,z,t) + 2(m\Delta x)^2 \frac{\partial^2}{2!\partial x^2}u + 2(m\Delta x)^4 \frac{\partial^4}{4!\partial x^4}u + \dots\right) \\
&+ \sum_{m=0}^{M} c_m \left(2u(x,z,t) + 2(m\Delta z)^2 \frac{\partial^2}{2!\partial z^2}u + 2(m\Delta z)^4 \frac{\partial^4}{4!\partial z^4}u + \dots\right).
\end{aligned}$$

As shown for the Leap-frog scheme, unlike the one dimensional case, we can get at most second order accuracy in time-space due to the cross shape of our stencil, and Lax-Wendroff analysis doesn't apply. Eliminating the lowest order terms, we get restrictions on

the coefficients:

$$
\begin{aligned}
&(1+\sum_{m=0}^{M} c_m)u = 0, \text{ consistency,}\\
&\Delta t^2 \frac{\partial^2}{\partial t^2}u + \sum_{m=0}^{M} c_m (m\Delta x)^2 \frac{\partial^2}{\partial x^2}u + \sum_{m=0}^{M} c_m (m\Delta z)^2 \frac{\partial^2}{\partial z^2}u = 0,\\
&\qquad \text{second order accuracy in space-time,}\\
&\sum_{m=0}^{M} c_m (m\Delta x)^4 \frac{\partial^4}{\partial x^4}u = 0, \text{ 4-th order accuracy in space } x,\\
&\vdots\\
&\sum_{m=0}^{M} c_m (m\Delta x)^{2M} \frac{\partial^{2M}}{\partial x^{2M}}u = 0, \text{ } 2M\text{-th order accuracy in space } x.
\end{aligned}
$$

When we ask for x-direction space accuracy, and we get the z-direction accuracy for free, due to isotropy. The system for coefficients is

$$\sum_{m=0}^{M} c_m = -1 \tag{3.20}$$

$$\sum_{m=0}^{M} c_m m^2 = -\gamma^2 \tag{3.21}$$

$$\sum_{m=0}^{M} c_m m^{2j} = 0 \qquad j = 2 \ldots M. \tag{3.22}$$

Numerical experiments have shown stability problems in the sense that, for most stencil widths M and CFL numbers γ, the schemes we obtain this way are often unstable.

3.1.4.2 Accuracy analysis in frequency domain

In this subsection, we will discuss the order of accuracy of the dispersion relation. As discussed before, the true dispersion is a linear function of the magnitude of the wavenumber, while the numerical dispersion depends on both wavenumber and propagation angle. We use the polar form with $K_x = K\cos(\phi)$ and $K_z = K\sin(\phi)$, and compute accuracy of the dispersion error at $K = 0$. This way, we get explicit accuracy in the propagation direction ϕ of the plane wave.

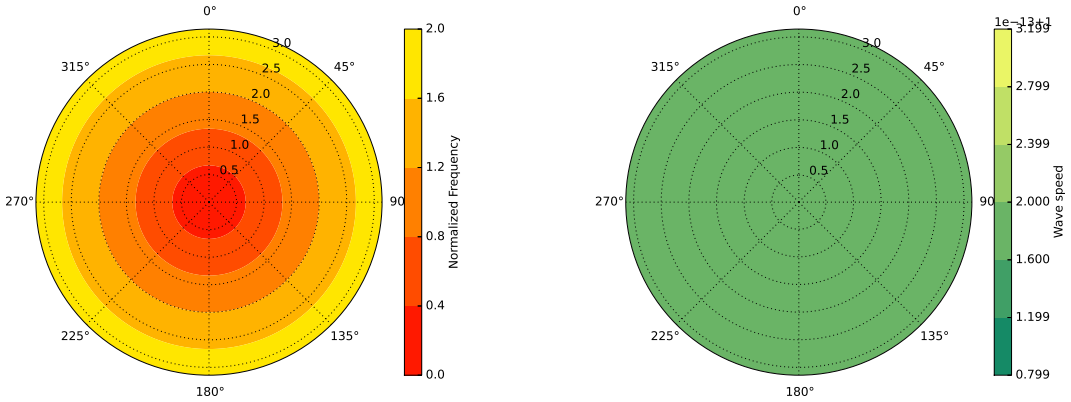

(a) With $\gamma = 0.6$, $\Omega = \gamma K$

(b) With $\gamma = 0.6$, $c = \frac{\Omega}{\gamma K}$

Figure 3.1: Normalized frequency as a function of propagation angle and normalized wavenumber, $\Omega = \gamma K$; true wave speed $c = \frac{\Omega}{\gamma K}$

Compute the Taylor expansion at the zero wavenumber for (3.17) in polar form:

$$
\begin{aligned}
LTE &= \sum_{i=0}^{\infty} \frac{(-1)^i}{(2i)!} \left(\Omega^{2i} + \sum_{m=0}^{M} c_m ((mK\cos(\phi))^{2i} + (mK\sin(\phi))^{2i}) \right) \\
&\qquad \text{(plug in the true dispersion } \Omega = \gamma K) \\
&= \sum_{i=0}^{\infty} \frac{(-1)^i}{(2i)!} \left((\gamma K)^{2i} + \sum_{m=0}^{M} c_m ((mK\cos(\phi))^{2i} + (mK\sin(\phi))^{2i}) \right) \\
&= \sum_{i=0}^{\infty} \frac{(-1)^i}{(2i)!} K^{2i} \left(\gamma^{2i} + \sum_{m=0}^{M} c_m ((m\cos(\phi))^{2i} + (m\sin(\phi))^{2i}) \right).
\end{aligned}
$$

Eliminate the lowest order terms to give accuracy in angle ϕ. Our design of schemes will be based on the following accuracy conditions at the zero wavenumber along propagation angle ϕ:

$$
\gamma^{2i} + \sum_{m=0}^{M} c_m ((m\cos(\phi))^{2i} + (m\sin(\phi))^{2i}) = 0 \qquad i = 0, \ldots, l. \tag{3.23}
$$

If we take $l = M$, then we get a full system for a scheme. As these conditions are the lowest order terms in a Taylor expansion, we shall choose one angle ϕ_0 in all the equations.

3.2 Dispersion reduction schemes

Similar to one dimension case, to reduce dispersion error, we would like to use wide stencils and design schemes targeting the reduction of dispersion errors. As in Chapter two, we aim to reduce dispersion error uniformly for all wavenumbers and/or propagation directions. Finkelstein and Kastner (2007) proposed three ways of interpolation, and we propose two new methods of uniform approximation, one in wavenumber and one in propagation angles. Obtaining good dispersion in all directions is of practical importance, as diving waves occur in seismic exploration for example. We start by analyzing schemes only enforcing accuracy of the dispersion relation at the zero wavenumber.

3.2.1 Only accuracy at the zero wavenumber

Taking $l = M$ in (3.23) and fixing $\phi = \phi_0$ give schemes that require the numerical dispersion to match the true dispersion up to the $2M$-th order at the zero wavenumber:

$$\gamma^{2j} + \sum_{m=0}^{M} c_m m^{2j} [\cos^{2j}(\phi_0) + \sin^{2j}(\phi_0)] = 0,\ j = 0, \ldots, M. \tag{3.24}$$

Each choice of ϕ_0 gives a scheme that would guarantee $2M$ order of accuracy in that direction. Liu and Sen (2009) take $\phi_0 = \frac{\pi}{8}$ as their optimal choice, for the numerical dispersion is periodic with period $\pi/2$, and $[0, \pi/4]$ is the mirror reflection of $[\pi/4, \pi/2]$. Since $\phi = \frac{\pi}{8}$ is the middle point of $[0, \pi/4]$, such schemes give accuracy in 8 uniformly spaced directions. This can be easily seen, as we let $f_{j,m}(\phi_0) = m^{2j}\left(\cos^{2j}(\phi) + \sin^{2j}(\phi_0)\right)$. Then

$$f_{j,m}(\phi_0) = m^{2j}\left(\cos^{2j}(\phi_0) + \sin^{2j}(\phi_0)\right) = \frac{m^{2j}}{2^j}\left((1 - \cos(2\phi_0))^j + (1 + \cos(2\phi_0))^j\right). \tag{3.25}$$

Figures 3.2, 3.3 and 3.4 show comparisons of dispersion relation

$$\Omega_{numerical} = \arccos(-\sum_{m=0}^{M} c_m(\cos(mK\cos(\phi)) + \cos(mK\sin(\phi)))) \tag{3.26}$$

as functions of angle and wavenumber. When the wavenumber is small, the numerical dispersion approximates the true dispersion nicely for all angles; when the wavenumber gets closer to π, dispersion gets worse for the $\pi/2$ direction no matter what we choose for ϕ_0 (that is, $\Omega_{numerical} < \Omega_{true}$). We also see, the smaller γ is, the better the approximation

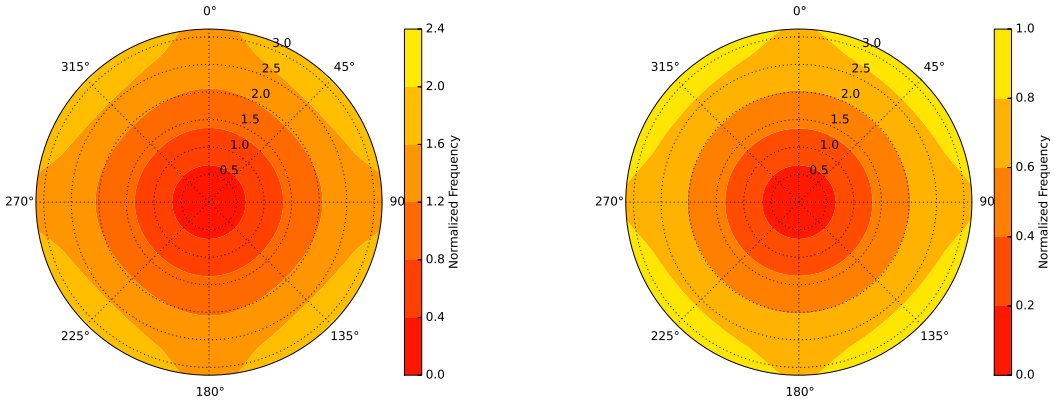

(a) With $\gamma = 0.6$, $\phi_0 = \pi/8$

(b) With $\gamma = 0.3$, $\phi_0 = \pi/8$

Figure 3.2: Normalized frequency as a function of propagation angle and normalized wavenumber: $\Omega_{numerical}$, Accuracy at the zero wavenumber along angle $\pi/8$, $M = 6$

is. For $\gamma = 0.6$, $\phi_0 = \pi/8$ approximates the dispersion better at lower wavenumbers, but $\phi_0 = \pi/4$ approximates the dispersion better at higher wavenumbers.

3.2.2 Exact dispersion at nonzero wavenumbers

For a fixed stencil width M, we reduce the number of accuracy requirements at zero wavenumber (with fixed propagation angle ϕ_0) to $l + 1$ and enforce $M - l$ exact phase dispersion conditions at non-zero wavenumbers and propagation angles. The system we have is:

$$
\begin{aligned}
&2c_0 + 2\sum_{m=1}^{M} c_m = -1 \\
&\sum_{m=0}^{M} c_m m^{2j}(\cos^{2j}(\phi_0) + \sin^{2j}(\phi_0)) = -\gamma^{2j}, j = 1, \ldots, l \\
&\sum_{m=0}^{M} c_m[\cos(mK_j\cos(\phi_j)) + \cos(mK_j\sin(\phi_j))] = -\cos(\Omega_j), j = l+1, \ldots, M,
\end{aligned}
$$

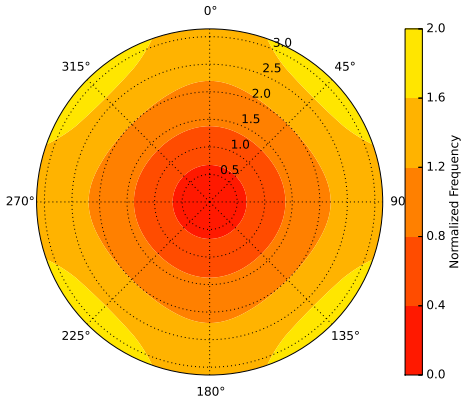

(a) With $\gamma = 0.6$, $\phi_0 = \pi/4$

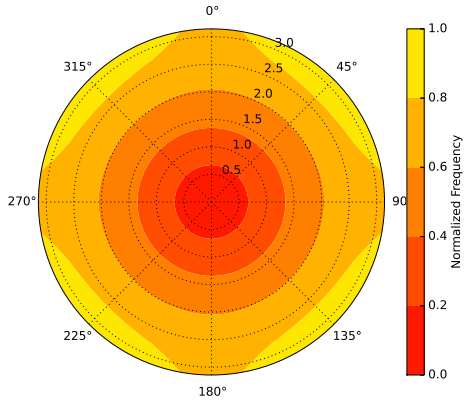

(b) With $\gamma = 0.3$, $\phi_0 = \pi/4$

Figure 3.3: Normalized frequency as a function of propagation angle and normalized wavenumber. Accuray at the zero wavenumber along angle $\pi/4$, $M = 6$, numerical dispersion $\Omega_{numerical}$.

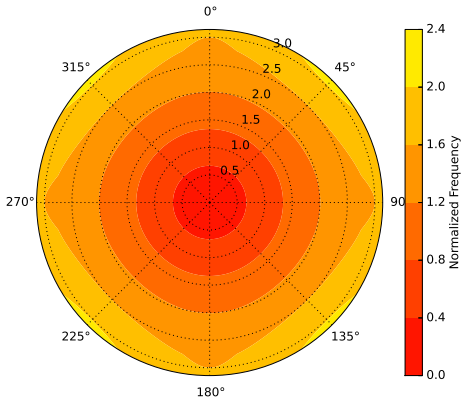

(a) $\gamma = 0.6$, $\phi_0 = \pi/2$

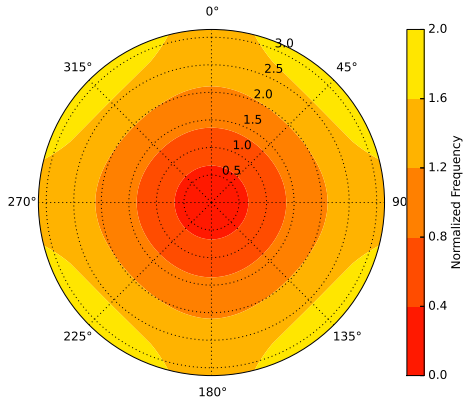

(b) $\gamma = 0.6$, $\phi_0 = \pi/3$

Figure 3.4: Normalized frequency as a function of propagation angle and normalized wavenumber. Accuray at the zero wavenumber along angle $\pi/2$ and $\pi/3$. $\gamma = 0.6$, $M = 6$ $\Omega_{numerical}$.

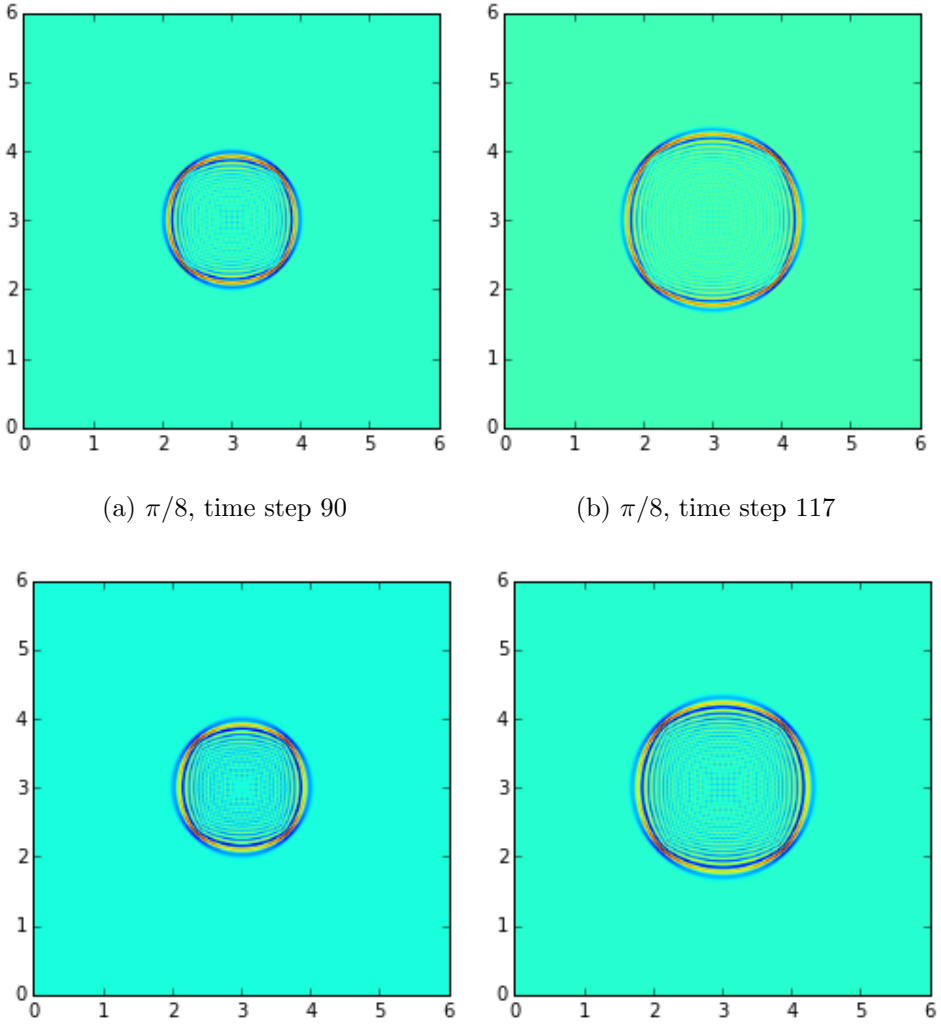

(a) $\pi/8$, time step 90

(b) $\pi/8$, time step 117

(c) $\pi/4$, time step 90

(d) $\pi/4$, time step 117

Figure 3.5: Wave propagation at: time step 90 and 117. Accuracy in $\pi/8$ and $\pi/4$. Scheme obtained via (3.23) taking $l = M$, with stencil width $M = 2$ and $\gamma = 0.6$. Choosing $\pi/8$ does not reduce anisotropy of wavefront significantly compared to taking $\pi/4$.

where exact dispersion is enforced by taking $\Omega_j = \gamma K_j$ in the last $M-l$ equations (enforced at directions ϕ_j):

$$\sum_{m=0}^{M} c_m[\cos(mK_j\cos(\phi_j)) + \cos(mK_j\sin(\phi_j))] = -\cos(\gamma K_j), j = l+1,\ldots,M.$$

According to (3.17), the above equation guarantees exact dispersion at the wavenumbers K_j.

To solve for 2D schemes, we solve the following system of equations for c_j:

$$\begin{pmatrix} 2 & 2 & 2 & \cdots & 2 & 2 \\ 0 & f_{1,1} & f_{1,2} & \cdots & f_{1,M-1} & f_{1,M} \\ \vdots & \vdots & \vdots & \vdots & \vdots & \vdots \\ 0 & f_{l,1} & f_{l,2} & \cdots & f_{l,M-1} & f_{l,M} \\ 2 & g_{l+1,1} & g_{l+1,2} & \cdots & g_{l+1,M-1} & g_{l+1,M} \\ \vdots & \vdots & \vdots & \vdots & \vdots & \vdots \\ 2 & g_{M,1} & g_{M,2} & \cdots & g_{M,M-1} & g_{M,M} \end{pmatrix} \cdot \begin{pmatrix} c_0 \\ c_1 \\ \vdots c_l \\ c_{l+1} \\ \vdots \\ c_M \end{pmatrix} = \begin{pmatrix} -1 \\ -(\gamma^2)^1 \\ \vdots \\ -(\gamma^2)^l \\ -\cos(\gamma K_{l+1}) \\ \vdots \\ -\cos(\gamma K_M) \end{pmatrix},$$

where $f_{j,m}(\phi_j) = m^{2j}\left(\cos^{2j}(\phi_j) + \sin^{2j}(\phi_j)\right)$ and $g_{j,m}(\phi_j) = \cos(mK_j\cos(\phi_j)) + \cos(mK_j\sin(\phi_j))$. Differentiate $g_{j,m}(\phi_j)$ for $2j$ times with respect to K_j to get

$$\partial_K^{(2j)} g_{j,m}(\phi_j) = (-1)^j[m^{2j}\cos^{2j}(\phi_j)\cos(mK_j\cos(\phi_j)) + m^{2j}\sin^{2j}(\phi_j)\cos(mK_j\sin(\phi_j))]. \tag{3.27}$$

Let $K_j \to 0$, then we rewrite the coefficients $f_{j,m}$ in terms of $g_{j,m}$:

$$\partial_K^{(2j)} g_{j,m}(\phi_j)\big|_{K_j=0} = (-1)^j[m^{2j}\cos^{2j}(\phi_j) + m^{2j}\sin^{2j}(\phi_j)] = (-1)^j f_{j,m}(\phi_j). \tag{3.28}$$

Now we write out the system with only $\{g_{j,m}\}$'s . This would be a $(M+1)\times(M+1)$ system $(g_{j,m})_{M+1}$, both j and m index from 0 to M:

$$\begin{pmatrix} \cos(0\cos(\phi_0)K_0) + \cos(0\sin(\phi_0)K_0) & \cdots & \cos(M\cos(\phi_0)K_0) + \cos(M\sin(\phi_0)K_0) \\ \cos(0\cos(\phi_1)K_1) + \cos(0\sin(\phi_1)K_1) & \cdots & \cos(M\cos(\phi_1)K_1) + \cos(M\sin(\phi_1)K_1) \\ \vdots & \vdots & \vdots \\ \cos(0\cos(\phi_M)K_M) + \cos(0\sin(\phi_M)K_M) & \cdots & \cos(M\cos(\phi_M)K_M) + \cos(M\sin(\phi_M)K_M) \end{pmatrix}$$

Use the sum-to-product formula

$$\cos(m\cos(\phi_j)K_j)+\cos(m\sin(\phi_j)K_j) = 2\cos\left(\frac{\cos(\phi_j)+\sin(\phi_j)}{2}mK_j\right)\cos\left(\frac{\cos(\phi_j)-\sin(\phi_j)}{2}mK_j\right).$$

to simplify the coefficient matrix.

If we take $\phi_0 = \cdots = \phi_M = \frac{\pi}{4}$, we get the easiest form for $g_{j,m}$:

$$g_{j,m}\left(\frac{\pi}{4}\right) = 2\cos\left(\frac{\sqrt{2}}{2}mK_j\right) = 2\cos(m\widetilde{K_j}), \tag{3.29}$$

where $\widetilde{K_j} = \frac{\sqrt{2}}{2}K_j$, with $\widetilde{K_j} \in \left[0, \frac{\sqrt{2}}{2}\pi\right]$. Then this system looks exactly like the system for one dimensional case with factors of powers of 2 (see the proof of Theorem 2.3.1), and thus we know this system has a solution.

Theorem 3.2.1. *There is a unique scheme that guarantees accuracy of dispersion relation at zero wave number of order l, and exact dispersion at all choices of $\{\widetilde{K_j}\}_{l+1}^{M} \subset (0, \frac{\sqrt{2}}{2}\pi]$ distinct and non zero. Moreover, the determinant of the coefficient matrix is*

$$|C(M, l+1)| = 2^{M+1}\cdot 2^1 \cdots 2^M \left(\prod_{n=l+1}^{M}(\cos(\widetilde{K_n})-1)\right)^{l+1} \prod_{l+1\le m<n\le M}\left(\cos(\widetilde{K_n})-\cos(\widetilde{K_m})\right).$$

With above existence theorem, there is a scheme that guarantees exact group velocity as well as phase velocity.

Corollary 3.2.2. *There exists a scheme to guarantee accuray of dispersion relation of order l at the zero wavenumber, exact phase velocity at $\widetilde{K_j}$, $j = l+3, \ldots, M$ and exact paired phase and group velocity at $\widetilde{K_{l+2}}$, as long as $\{\widetilde{K_j}\}_{l+2}^{M} \subset (0, \frac{\sqrt{2}}{2}\pi]$ are distinct and nonzero.*

For general propagation angle ϕ, we study the existence of schemes case by case. In particular, we do several experiments with the angle $\frac{\pi}{8}$ proposed by Liu and Sen (2009). Similar to the one dimension case, it is essential the existence theorem holds for the Remez algorithm to work in later subsections. Figures 3.16a and 3.16b show wave propagation simulated by schemes obtained this way with $\frac{\pi}{4}$. In all the experiments we do in this subsection and subsection 3.2.3, we will choose $\phi_j = \phi$ for $j = l+1, \ldots, M$. More general choices for the pair (K_j, ϕ_j) will be summed up in subsection 3.2.4.

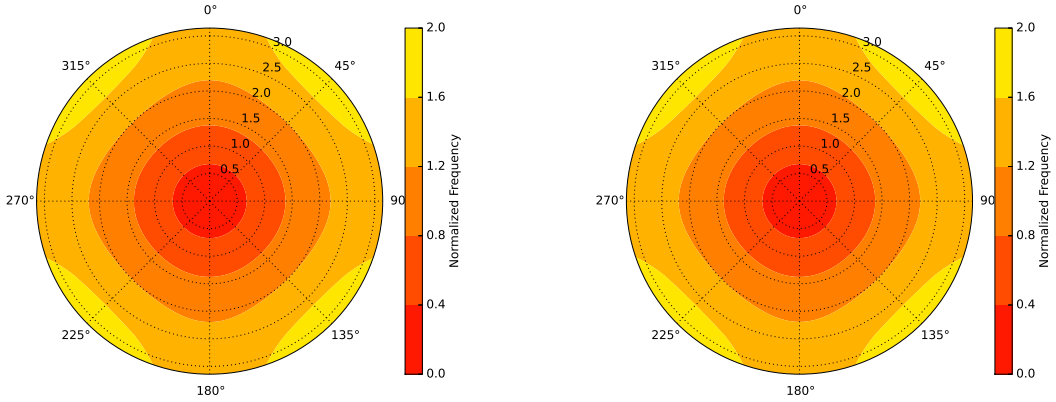

(a) With exact phase velocity at `K=np.linspace(0.25*np.pi,0.5*np.pi,3)`

(b) With exact phase velocity at `K=np.linspace(0.05*np.pi,0.75*np.pi,3)`

Figure 3.6: Normalized frequency as a function of propagation angle and normalized wavenumber, $\phi_0 = \pi/4$ and exact dispersion at several wavenumbers. $M = 6$, $\gamma = 0.6$.

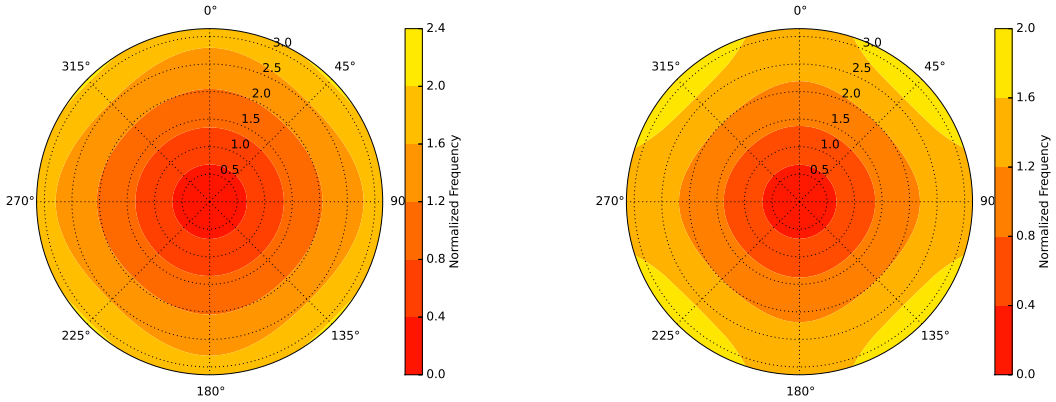

(a) With $M = 16$, $\phi_0 = \pi/4$, $\phi = \pi/8$ and `K=np.linspace(0.05*np.pi,0.75*np.pi,3)`

(b) With $M = 16$, $\phi_0 = \pi/4$, $\phi = \pi/4$ and `K=np.linspace(0.05*np.pi,0.5*np.pi,10)`

Figure 3.7: Normalized frequency as a function of propagation angle and normalized wavenumber, $\phi_0 = \pi/4$ and exact dispersion at several wavenumbers. $M = 16$, $\gamma = 0.6$.

3.2.3 Minimizing in wavenumber

As shown in the previous subsection, if we take $\phi_0 = \cdots = \phi_M = \frac{\pi}{4}$, the interval in wavenumber is $(0, \frac{\sqrt{2}}{2}\pi]$. Because all the theorems on minimax approximation follow on this interval , we can find schemes using Remez algorithm that guarantee minimum L^∞ norm of the error function (3.17) for the fixed angle $\frac{\pi}{4}$. Similarly, we can also preset several wavenumbers to get exact phase and group velocity, while minimizing the L^∞ error norm.

Consider a function of K: $f(K) = \cos(\gamma K)$, where $K \in \left(0, \frac{\pi}{\sqrt{2}}\right)$, and a function with parameter ϕ:

$$p(K) = -\sum_{m=0}^{M} c_m[\cos(mK\cos(\phi)) + \cos(mK\sin(\phi))]. \tag{3.30}$$

Here we take $\phi = \frac{\pi}{4}$. Then our goal is to find a best minimax approximation to f from the linear space:

$$\begin{aligned} P = &\{p | p \in span\{\cos(mK/\sqrt{2})\}_{m=0}^{M}, \\ &\sum_{m=0}^{M} c_m m^{2j}(\cos^{2j}(\phi_0) + \sin^{2j}(\phi_0)) = -\gamma^{2j}, j = 0, \ldots l\}, \end{aligned}$$

where we put restrictions on accuracy conditions at the zero wavenumber along direction ϕ_0. We can take ϕ_0 to be $n\pi/4$, with $n = 1, 3, 5, 7$.

The corresponding null space is still a Haar space, and we can still do minimization in wavenumbers. Similar as before, we can still specify exact dispersion (phase or group) at preset wavenumbers.

3.2.3.1 Remez Algorithm IV

1. Pick a set of reference points $\{K_i\}_{i=1}^{M+1-l} \in (0, \frac{\pi}{\sqrt{2}})$, denote $h = f(K_1) - p(K_1)$.

2. Find the first polynomial $p(K) = \sum_{m=0}^{M} c_m \cos(mK)$ with

$$\begin{aligned} p(0) &= 1, \qquad j = 0 \\ p^{(2j)}(0) &= (-1)^j \gamma^{2j}, \qquad j = 1, \ldots, l \\ p(K_i) &= (-1)^{i+1} h, \qquad i = 2, \ldots, M+1-l. \end{aligned}$$

3. Compute the error function $e(K) = f(K) - p(K)$. Find η, a point where $|f(\eta) - p(\eta)| = ||f - p||$, and denote $\delta = |f(\eta) - p(\eta)| - |h|$. If the difference δ is within the preset accuracy, stop and take p to be the best approximation.

4. If not, replace a point from $\{K_i\}_{i=1}^{M+1-l}$ with η, denote the new set of reference points by $\{K_i^+\}_{i=1}^{M+1-l}$. Let $h = f(K_1^+) - p(K_1^+)$.

5. Repeat above until the difference is below the preset error bound.

Remez algorithm minimizing dispersion error in two dimensions. Minimize in wavenumbers, with fixed propagation angle $\phi = \phi_0 = \pi/4$.

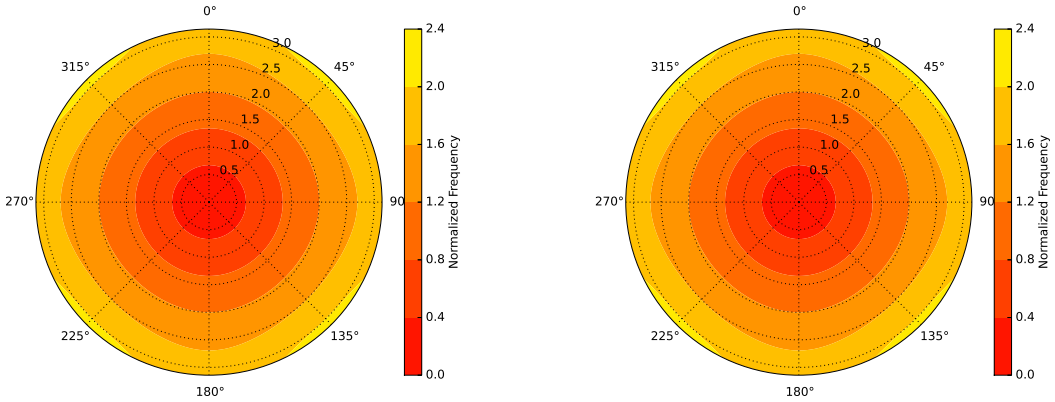

(a) $M = 6$, $l = 3$, $\phi_0 = \phi = \pi/4$ (b) $M = 6$, $l = 3$, $\phi_0 = \pi/4$,$\phi = \pi/8$

Figure 3.8: Normalized frequency $\Omega_{numerical}$ as a function of propagation angle and normalized wavenumber. Schemes obtained by optimization in wavenumber with $\gamma = 0.6$.

3.2.4 Interpolation in propagation angle

In higher dimensional case, we are more interested in angle dependence of the dispersion relations. Therefore, we start the analysis with reducing dispersion error by forcing exact phase velocity at specific propagation angles while we still keep accuracy conditions:

$$\gamma^{2i} + \sum_{m=0}^{M} c_m((m\cos(\phi_0))^{2i} + (m\sin(\phi_0))^{2i}) = 0 \qquad i = 0, \ldots, l$$

$$\cos(\gamma K_i) + \sum_{m=0}^{M} c_m[\cos(mK_i\cos(\phi_p)) + \cos(mK_i\sin(\phi_p))] = 0 \qquad i, p = 1, \ldots, M - l.$$

We will take one angle ϕ_0 in all the accuracy conditions, as higher order accuracy conditions at some angle ϕ_0 would not make sense if there is no lower order accuracy conditions at the same angle. As for the exact dispersion conditions, similar to the discussion in Finkelstein and Kastner's work of 2007 and Liu and Sen's work of 2009, there are several options for obtaining schemes:

1. Take distinct wavenumbers, but the same propagation angles. This case is interpola-

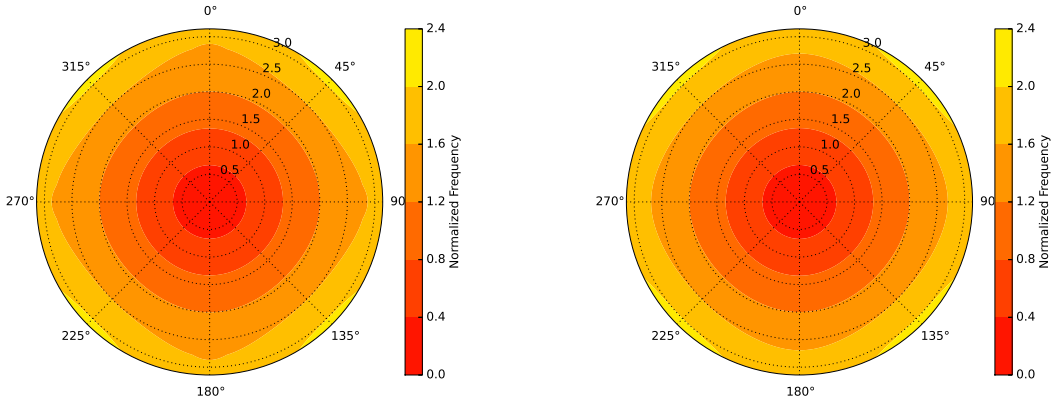

(a) $M = 6$, $l = 3$, $\phi_0 = 0$, $\phi = \pi/8$ (b) $M = 6$, $l = 3$, $\phi_0 = \pi/4$,$\phi = \pi/8$

Figure 3.9: Normalized frequency as a function of propagation angle and normalized wavenumber. Schemes obtained by optimization in wavenumber with $\gamma = 0.6$.

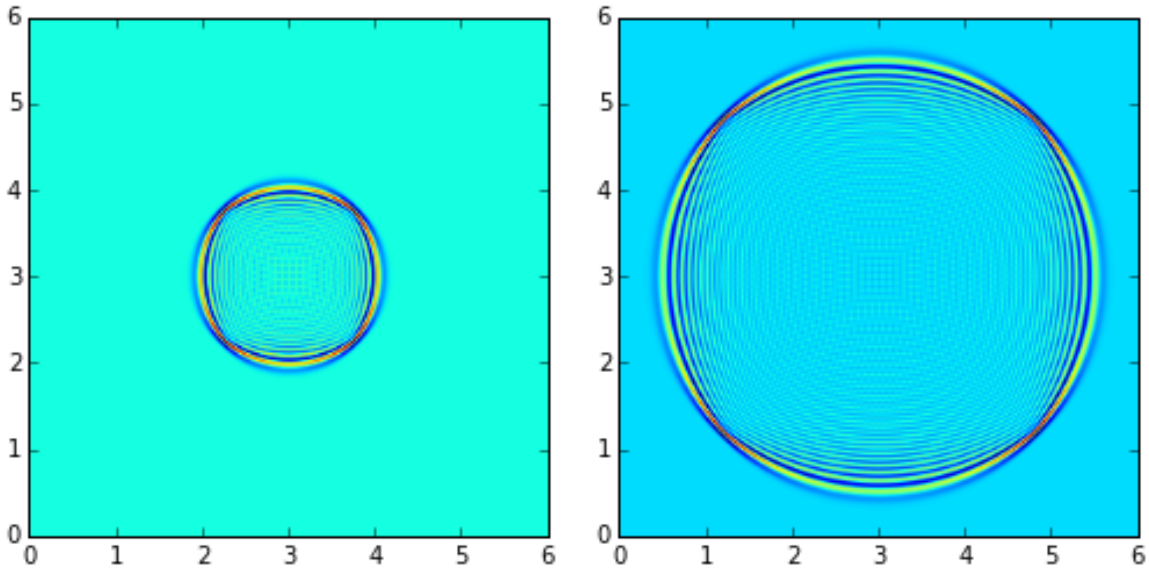

(a) At time step 100 (b) At time step 224

Figure 3.10: Wave propagation after 100 and 224 time steps, Remez algorithm in K, with $\gamma = 0.6$, $l = 2$, $M = 6$, $\phi = \phi_0 = \pi/4$.

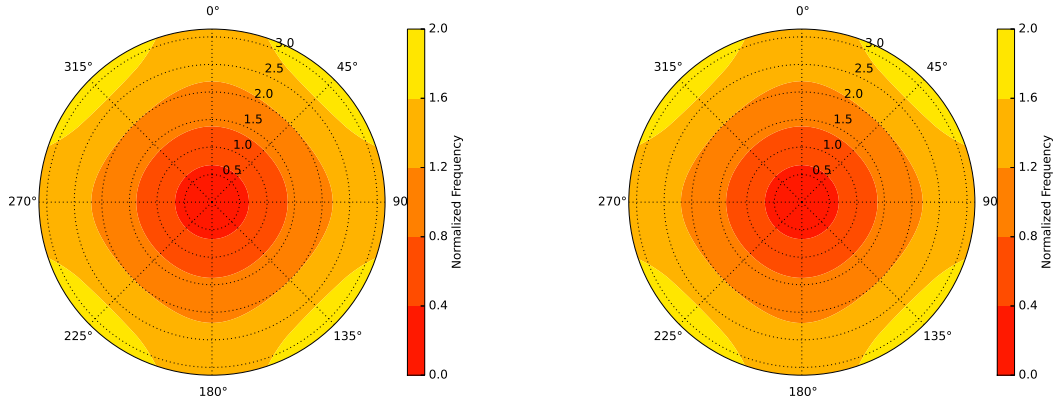

(a) `K= np.linspace(0.25*np.pi,0.75*np.pi,3)` (b) `K=np.linspace(0.25*np.pi,0.75*np.pi,3)`

Figure 3.11: Normalized frequency as a function of propagation angle and normalized wavenumber. Accuray at the zero wavenumber along angle $\pi/4$ with exact dispersion along $\pi/4$ and various wavenumbers, $\gamma = 0.6$, $M = 6$, $\Omega = \arccos(-\sum_{m=0}^{M} c_m(\cos(mK\cos(\phi)) + \cos(mK\sin(\phi))))$.

tion in wavenumber, as discussed in section 3.2.2.

$$\cos(\gamma K_i) + \sum_{m=0}^{M} c_m[\cos(mK_i\cos(\phi)) + \cos(mK_i\sin(\phi))] = 0 \qquad i = 1, \ldots, M-l. \tag{3.31}$$

2. Take distinct propagation angles, but same wavenumber

$$\cos(\gamma K) + \sum_{m=0}^{M} c_m[\cos(mK\cos(\phi_i)) + \cos(mK\sin(\phi_i))] = 0 \qquad i = 1, \ldots, M-l. \tag{3.32}$$

3. Take distinct wavenumbers, propagation angles pairs (K_i, ϕ_i)

$$\cos(\gamma K_i) + \sum_{m=0}^{M} c_m[\cos(mK_i\cos(\phi_i)) + \cos(mK_i\sin(\phi_i))] = 0 \qquad i = 1, \ldots, M-l.$$

In all three different cases, choices of K can be determined upon the incoming signal.

3.2.5 Uniform approximation in propagation directions

Due to the existence of diving waves, where the direction of wave propagation changes, it is reasonable to design schemes that give good dispersion approximations in all directions. Still we require $(l+1)$ accuracy conditions at the zero wavenumber.

$$\gamma^{2i} + \sum_{m=0}^{M} c_m((m\cos(\phi_0))^{2i} + (m\sin(\phi_0))^{2i}) = 0 \qquad i = 0, \ldots, l,$$

where ϕ_0 is a fixed angle. It is easy to see, if we take $\phi_0 = \pi/4$, the $l+1$ equations are linearly independent. We can leave the rest of the degrees of freedom for the minimax approximation.

Consider a constant function of ϕ: $f(\phi) = \cos(\gamma K)$, where $K \in (0, \pi)$ is a preset parameter, and consider the function

$$p(\phi) = -\sum_{m=0}^{M} c_m[\cos(mK\cos(\phi)) + \cos(mK\sin(\phi))]. \tag{3.33}$$

Our goal is to find a best minimax approximation to f from the linear space:

$$\begin{aligned} P = &\{p | p \in span\{\cos(K\cos(\phi)), \cos(mK\sin(\phi))\}_{m=0}^{M}, \\ &\sum_{m=0}^{M} c_m m^{2j}(\cos^{2j}(\phi_0) + \sin^{2j}(\phi_0)) = -\gamma^{2j}, j = 0, \ldots l\}. \end{aligned}$$

We again look at the corresponding null space:

$$\begin{aligned} P_0 = &\{p_0 | p_0 \in span\{\cos(K\cos(\phi)), \cos(mK\sin(\phi))\}_{m=0}^{M}, \\ &\sum_{m=0}^{M} c_m m^{2j}(\cos^{2j}(\phi_0) + \sin^{2j}(\phi_0)) = 0, j = 0, \ldots l\}. \end{aligned}$$

If P_0 is a Haar space, i.e., if the system has only trivial solution

$$\begin{aligned} &\sum_{m=0}^{M} c_m m^{2j}(\cos^{2j}(\phi_0) + \sin^{2j}(\phi_0)) = 0, j = 0, \ldots l \\ &\sum_{m=0}^{M} c_m[\cos(mK\cos(\phi_p)) + \cos(mK\sin(\phi_p))] = 0 \qquad p = 1, \ldots, M - l \end{aligned}$$

for distinct ϕ_p, $p = 1, \ldots, M - l$, then we can still obtain the alternating property for a Remez-type algorithm. From numerical experiments, we see that there are schemes obtained this way that are stable. Here is an example of such scheme.

Example 3.2.3 (Stable scheme)**.** The following computation gives a stable scheme for minimizing the dispersion relation as a function of ϕ.

```
k=0.5*np.pi #
l=2
M=10
gamma=0.6
phi0=0.25*np.pi


from remez2d import *
('condition number of the LHS', 358740206535053.56)
[[ -1.45755122e-01]
[ -2.97529648e-01]
[ -1.40963862e-01]
[  1.47871212e-01]
[ -9.28623063e-02]
[  3.76990211e-02]
[ -1.01014412e-02]
[  1.85806768e-03]
[ -2.33855679e-04]
[  1.86638533e-05]
[ -7.28783153e-07]] flag
Stability factor, max = 0.5669740394358797, min=-0.9999999999999998
```

Comparing Figures 3.13 and 3.10, we see that although both schemes maintain sharp wave fronts, schemes aiming to reduce dispersion error in all directions reduce anisotropy generated for the grid functions.

3.2.6 Numerical experiments in two dimensions

In this subsection we compare the results of four schemes with stencil width $M = 10$, CFL number $\gamma = 0.6$. All programs are written in Python. The schemes are:

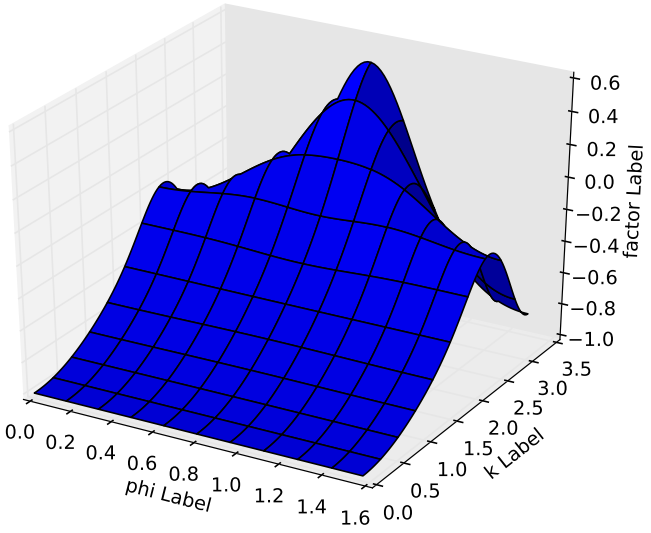

Figure 3.12: Stability factor for amplification polynomial $g^2 + 2zg + 1 = 0$: $|z|$ as a function of K and ϕ. Scheme obtained with Remez algorithm in ϕ

1. `accu2d.py` from (3.23) with $\phi_0 = \pi/4$. Here we do experiments with both $M = l = 10$ and $M = l = 2$.

2. `accu2d_exactphase_wavenumber.py` from (3.31) with $\phi_0 = \pi/4$, $\phi = \pi/4$, and exact phase velocity at 8 wavenumbers $K =$ `np.linspace(0.05*np.pi,0.9*np.pi,8)`.

3. `remez2d_angle.py` from Example 3.2.3, with $K = 0.5\pi$, $l = 2$, $\phi_0 = \pi/4$.

4. `remez2d_wavenumber.py` from algorithm 3.2.3.1, with $\phi_0 = \pi/4$, $\phi = \pi/4$, $l = 2$, and optimization interval is $K \in [0.01, 0.8\pi]$. Notice that increasing l will increase the accuracy. Here for comparison with the result of `remez2d_angle.py`, we only use $l = 2$.

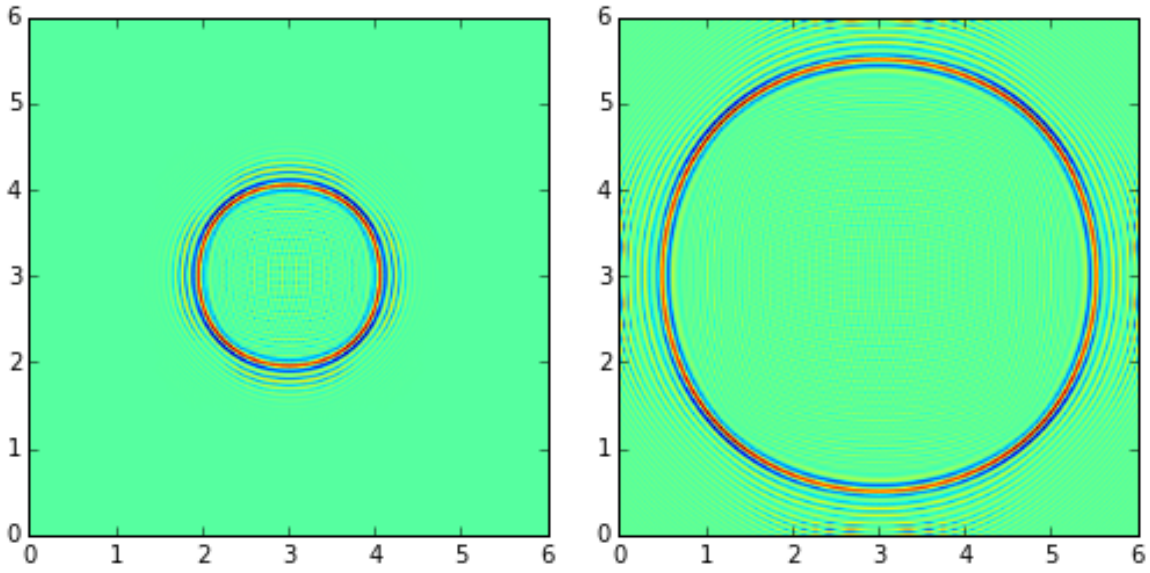

(a) After 100 time steps

(b) After 224 time steps

Figure 3.13: $K = \pi/2$, $l = 2$, $M = 6$, $\gamma = 0.6$, $\phi_0 = \pi/4$. Wave propagation at time step 100 and 224, scheme computed with Remez algorithm in propagation angle.

In general, it is hard to obtain stable schemes in two dimensions with exact dispersion requirements in propagation angle or with minimized dispersion error in angle. One of the few stable schemes we found for `remez2d_angle.py` all require $l = 2$. In order to compare with scheme from Figure 3.13, we will use second order accuracy for all schemes mentioned above.

From Figure 3.14, we see that all schemes give nice wave speeds for small wavenumbers. Schemes for wider stencils give better wave speeds at higher wavenumber. Scheme `remez2d_angle.py` which targets to reduce dispersion error at all directions, increases wave speed for all directions.

Figure 3.16 shows snapshots of wave propagation with source term of a Ricker wavelet. The left column shows the wave at time step 100, and the right column shows a snapshot at time step 200. Wave computed by `remez2d_angle.py` shows smaller anisotropy for the grid function. With minimization in wavenumbers, lower accuracy schemes give wave fronts as sharp as higher accuracy schemes.

3.3 Elliptical Anisotropic Media

In this section, we develop schemes for the elliptical anisotropic media. The differential equation we study is:

$$\frac{\partial^2 u}{\partial t^2} - (c_x^2 \frac{\partial^2 u}{\partial x^2} + c_z^2 \frac{\partial^2 u}{\partial z^2}) = 0 \tag{3.34}$$

where c_x denotes the wave speed in x-direction and c_z denotes the wave speed in z-direction. We assume $c_x^2 = (1 + 2\epsilon)c_z^2$ with $\epsilon > 0$, as horizontal reflectors work as a deceleration factor for vertical waves in the media. The general scheme is of form

$$U_{l,j}^{n+1} + U_{l,j}^{n-1} + 2c_0 U_{l,j}^n + \sum_{m=1}^{M} c_m (U_{l+m,j}^n + U_{l-m,j}^n) + \sum_{m=1}^{M} d_m (U_{l,j+m}^n + U_{l,j-m}^n) = 0 \tag{3.35}$$

$$U_{l,j}^{n+1} + U_{l,j}^{n-1} + \sum_{m=0}^{M} c_m (U_{l+m,j}^n + U_{l-m,j}^n) + \sum_{m=0}^{M} d_m (U_{l,j+m}^n + U_{l,j-m}^n) = 0. \tag{3.36}$$

Due to the form of the differential equation, it is reasonable to take $c_m = (1 + 2\epsilon)d_m$ if we take $\Delta x = \Delta z$. If we take $c_m = d_m$ as in the isotropic case, we would take $\Delta z = \sqrt{1 + 2\epsilon}\Delta x$. In the following two sections, we will show the equivalence of the isotropic case and elliptical case via a simple change of variable.

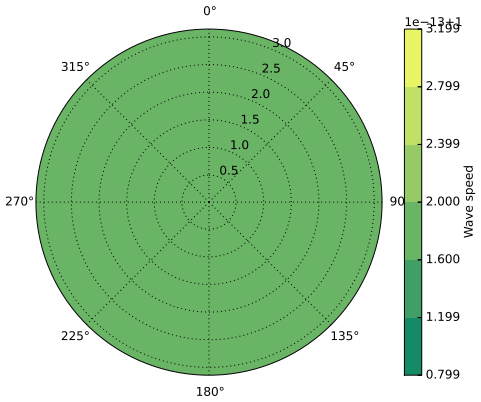

(a) True wave speed $\Omega/\gamma K = 1$ for comparison. Notice true speed is independent of K or ϕ

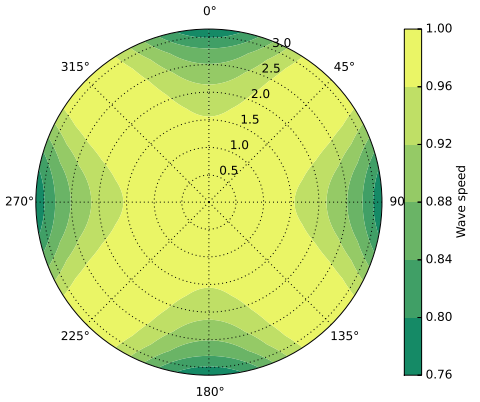

(b) `accu2d.py`, with $M = 10$, Max of dispersion error, max=0.0000000003533707

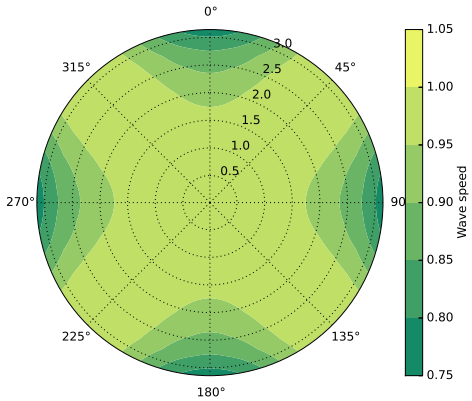

(c) `accu2d_exactphase_wavenumber.py`, Max of dispersion error, max=0.0000011011305976

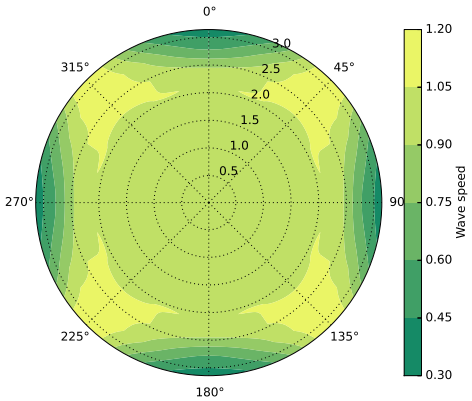

(d) `remez2d_angle.py`, Max of dispersion error, max=0.1536829480601596

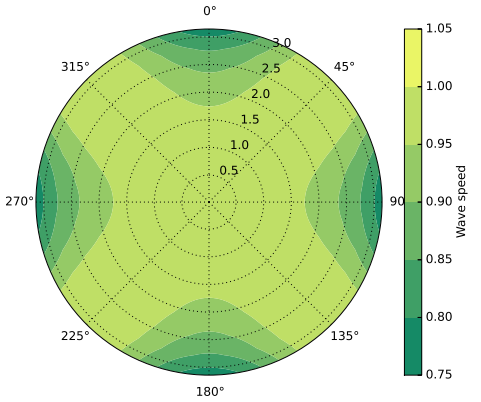

(e) `remez2d_wavenumber.py`, Max of dispersion error, max=0.0000001296140106

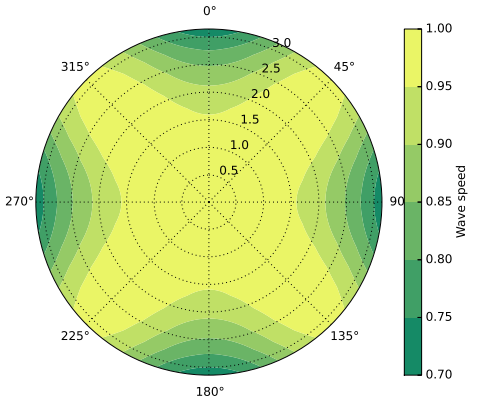

(f) `accu2d.py`, with $M = 2$, Max of dispersion error, max=0.0000000000004988

Figure 3.14: Comparison of numerical phase velocity for different schemes

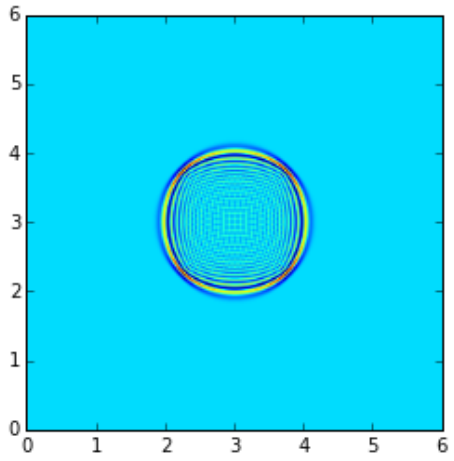

(a) `accu2d.py`, $l = 2, M = 2$

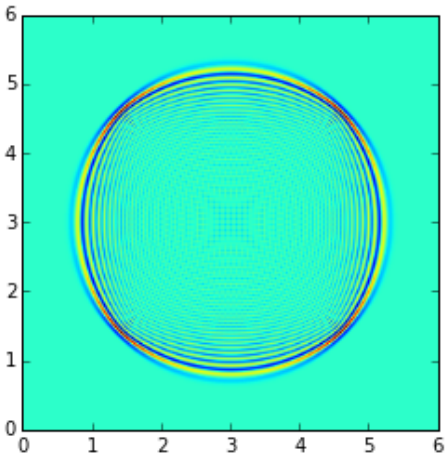

(b) `accu2d.py`, $M = l = 2$

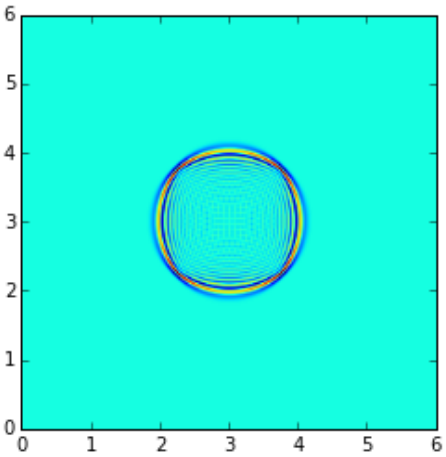

(c) `accu2d.py`, $M = l = 10$

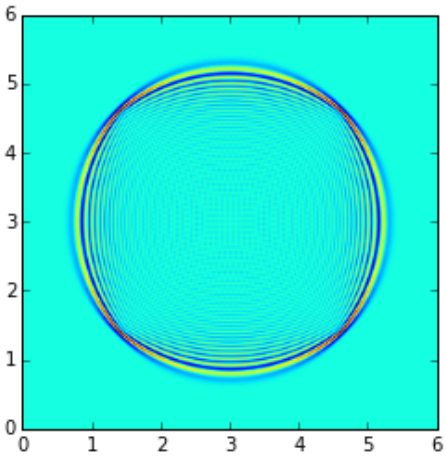

(d) `accu2d.py`, $M = l = 10$

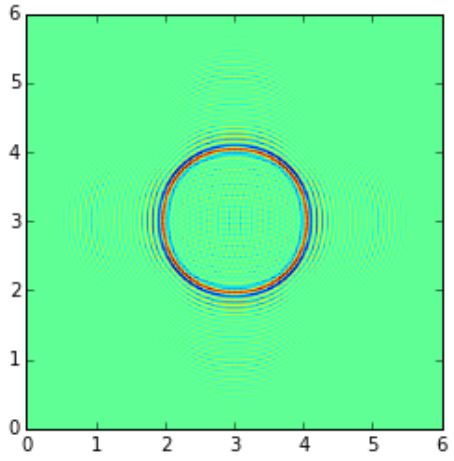

(e) `remez2d_angle.py`, $M = 10, l = 2$

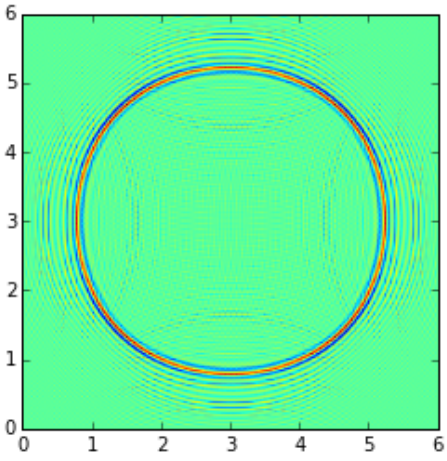

(f) `remez2d_angle.py`, $M = 10, l = 2$

Figure 3.15: Wave propagation at: time step 100 and 200.

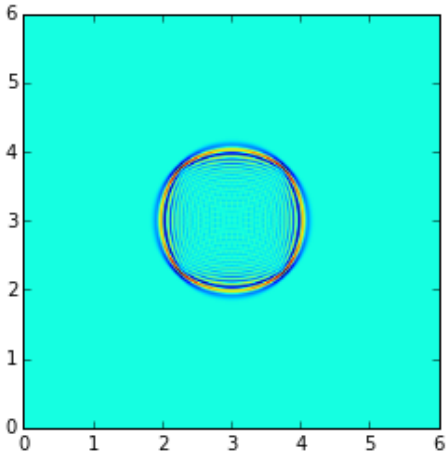

(a) `accu2d_exactphase_wavenumber.py`, $l = 2, M = 10$

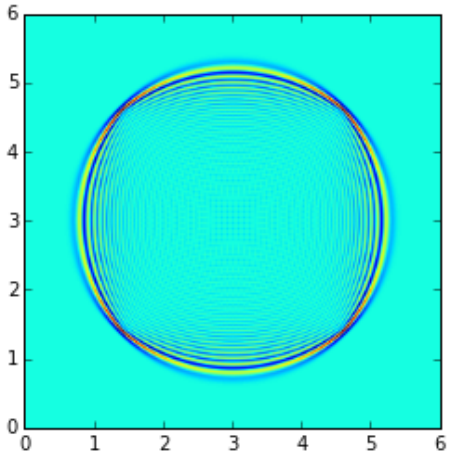

(b) `accu2d_exactphase_wavenumber.py`, $l = 2, M = 10$

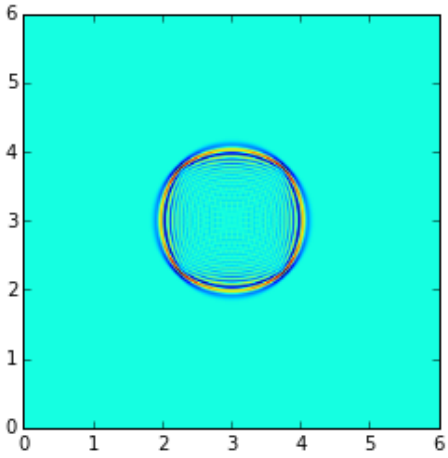

(c) `remez2d_wavenumber.py`, $M = 10, l = 2$

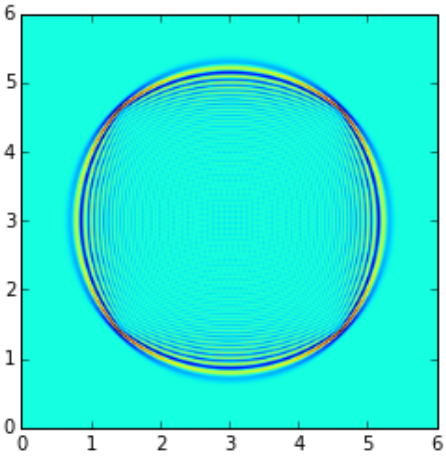

(d) `remez2d_wavenumber.py`, $M = 10, l = 2$

Figure 3.16: Wave propagation at: time step 100 and 200.

3.3.1 Dispersion analysis

The true dispersion can be obtained from the differential equation (3.34)

$$\omega^2 = c_x^2 k_x^2 + c_z^2 k_z^2. \tag{3.37}$$

We will show that by taking $\Delta z = \sqrt{1+2\epsilon}\Delta x$, the dispersion relation is equivalent to the isotropic case:

$\omega^2 = c_x^2 k_x^2 + c_z^2 k_z^2$

$(\omega\Delta t)^2 = (c_x\Delta t)^2 k_x^2 + (c_z\Delta t)^2 k_z^2$

(Use $c_x^2 = (1+2\epsilon)c_z^2$)

$(\omega\Delta t)^2 = (1+2\epsilon)(c_z\Delta t)^2 k_x^2 + (c_z\Delta t)^2 k_z^2$

$(\omega\Delta t)^2 = (1+2\epsilon)\dfrac{(c_z\Delta t)^2}{(\Delta x)^2}(k_x\Delta x)^2 + \dfrac{(c_z\Delta t)^2}{(\Delta z)^2}(k_z\Delta z)^2$

(take $\Delta x = \Delta z\sqrt{1+2\epsilon}$ to obtain dispersion relation identical to the isotropic case)

$\Omega^2 = \gamma^2(K_x^2 + K_z^2)$

where $\Omega = \omega\Delta t$, $\gamma^2 = \frac{(c_z\Delta t)^2}{(\Delta z)^2}$, $K_x = k_x\Delta x$ and $K_z = k_z\Delta z$.

The numerical dispersion for the isotropic case is

$$\cos(\Omega) + \sum_{m=0}^{M}[c_m\cos(mK_x) + c_m\cos(mK_z)] = 0. \tag{3.38}$$

Similarly, the numerical dispersion for the elliptical anisotropic case is

$$\cos(\Omega) + \sum_{m=0}^{M}[c_m\cos(mK_x) + d_m\cos(mK_z)] = 0. \tag{3.39}$$

3.3.2 Accuracy analysis

Since for differential equations (3.1) and (3.34), a simple change of variable $\widetilde{z} = \sqrt{1+2\epsilon}\, z$ can convert (3.34) into (3.1), it is reasonable that above conclusion holds for the difference equations as well, with $c_m = (1+2\epsilon)d_m$. Similar to the numerical dispersion case, we plug

in the true solution to the difference equation for elliptical anisotropic case:

$$
\begin{aligned}
&U_{l,j}^{n+1} + U_{l,j}^{n-1} + \sum_{m=0}^{M} c_m (U_{l+m,j}^{n} + U_{l-m,j}^{n}) + \sum_{m=0}^{M} d_m (U_{l,j+m}^{n} + U_{l,j-m}^{n}) \\
&= 2u + 2\frac{\Delta t^2}{2!}\partial_t^2 u + 2\frac{\Delta t^4}{4!}\partial_t^4 u + \dots \\
&+ \sum_{m=0}^{M} c_m \left(2u + 2\frac{(m\Delta x)^2}{2!}\partial_x^2 u + 2\frac{(m\Delta x)^4}{4!}\partial_x^4 u + \dots \right) \\
&+ \sum_{m=0}^{M} d_m \left(2u + 2\frac{(m\Delta z)^2}{2!}\partial_z^2 u + 2\frac{(m\Delta z)^4}{4!}\partial_z^4 u + \dots \right).
\end{aligned}
$$

Taking $c_m = (1 + 2\epsilon)d_m$ and $\Delta z = \sqrt{1 + 2\epsilon}\Delta x$ gives the exact same form of the isotropic case, with a minor adjustment of the c_0 and d_0 terms.

3.3.3 Stability analysis

For the schemes we get to be stable, we enforce:

$$
|z| = \left| c_0 + \sum_{m=1}^{M} [c_m \cos(mK_x) + d_m \cos(mK_z)] \right| \leq 1. \tag{3.40}
$$

It is even harder to find stable schemes for the elliptical anisotropic media.

Conclusion

We conclude that, for the elliptical anisotropic case, we can compute the coefficients as usual. The schemes apply to a stretched medium.

Chapter 4

CONCLUSIONS

In this work, we have developed a unified methodology for obtaining dispersion reduction finite difference schemes. The method is based on obtaining a uniform approximation to the true dispersion relation for all wavenumbers in the proper domain, while keeping the traditional requirement of order of accuracy. All accuracy analyses are done in the spectral domain, using the spectral order of accuracy proposed by Finkelstein and Kastner (2009). We have proved the existence of schemes based on interpolation of the dispersion relation proposed by Finkelstein and Kastner (2007, 2008) and Liu and Sen (2009) for arbitrary choice of wavenumbers. The existence result further guarantees the possibility of designing a Remez-like algorithm, with enforced exact phase/group dispersion relation at preset non-zero wavenumbers.

In one dimension case, the minimization of dispersion error is done in the wavenumber domain. Decrease in numerical dispersion error for all wavenumbers is observed. One drawback of our new method is that, unlike traditional scheme where the numerical wave speed is always smaller than the true wave speed, in the new method, it is possible that the numerical speed is higher than the true wave speed (see Figure2.14a). This is not surprising, as such errors are in the nature of the Remez algorithm. Another remark to make is on the choice of the optimization interval. Since the null spaces needed for the algorithm are not Haar on the full domain $[0, \pi]$, it is reasonable to do minimization only on $[0, K_{max}]$ with some $K_{max} < \pi$. Schemes corresponding to Figure 2.14 are obtained by optimizing with $K_{max} = 0.9\pi$. With exact dispersion requirements at preset wavenumber K_0 for example, we need to either change the optimization interval to avoid K_0, or to change the alternating requirements to rule out the zero at K_0. Figure 2.17 is produced with exact phase velocity at 0.5π and optimization interval $[0, 0.49\pi]$; the overall dispersion error is reduced.

In the two dimension case, the dispersion relation depends on both wavenumber and

propagation angle. As in one dimension case, we build new schemes from accuracy conditions at the zero wavenumber. These conditions depend on propagation angles, and we choose the angle $\pi/4$ in the accuracy conditions. This choice guarantees the possibility of Remez algorithm in wavenumber, and doesn't increase dispersion error much compared to $\pi/8$, the choice made by Liu and Sen. Similar to the one-dimension case, we seek schemes that minimize dispersion error uniformly. The minimization is done either in wavenumber with a fixed propagation angle or in angle with a fixed wavenumber. Although the Remez algorithm in wavenumber is guaranteed by our results to work if we take $\pi/4$, the Remez algorithm in propagation angle is not guaranteed to always work. Both ways show improved dispersion accuracy in propagation angles. It is in general hard to find stable schemes in two dimensions using these methods. Schemes that guarantee minimized dispersion for all angles are also hard to find. It would be an interesting question to study the criteria for determining stable schemes using these methods.

BIBLIOGRAPHY

1. Alford, R. M., Kelly, K. R., Boore, D. M., 1974, Accuracy of finite-difference modeling of the acoustic wave equation Geophysics, VOL.39, NO.6, P. 834-842.

2. Alkhalifah, T., and I. Tsvankin, 1995, Velocity analysis for transversely isotropic media: Geophysics, 60, 1550-1566.

3. Alkhalifah, T., 1998, Acoustic approximations for processing in transversely isotropic media, GEOPHYSICS, 63(2), 623-631.

4. Alkhalifah, 2000, Geophysics, VOL 65, NO.4(JULY-AUGUST 2000), P.1239-1250, An acoustic wave equation for anisotropic media

5. Bube et al, 2012, Geophysics, VOL 77, NO. 5(SEP-OCT 2012), P.T171-T186, On the instability in second-order systems for acoustic VTI and TTI media

6. Burridge, Some mathematical topics in seismology, Courant Institute of Mathematical Sciences Lecture Notes, New York University, 1976

7. Chapman, C., 2004, Fundamentals of Seismic Wave propagation, Cambridge University Press, ISBN-13 978-0-521-81538-3

8. Cowin, S. C., Mehrabadi, M. M. and Sadegh, A. M., (1991) Kelvin formulation of the anisotropic Hooke's law, in J. J. Wu, T. C. T. Ting and D. M. Barnett (eds.) Modern Theory of Anisotropic Elasticity and Applications, SIAM, Philadelphia, pp. 340-356

9. Duveneck et al, 2008, SEG Las Vegas 2008 Annual Meeting, Acoustic VTI wave equations and their application for anisotropic reverse-time migration

10. Finkelstein, B., Kastner, R., 2007, Finite difference time domain dispersion reduction schemes, J. Comput. Phys. 221(2007) 422-438

11. Finkelstein, B., Kastner, R., 2008, A Comprehensive New Methodology for Formulating FDTD Schemes With Controlled Order of Accuracy and Dispersion, IEEE Trans. Antennas Propag.,VOL. 56, NO.11, NOV 2008

12. Finkelstein, B., Kastner, R., 2009, The spectral order of accuracy: A new unified tool in the design methodology of excitation-adaptive wave equation FDTD schemes, J. Comput. Phys. 228(2009) 8958-8984

13. Helbig, K., 1983, Elliptical anisotropy-Its significance and meaning, Geophysics, VOL.48, NO.7,JULY 1983

14. Karlin, S., Studden, W. J., Tchebycheff Systems: with applications in analysis and statistics, Interscience Publishers 66-13398, 1966

15. Kelly, K. R., Ward, R. W., Treitel, S., Alford, R. M., 1976, Synthetic seismograms: a finite-difference approach, Geophysics, VOL.41, NO.1, P. 2-27.

16. Kimchi, E., Richter-Dyn, N, Best Uniform Approximation with Hermite-Birkhoff Interpolatory Side Conditions, Journal of Approximation Theory, 15, 85-100(1975)

17. Kimchi, E., Richter-Dyn, N, Properties of Best Approximation with Interpolatory and Restricted Range Side Conditions, Journal of Approximation Theory, 15, 101-115(1975)

18. Kosloff, D., 2008, Numerical Solution of the Constant Density Acoustic Wave Equation by Implicit Spatial Derivative Operators, SEG Las Vegas 2008 Annual Meeting

19. Kosloff, D., Pestana, R. C., and Tal-Ezer, H., Acoustic and elastic numerical, wave simulations by recursive spatial derivative operators. GEOPHYSICS, VOL.75, NO.6(NOVEMBER-DECEMBER 2010); P. T167T174

20. Kreiss, H., Oliger, J., 1973, Methods for the approximate solution of time dependent problems, International Council of Scientific Unions, World Meteorological Organization, 1973

21. Lax, Hyperbolic Partial Differential Equations, Courant lecture notes, ISSN 1529-903I; 14. 2006

22. Levander, A. R., 1988, Fourth-order finite-difference P-SV seismograms, Geophysics, VOL.53, NO.11, P. 1425-1436.

23. LeVeque, R. J., 2007, Finite Difference Methods for Ordinary and Partial Differential Equations, SIAM

24. Liu, Y., Sen, M. K., 2009, A new time-space domain high-order finite-difference method for the acoustic wave equation, J. Comput. Phys. 228(2009)8779-8806

25. Lorenz, G.G. Approximation of Functions, Holt, Rinehart and Winston, Inc. 1966 66-13296

26. Powell, M. J. D., Approximation theory and methods, Cambridge University Press, ISBN 0-521-29514-9, 1996

27. Sanna, M., Numerical Simulation of Fluid-Structure Interaction Between Acoustic and Elastic Waves, Jyväskylä Studies in Computing, ISBN 978-951-39-4439-1 (PDF) 2011

28. Trefethen, L. N., 1982, Group velocity in finite difference schemes, SIAM REVIEW Vol.24, No.2

29. Trefethen, L. N., Finite Difference and Spectral Methods for Ordinary and Partial Differential Equations, unpublished text, 1996, available at

    http://people.maths.ox.ac.uk/trefethen/pdetext.html

30. Tsvankin I. P-wave signatures and notation for transversely isotropic media: An overview. Geophysics, 1996,61(2):467483

31. Tsvankin, Seismic Signatures and Analysis of Reflection Data in Anisotropic Media, ISBN: 0-08-043649-8, 2001

32. Virieux, J., 1984, SH-wave propagation in heterogenneous media: Velocity-stress finite-difference method, Geophysics, VOL.49, NO.11, P. 1933-1957, 15 FIGS. 1 TABLE

33. Virieux, J., 1986, P-SV wave propagation in heterogeneous media: Velocity-stress finite-difference method, Geophysics, VOL.51, NO¿4, April 1986

34. Wang, S., Teixeira, F. L., 2003, Dispersion-Relation-Preserving FDTD Algorithms for Large-Scale Three-Dimensional Problems IEEE TRANSACTION ON ANTENNAS AND PROPAGATION, VOL.51, NO.8

35. Whitham, G. B., 1974, Linear and nonlinear wave, Wiley-Interscience, ISBN: 0471940909

36. Zhang et al, 2005, Geophysical Prospecting, 2005, 53, 843-852, Finite-difference modeling of wave propagation in acoustic tilted TI media